Master's thesis

NTNU
Norwegian University of Science and Technology
Faculty of Information Technology and Electrical Engineering
Department of Electric Power Engineering

Vebjørn Hjelle

Energy Storage for Reinforcement of a High Voltage Distribution Grid

Master's thesis in Energy and Environmental Engineering
Supervisor: Trond Leiv Toftevaag
June 2019

NTNU
Norwegian University of Science and Technology

Vebjørn Hjelle

Energy Storage for Reinforcement of a High Voltage Distribution Grid

Master's thesis in Energy and Environmental Engineering
Supervisor: Trond Leiv Toftevaag
June 2019

Norwegian University of Science and Technology
Faculty of Information Technology and Electrical Engineering
Department of Electric Power Engineering

NTNU
Norwegian University of
Science and Technology

Preface

This thesis is the result of work carried out during winter and spring 2019 as the final stage of a master's degree at the Norwegian University of Science and Technology. The subject for the work was initiated by Stryn Energi AS, which has granted access to power system data of their distribution system. This has enabled the analysis to be based on a real-world system, making the project work highly motivating and inspiring.

I wish to express thanks to my supervisor, Docent Trond Leiv Toftevaag at the Department of Electric Power Engineering, for his support throughout the project. Trond has been a great assistance when problems have occurred, and also an excellent discussion partner on a number of topics. Additionally, I would like to thank Chief Operating Officer Hans Ørjasæter at Stryn Energi AS for providing the opportunity of working with such an inspiring project, and for always being available for discussions throughout the year.

Vebjørn Hjelle

Trondheim, June 2019

Abstract

A 22 kV distribution system consisting presently of 350 cottages has in this thesis been analyzed. A forthcoming expansion including about 180 cottages is planned, while the area is regulated for a total of 1000. As the existing connection to the external grid is not dimensioned for such demand, the load may cause congestion in the supply. The purpose of this thesis is therefore to analyze the viability of using energy storage in the cottage area instead of conducting traditional grid reinforcement.

Technical aspects of several reinforcement alternatives are investigated by modeling the given power system in an analysis tool, using this model to run simulations in different load scenarios. A load profile is estimated based on the distinctive characteristics of the consumer group, resulting in a long high-demand period of over eight hours. Energy storage is implemented into this model with the peak shaving application in mind, and through the simulations the impact of installing energy storage is compared to traditional reinforcement alternatives. Further, the costs of battery energy storage systems are surveyed and utilized in an economic analysis, where lifetime costs for different supply alternatives were compared.

The simulations show that energy storage is able to provide the necessary power during peak demand to mitigate congestion in the grid, but that a large energy capacity is required due to the prolonged high-demand period. When the load demand incurs a maximal loading of 97% in the existing supply, a battery of 1.2 MW/10 MWh is able to reduce the loading to 80% during the entire simulation period. Lower loading, and losses, are however obtained when the supply lines are replaced or a new cable connection is constructed, implying that these alternatives might be technically more robust than a battery alternative. During the economic analysis it is found that a battery installation is not an economically viable alternative for the given system, due to the energy capacity resulting in an expensive capital investment. For the critical load scenario, it is found that the battery is over eight times more expensive than replacing the cable connection of 2 km. With current battery costs a battery investment is shown to be economically beneficial when the length of cable needing replacement exceeds 37 km, while it is found to be 17 km when using an estimated future cost of batteries.

Samandrag

Eit 22 kV distribusjonsnett som forsyner eit hyttefelt bestående av 350 hytter har i dette prosjektet blitt analysert. Ei planlagt utviding på rundt 180 hytter er forestående, og feltet er regulert for totalt omkring 1000 hytter. Den noverande forsyninga til området er ikkje dimensjonert for ei slik belasting, noko som kan føre til overbelasting dersom forbruket aukar. Føremålet med dette prosjektet er difor å analysere om installasjon av energilagring i hyttefeltet er eit godt alternativ til å gjennomføre tradisjonell forsterking av forsyninga.

Tekniske aspekt ved ulike oppgraderingsalternativ er undersøkt ved å modellere nettområdet i eit analyseverktøy, og å nytte denne modellen til å gjere simuleringar for ulike lastscenario. Ein lastprofil er estimert basert på det karakteristiske forbruksmønsteret til kundegruppa, noko som har resultert i ein høglastperiode på over åtte timar. Energilagring er implementert i modellen med mål om å redusere makslasta som må importerast via forsyninga. Verknaden av å installere energilageret er vidare samanlikna med tradisjonell nettforsterking gjennom simuleringar. Vidare har undersøkingar blitt gjort for å finne totalkostnaden for ein batteriinstallasjon, og denne er nytta i ei økonomisk analyse der levetidskostnadane for dei ulike forsyningsalternativa er vurdert.

Simuleringane viser at det er mogleg å nytte energilagring for å redusere toppbelasting i forsyninga, men at ein høg energilagringskapasitet er naudsynt grunna den lange høglastperioden. Når forbruket tilseier ei maksimal belasting på 97% for forsyninga var eit batteri med parametrar 1.2 MW/10 MWh i stand til å redusere belastinga til 80% gjennom heile simuleringsperioden. Både lågare belasting og tap er likevel observert dersom forsyninga i staden er forsterka ved å bytte den noverande med nye kablar, eller ved å bygge ein ekstra forsyningsveg, noko som tyder på at desse alternativa er meir robuste enn å installere batteri. Den økonomiske analysa viser at installasjona av batteri ikkje er lønnsomt i forhold til å oppgradere kabelforsyninga i dette spesifikke tilfellet. På grunn av den store kapasiteten some er naudsynt i batteriet vert investeringskostnaden særs høg. For det kritiske lastscenariet er det over åtte gongar dyrare å nytte batteri enn å oppgradere forsyningsvegen på 2 km. Med dei noverande batterikostnadane viser analysa at alternativet med batteri er lønnsomt dersom 37 km eller meir kabel må byttast, medan avstanden er 17 km dersom eit anslag på ein framtidig batterikostnad er nytta.

Contents

List of Tables

List of Figures

Abbreviations

BESS	Battery energy storage system
BMS	Battery management system
BOS	Balance of system
CENS	Cost of energy not supplied
DOD	Depth of discharge
DSO	Distribution system operator
EMS	Energy management system
EPC	Engineering, procurement, and construction
EV	Electric vehicle
LV	Low voltage
MV	Medium voltage
O&M	Operation and maintenance
PV	Present value
QDSL	Quasi-dynamic simulation
SOC	State of charge
VRFB	Vanadium redox flow battery

Chapter 1

Introduction

1.1 Background

Stryn Energi is the distribution system operator in the municipality of Stryn, supplying a total of approximately 4500 customers including households, industry, businesses, agriculture and holiday residents. A semi-rural area consisting of cottages have the last couple of years experienced rapid expansions, and the customer mass is expected to continue its growth. As the grid connection to the area is considered weak, the growing demand might become a problem for the power supply.

Because of this, the distribution system operator may need to reinvest in the supply to the area. There are several measures that could be done to reinforce the power supply, and using battery energy storage has emerged as one of the opportunities. There have previously been conducted studies on the usage of utility-scale stationary batteries for different applications, which also has investigated the viability of batteries compared to traditional reinforcement. The Norwegian research project "Flexibility in the future smart distribution grid - FlexNett" [1] looked into several cases where batteries were installed as a grid component. The focus was especially on postponement of grid investments, reducing the costs of energy not supplied, short-duration peak shaving and voltage support. The grid area that has been analyzed for this thesis consists of a homogeneous consumer group, as the entire area consists of cottages. Characteristic for this group is a large demand during weekends and holidays, while otherwise having a small consumption. This results in a distinctive consumption pattern, which differentiates the analysis from what was investigated in the FlexNett project.

The present project is a continuation of a project conducted during fall 2018 on the same topic [2]. That project focused especially on developing a simulation model of the given power system and investigating energy storage technologies and applications for grid utilization. As a result, these findings and outcomes are utilized and further improved in this master's thesis project.

1.2 Problem description

To investigate the viability of battery energy storage in comparison to traditional reinforcement through the peak shaving application, the following points are a focus for the study:

- Further development of the simulation model, including an adaption of the consumption characteristics of the consumer group.
- Describe and add relevant reinforcement alternatives to the simulation model.
- Modify the general control algorithm of the energy storage system for the peak-shaving application.

- Simulate and analyze various reinforcement alternatives in different load situations, including the impact of installing energy storage.
- Investigate present and future cost predictions for energy storage via market and literature studies.
- Conduct an economic assessment of relevant reinforcement alternatives for the given power system, including the energy storage alternative.

1.3 Objective

The objective of this project is to investigate if energy storage is a viable option to traditional grid reinforcement of the 22 kV distribution system in a rural area consisting of cottages. Additionally, a target is to gain insight on how techno-economical analyses are conducted in order to select the best alternative of grid reinforcement.

1.4 Limitations

The given power system is modeled on a high-voltage distribution grid level (22 kV), meaning that the low-voltage distribution grid (230 V and 415 V) is not taken into consideration. Because of this, all loads under a transformer are aggregated to refer it to the 22 kV level. The data quality of the analyzed system is not sufficient to correctly replicate the supply situation. Therefore, load estimations based on the real data are done, where a pessimistic approach is taken in order to analyze the worst case scenario. No dynamic or transient effects have been considered since a quasi-dynamic simulation approach is chosen. Additionally, zero-sequence elements are neglected as it is assumed that only balanced loads are present. Due to lack of data and the time constraint, some elements have been neglected during the economic analysis. These are the cost of energy not supplied, congestion costs, and the salvage value of the equipment.

1.5 Software

Modeling and simulation are done in the power system analysis tool DIgSILENT PowerFactory [3]. Load data is gathered from the DSO's distribution management system, which called is Validér Dashbord and is made by Powel [4]. Microsoft Excel is utilized for handling the data and to perform calculations for the economic analysis.

1.6 Structure of the report

Chapter 2 gives an executive description of the power system to be analyzed, and also present its grid topology. Chapter 3 present the principle of socioeconomic analysis of grid upgrades, and introduce the fundamentals of the utilized economic principles. Chapter 4 describes the four reinforcement alternatives that are looked into, while chapter 5 gives a short introduction to the most important principles of batteries. Chapter 6 describe how the power system and

energy storage is modeled, and also addresses the creation of the characteristic load profile. Chapter 7 describe two load scenarios, and present results and analysis of the conducted simulations for all the relevant reinforcement alternatives in each of the scenarios. Further, chapter 8 discusses the method of the economic analysis, and present market and literature studies regarding the cost of a battery energy storage system. Chapter 9 present results and a discussion of the economic analysis, while chapter 10 deals with sensitivity analyses based on these results. Chapter 11 gives a broader perspective on energy storage in relation to the results obtained, while chapter 12 present the conclusions of the work. Recommendations for further work are described in chapter 13.

Chapter 2

Power system description and topology

This chapter is in its entirety gathered from [2], as the system to be analyzed is equal. The analyzed power system represents a semi-rural area consisting of holiday cottages and a ski resort. Figure 2.1 shows a map of the area. Today there are approximately 350 cottages which are connected to the grid, where a large share of them are large, newly built and have a lot of amenities. The total customer base usually has a low consumption during the working days since few of them are present these days. During weekends and holidays, however, a large amount of the consumers may use their cottages, creating a large load demand these periods. Christmas, Easter and winter weekends are expected to have an especially high consumption because many customers are present, and because the heating demand increases due to low winter temperatures. [5]

The cottage area is supplied by a high voltage distribution network at 22 kV. In the area itself the transmission is done by underground cables in a radial configuration, while the external supply connection consist of a combination of overhead lines and cables. These lines, which are circled in fig. 2.1, are the only connection to the external grid, thus there is no alternate method of supply. The 350 load points are distributed between 11 transformers stations which supplies mostly 415 V to the low distribution grid. Essentially all customers have installed the smart metering system, which provides hourly consumption data for each measuring point.

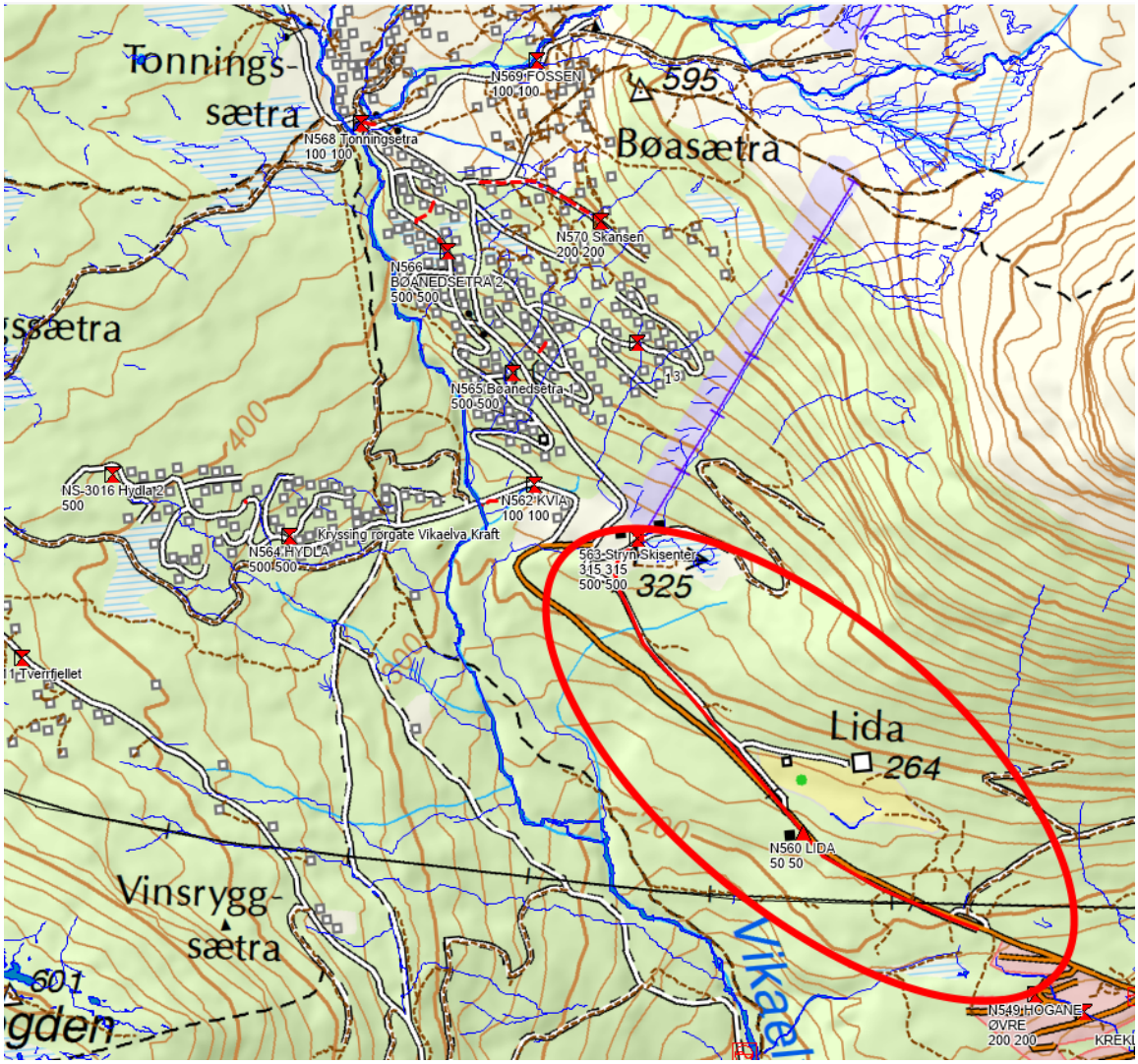

Figure 2.1: Map of cottage area with connection to external grid.

Several overhead lines and cables of the supply have low transmission capacity which can lead to congestion, or at least severely increased loss in the lines. Even though the situation might not be critical at this point, the cottage area is regulated for around 650 additional cottages. In this situation the peak load demand might become critical for the weak lines. There are several line sections that are weak points, but the worst one is regarded as the bottleneck of the system. This line is marked by an arrow in fig. 2.2, and is denoted as line section 2. Figure 2.2 shows a simplified single-line diagram of the cottage area at the 22 kV level. The additional weak connections are colored red in the simplified single-line diagram. The full single-line diagram made in PowerFactory can be seen in fig. A.1 of appendix A. Note that each line segment is numbered in order to easily refer to a specific section in the grid. These numbers are consistent between figs. A.1 and 2.2, while table A.3 specify the line type of each section. These types are referred to the overhead line and cable parameters of tables A.1 and A.2. Appendix A also present data for transformers and load consumption. The distribution system modeling approach is described in chapter 6.

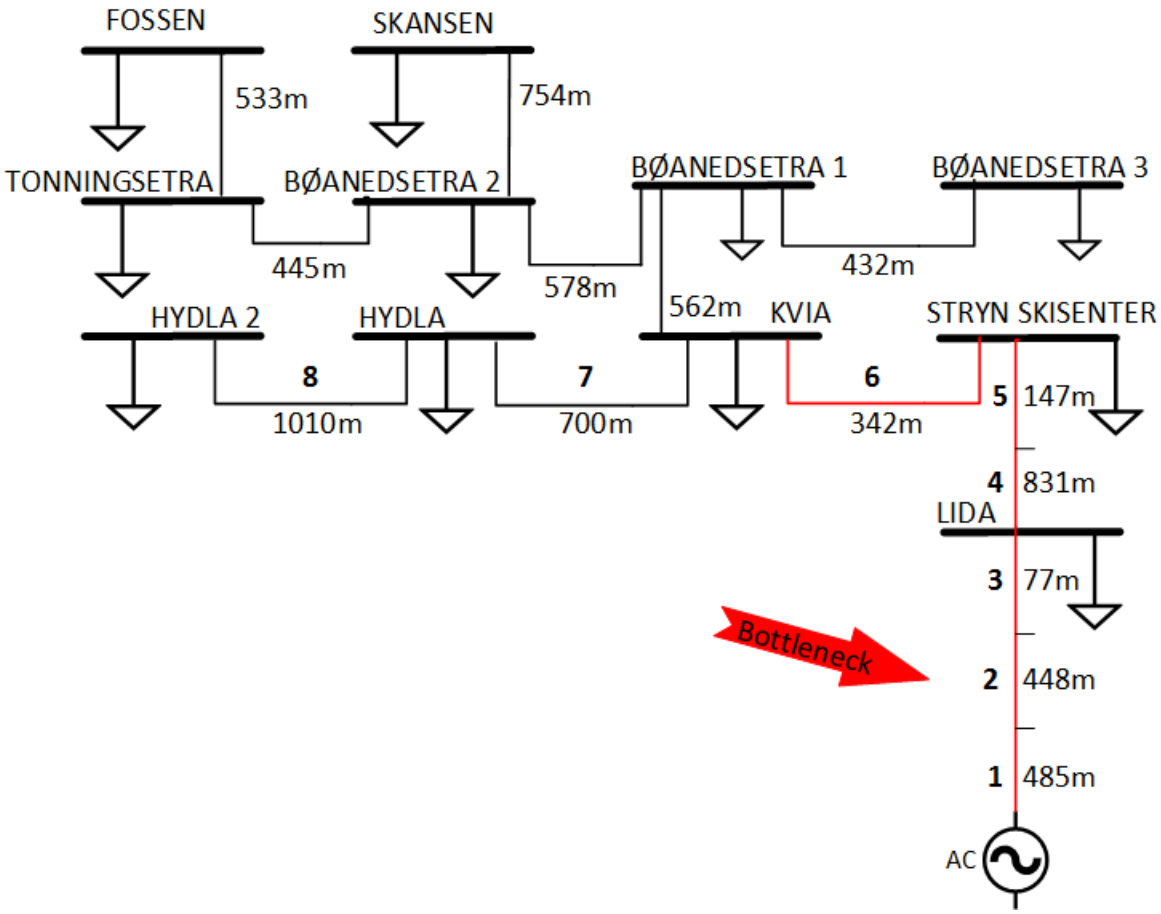

Figure 2.2: Simplified single-line diagram of cottage area showing line section numbers and length.

Chapter 3

Economics

3.1 Socioeconomic analysis of grid upgrades

The Norwegian energy act states that a development should be socioeconomically rational. Thus it is a requirement to conduct socioeconomic analysis of relevant solutions when applying for allowances to build grid infrastructure. In "Veileder for kraftsystemutredninger" it is specified that a socioeconomic analysis should be carried out for different load and production scenarios [6]. A socioeconomic analysis starts with a description of the problem and goals with the grid upgrade. After this, relevant actions for solving the problem are described and analyzed. Then the cost and benefits for each action is identified and compared. This is used to calculate the socioeconomic profitability for each action, often through the use of the net present value method. Sensitivity and scenario analysis related to change in important parameters should then be conducted to highlight potential pitfalls when choosing which action to select. Additionally, effects that not are measured in money is considered. This may be e.g. groups that are negatively affected by the infrastructure or recreational area such as parks and untouched nature. Based on the socioeconomic analysis, with all these considerations in mind, the best action should be conducted.

In the socioeconomic analysis for grid upgrades NVE states that five cost and benefit impacts should be included. These are investment costs, operation and maintenance costs, cost of electrical losses, cost of energy not supplied and bottleneck costs. By minimizing the total cost of these elements, the socioeconomic optimum is found. The fundamentals of these costs are presented in sections 3.1.1 to 3.1.4. The bottleneck costs are not covered further in this report, as they typically are relevant at higher voltage levels ie. from 132 kV. [7]

3.1.1 Investment cost

The investment cost is the initial cost to get a project to an operable status. It should include equipment, labor for construction, transport and payment to land tenures. The size of these costs should be based upon the current prices in the market and experience from earlier projects. [7]

3.1.2 Cost of electrical losses

In the Norwegian power system the energy losses amount to about 8% of the annual production, while the power losses in the peak hour is around 15% of the generated power [8]. The power losses in the system have many sources, some of them being transformers, overhead lines and cables both in the high and low voltage equipment. The copper loss in a line or cable due to the internal resistance is given by eq. (3.1).

$$\Delta P = R \cdot I^2 \tag{3.1}$$

These losses cause the necessary generation to be higher, and they also occupy transmission capacity in the grid. Therefore, increased investments in production and transmission capacity is caused by the losses. It is therefore necessary to put a cost on the losses in such a way that it induces correct dimensioning seen from a socioeconomic point of view. To account for the energy and power loss, the cost of losses can be expressed as given in eq. (3.2). [7]

$$C_{loss} = k_p \cdot \Delta P_{max} + \int k_w(t) \cdot \Delta P(t) dt \tag{3.2}$$

In eq. (3.2) C_{loss} is the annual cost of losses in NOK/yr, $k_w(t)$ is the energy cost in time t (NOK/kWh), k_p is the cost of maximum power losses (NOK/kW yr), while ΔP_{max} and $\Delta P(t)$ is the maximum power losses and power losses in time t respectively (kW). [8]

By simplifying eq. (3.2) the equation can be written as in eq. (3.3).

$$C_{loss} = (k_p + k_{weq} \cdot T_t) \cdot \Delta P_{max} \tag{3.3}$$

Here, k_{weq} is the annual equivalent cost of energy losses (NOK/kWh). T_t is called the utilization time for electrical losses, and is defined by eq. (3.4). It expresses the duration of the maximum power loss where it induces the same energy losses as the annual energy losses, as shown in fig. 3.1. By utilizing this formula it is sufficient to do only one power flow simulation in the maximum power hour, as ΔP_{max} is the total loss in this hour and can then be utilized to find the annual losses. [8]

$$T_t = \int \frac{\Delta P(t)}{\Delta P_{max}} dt \tag{3.4}$$

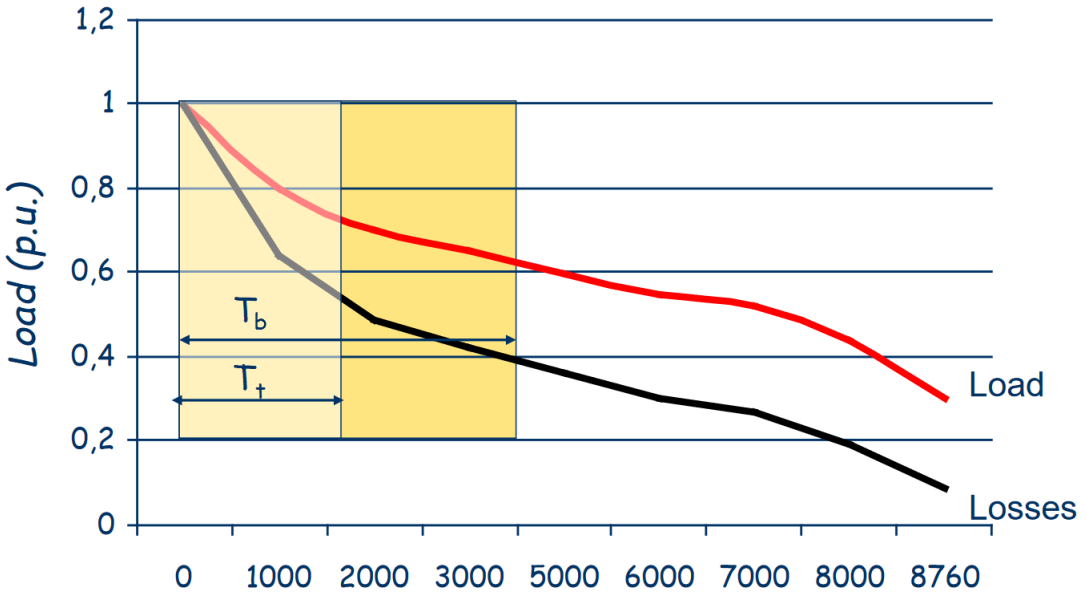

Figure 3.1: Utilization time for electrical loads and losses [9].

3.1.3 Operation and maintenance cost

Operation and maintenance (O&M) costs may be difficult to determine for a project, since it varies greatly with many factors. It is therefore common to associate these costs with previous experience from equivalent projects. If this is not available the costs have to be estimated, for example as an annual percentage of the investment cost. The O&M costs should cover costs for equipment, supplies, transport and labor for all years in the analysis period. [7, 10]

3.1.4 Cost of energy not supplied

A power outage is in the Norwegian regulation defined as an event where the voltage at one or more end users is below 5% of the nominal voltage. Outages are classified as short when the duration is below three minutes and long when the duration is above three minutes. The socioeconomic costs of an outage expresses the economic loss for the society during the outage and includes the costs for end users and the system operator. These costs may be monetary and non-monetary. The monetary costs are easily determined, e.g. costs for broken equipment or lost production. Non-monetary costs are especially relevant for households, and cannot be directly determined. This may include costs for an uncomfortable indoor temperature and not being able to cook. Both monetary and non-monetary costs can also be split into direct or indirect costs. Direct costs occur directly as a result of the outage, such as the need to replace broken equipment. Indirect costs, on the other hand, have no direct correlation with the outage. This may be e.g. loss of trust and fear for when the next outage is going to happen. [7, 11, 12]

3.1.5 Analysis period and calculation interest rate

The calculation interest rate takes into consideration the time value of money, meaning that costs and benefits in the future is valued less than costs and benefits today. By using this, the future cash flows are discounted, meaning that the present value of the payments are found. The calculation interest rate also accounts for risk free interest rate and a risk premium for the project. NVE and the Ministry of Finance provides a recommended calculation rate for socioeconomic analysis. It is common for a DSO to use this interest rate as its required rate of return, which for 2019 is set to 5.82% [13]. [14, 15]

The analysis period is the time frame set for the analysis. Since a grid upgrade or renewal will have an effect for many years the analysis period often is in the range 15 to 30 years. Usually the analysis period should equal the economic life of the project. The economic life is the number of years where the asset has a positive benefit compared to replacing it with a facility with the same purpose. Economic life is equal to, or less than, the physical life. The physical life is the amount of time it takes for the equipment to no longer function, meaning that it definitely has to be replaced. Costs and earnings for all years in the analysis period should be included in the analysis. As the future is highly uncertain, it is difficult to determine the cash flows for the entire period. The load situation could be one of the parameters which is difficult to determine, and as such an estimate has to be used. By using the interest rate for discounting, the uncertain cash flows at the end of the analysis period has lesser impact on the present value than the more certain cash flows at the start of the analysis. [14, 16, 17]

3.1.6 Present value

The present value (PV) is today's value of a future cost or earning. The present value for a project at a given time, often the investment or calculation date, is found by discounting all costs and earnings back to the chosen time point. The present value of all future costs during the analysis period can be calculated as investment cost plus the annual cost of each year, which can be expressed as in eq. (3.5). [14]

$$PV = B_0 + \sum_{t=1}^{N} \frac{C_t}{(1+r)^t} \tag{3.5}$$

Here, B_0 is the investment cost in year 0, N is the number of years in the analysis period and r is the interest rate. C_t is the annual cost for year t after subtracting possible earnings. This concept is often expanded in order to compare several projects. This is called the net present value method, which is given by eq. (3.6). Here B_0 is still the investment cost for the relevant project, while U_t is the net benefit (earnings - cost) that the investment produce in year t. For example when upgrading the cross section of a cable, the annual net benefit would be the reduction of cost of losses compared to the case when no upgrade was done. If the PV of the total cost reduction is larger than the investment cost, the NPV will be positive. This indicates that the project is economically profitable. [14]

$$NPV = -B_0 + \sum_{t=1}^{N} \frac{U_t}{(1+r)^t} \tag{3.6}$$

Chapter 4

Reinforcement alternatives

To fix the potential problem of the 22 KV distribution grid being to weak to supply the cottage area at peak demand, there are several reinforcement options to consider. To find the technically and economically optimal solution, they have to be compared in order to find strengths and weaknesses of each option. In this chapter some relevant solutions will be introduced and described, and these will be used further in the technical and economic analysis.

4.1 Alternative 1: Do nothing

The existing supply connection was built in 1987 and is at this point in time not showing any signs that its physical condition is unsatisfactory [18]. Thus the physical life of the supply is not at its end, meaning that a reinvestment because of this is not needed. As a result it becomes an alternative to do nothing to the grid, which will be assigned to alternative 1. A potential reinforcement must therefore be driven by an increased demand such that the critical thermal level of the supply is reached, or that the losses in the system indicates that a reinforcement is needed, during the analysis period.

4.2 Alternative 2: Refurbish existing connection

The most obvious solution to increase the supply capacity to the cottage area may be to refurbish the existing overhead lines and cables. This way the current route can be utilized by demolishing the existing grid and build a new supply line with higher supply capacity. The DSO inform that, even though the existing supply is partly overhead lines, a new connection in this route would be built solely as a cable connection. This may be due to aesthetic reasons, or that a cable connection is less prone to outages than a overhead line since it is not as exposed to e.g. threes falling over the line. As the connection is the only supply to the area, a more physically robust solution may be preferred in order to decrease the probability of outages.

Building a new supply line in the existing path would mean to exchange sections 1 to 6 of fig. 2.2 with the new cable, as all these sections are regarded as weak. This amounts to a total length of 2.34 km.

4.3 Alternative 3: Add new connection

Another relevant opportunity for the DSO to improve the supply capacity to the cottage area is to add a new connection to the node “Hydla 2”. This would connect the transformer station with an additional external grid, enabling the area to be supplied by two different connections.

This adds robustness to the supply if both connections are able to supply the area on its own, as the supply would not be interrupted if one of them should experience a fault.

According to the DSO a cable connection also for this alternative is most appropriate. The line must be connected through an area used for recreational activities such as hiking and skiing, and as such it is desired to avoid the aesthetic strain an overhead line could cause for the area. A cable connection could therefore be built alongside a path used for skiing tracks, which would mean a total distance of 4.5 km to the nearest grid connection.

This alternative possibly also has a future benefit for the DSO, as the connection would create an extra supply path to a highly populated area downstream of what is regarded as the external grid in fig. A.1. This populated area is the core supply area for the DSO, and it is as such a priority to keep the supply up and running. For this to work, however, sections 1 to 7 in the cottage area also has to be upgraded or bypassed due to the limited capacity. An assessment of this situation is thus beyond the scope of this project, and will therefore not be discussed further.

4.4 Alternative 4: Install battery

Installing a battery in the cottage area could contribute to the supply by providing peak shaving, and other services such as voltage support. The battery will in peak shaving operation provide power whenever the supply lines are heavily loaded, and charge during low demand periods. Depending on the demand magnitude the battery may be able to prevent outage in the cottage area. This requires the rated power to be minimum as large as the demand, and the energy capacity large enough to sustain the required power for the outage period. This may be viable for shorter outages, but for extended periods of outages an additional supply, as described in section 4.3, is more appropriate. [2]

Chapter 5

Principles of batteries

During the initial phase of this project [2] a literature study was conducted on various aspects of batteries. For example the working principle of batteries, various parameters, modes of operation and different technologies were studied. In this chapter some of the most important parameters and features that were discovered will be repeated. Some sections are gathered directly from [2] and shortened to provide the necessary basis for this report. Important aspects in regards to battery technologies are presented in section 8.3.

5.1 Energy capacity

The capacity of a battery is an important parameter to determine its performance. The capacity is often measured in ampere-hours (Ah), which is the product of current and time in hours. Thus, the capacity expresses the current a battery can deliver over a time period for a given nominal voltage and at a specified discharge rate. This means that the capacity is a measure of charge as shown in eq. (5.1) [19, 20]. Q is the capacity measured during discharge, I is the discharge current while t_1 and t_2 is the start and end time of the discharge period.

$$Q = \int_{t_1}^{t_2} I dt \tag{5.1}$$

The most common way of expressing the capacity of a battery is by this ampere-hour rating. Load consumption and billing, however, is expressed in terms of energy by kWh. To relate the capacity to the rest of the power system, a battery capacity in terms of kWh is desired. To accurately express the energy capacity of the battery is quite a difficult task, as the voltage is not constant. The voltage does in fact decrease as a function of the state of charge, and the energy capacity can therefore not be easily calculated precisely. A common approach is thus to estimate the energy capacity by eq. (5.2) through using the nominal voltage. Here, E is the energy capacity, V_{rated} is the nominal voltage and Q is the capacity as defined in eq. (5.1) [21]. [20]

$$E = V_{rated} \cdot Q \tag{5.2}$$

5.2 Power

The power of a battery is the product of the current I and the voltage V as shown in eq. (5.3). The power is thus dependent on the charge/discharge rate and the voltage. Since these values are not necessarily the same for charge and discharge, the power output and power input may be different [21].

$$P = V \cdot I \tag{5.3}$$

For many applications, the specific power is an important parameter. This expresses the power per kg of battery, which is especially relevant in mobile battery applications such as electric vehicles. In a stationary application like grid utility, however, it is often irrelevant.

5.3 State of charge and depth of discharge

The state of charge (SOC) express the share of the total capacity that is remaining in the battery, most often given in percent as in eq. (5.4).

$$SOC = \frac{Q}{Q_{rated}} \cdot 100\% \tag{5.4}$$

Here, Q is the battery charge as given in eq. (5.1) and Q_{rated} is the nominal battery capacity in Ah [22]. With a SOC of 100% the battery is fully charged, and the remaining capacity is equal to the rated capacity. When the SOC is 0%, the battery is fully discharged.

The depth of discharge (DOD) indicates how much of the total capacity is discharged. I.e. if the battery is discharged from 100% SOC to 40% SOC the DOD is 60%. For many battery technologies the DOD severely impacts the cycle life, which is the amount of cycles a battery can withstand before the nominal capacity fall below 80% of its initial value [21]. A high DOD increases the battery degradation dramatically, meaning that the cycle life of the battery is decreased [23]. The principle of this is illustrated by a typical deep-cycle lead-acid battery in fig. 5.1, where it is evident that the number of cycles is decreasing when the DOD increases. Because of this, each battery has a recommended maximum and minimum SOC where it is supposed to operate. A common manufacturer recommendation for lithium-ion batteries is to operate with a DOD of maximum 80%, between 10% and 90% SOC [24].

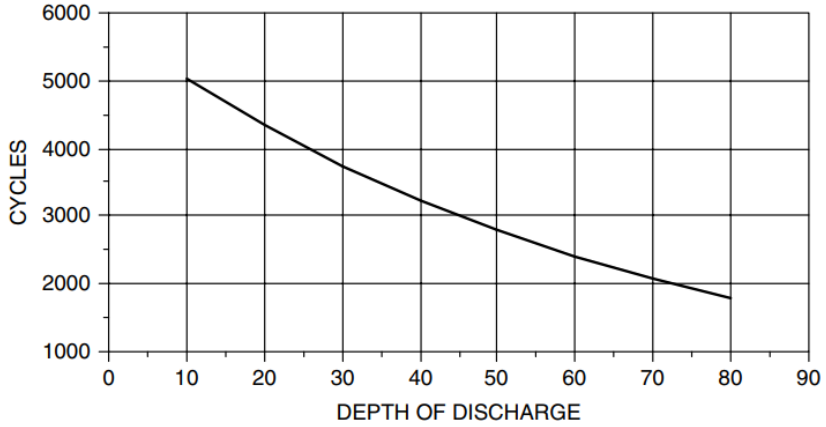

Figure 5.1: Impact of depth of discharge on the cycle life in a lead-acid battery [20].

5.4 Efficiency

Figure 5.2 shows the Thevenin equivalent circuit for a battery. V_B is the battery voltage, R_i is the internal resistance and V is the terminal voltage. The terminal voltage has to be greater than V_B for the battery to charge, and vice versa for discharging. During the power exchange the internal resistance will cause I^2R power losses in the battery. As faster charge/discharge lead to higher currents, it will cause greater losses [20].

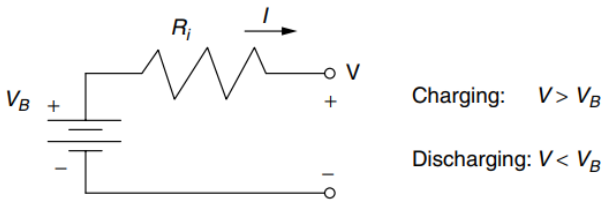

Figure 5.2: Thevenin equivalent circuit of a 12 V battery [20].

The efficiency of a battery, often called the round trip efficiency, is the product of charge efficiency and discharge efficiency. This means that the loss of both charging and discharging is included. Equation (5.5) express the energy efficiency of a battery during a cycle, where E_{ch} is the energy input over the charging period and E_{disch} is the energy output during the discharge period. [20, 25]

$$\eta = \frac{E_{disch}}{E_{ch}} \tag{5.5}$$

Chapter 6

Modeling

The PowerFactory model utilized in this project is an extension of the one developed in [2]. In this chapter the main takeaways and aspects of the modeling approach will be summarized, while changes done during this project will be elaborated on more thoroughly. Figure A.1 show the full single-line diagram of the PowerFactory model.

6.1 Grid modeling

The grid topology is modeled in PowerFactoy based on topology and component data from the DSO's information system. The 22 kV medium voltage distribution grid is supplying an area consisting of approximately 350 cabins, while several expansions are expected the coming years. Because of the large number of individual loads, only the 22 kV grid is modeled in order to simplify the modeling. Thus, it is assumed that the low voltage grid does not induce any problems for the supply. This means that the 230/415 V low voltage distribution grid is not modeled, and that all loads under each MV/LV transformer are aggregated to one load which are modeled as a MV load in PowerFactory. [2]

Technical data for overhead lines and cables that are used in the model is gathered from [26], and data for the relevant components are given in tables A.1 and A.2 of appendix A. Table A.3 present the component type for all sections of the area before any changes is done. Further, tables A.4 and A.5 summarizes the prerequisites used for the given rated thermal current limit for overhead lines and cables respectively. The thermal current limit is the determining factor when the maximum power flow in a line is investigated.

6.2 Load modeling

As mentioned previously the simulation model used in this project is made at the 22 kV level, which means that the LV/MV transformers are representing the loads of the system. Each transformer experiences the aggregated load of all consumer loads connected to it by the low voltage grid, which is the desired load to implement in the model. Obtaining this aggregated time series load directly is, however, not possible even if almost every consumer has installed a smart metering system. This is due to the functionality not yet being implemented into the information system connected to the smart metering system. One solution to the problem could have been to install smart meters in the transformer station, which would have provided the hourly aggregated consumption, but this has not been done in time for the purpose of this project.

6.2.1 Peak load estimation

As a result of lacking consumption data on the transformer level, estimations have been done during the first stage of this project [2] in order to establish a consumption profile for the cottage area. 16 arbitrary measuring points under the transformer "Hydla", which consist of newly built and large cottages, was investigated to find each point's peak load. These values were then used to calculate an average value for peak demand of each consumer. This average was then multiplied with the number of customers under each transformer, leading to a coarse estimation of the aggregated peak load. The calculation of the average peak load is shown in table A.6 of appendix A.2, while table A.7 show the resulting peak load for each transformer node. It has to be noted that this peak estimation assumes that the peak of every consumer occurs at the same instant, which is not a very likely situation. Due to the homogeneous customer group, however, it is not unthinkable that a large share are present and using a lot of power at the same time. Regardless, the peak load will represent the worst case scenario for the supply. [2]

6.2.2 Reactive load estimation

An assessment of the reactive load elements has been conducted in a similar way as the active power demand. The smart meters installed in the area track both active and reactive consumption every hour for each measuring point. By inserting P and Q for a given time point into the equation for the power factor shown in eq. (6.1), the power factor of each load node can be found. This can be inserted into PowerFactory, enabling the load flow analysis to account for reactive behaviour.

$$cos\phi = \frac{P}{S} = \frac{P}{\sqrt{P^2 + Q^2}} \tag{6.1}$$

The PowerFactory analysis model is, as mentioned in section 6.2.1, built on a medium voltage level, meaning that all consumer load nodes under a transformer is aggregated to one load in the model. As aggregated data for each transformer is not available, an estimation has to be done. Therefore, some measuring points under the transformer node "Hydla" was arbitrarily chosen to be investigated, using them to estimate a common power factor for the cottage area in a similar way as the peak load estimation presented in the previous section. Active and reactive power values for randomly chosen time points for each measuring node was gathered. These values was then used to calculate the power factor for each time point by using eq. (6.1). The collected values are shown in appendix A.3. Note that all these values are inductive. After comparing the reactive consumption and production values for a couple of measuring points, it became evident that the consumption data generally had the largest values. As one have to choose an inductive or capacitive power factor for the entire simulation period in PowerFactory, the inductive data was used. The average of these values were found to be approximately 0.97.

Obviously, doing such an estimation will not give a precise value for the power factor as it is largely dependent on the selection of measuring nodes and points of time. It can, however, provide an indication on the order of magnitude in question. Comparing it to other sources, and using experience from similar situations, a power factor of 0.95 was chosen for all medium voltage loads in the system. This slightly worse power factor was chosen in order to have some leeway by not using a too optimistic value.

6.2.3 Load profile

Due to the lack of consumption data on the transformer level, [2] utilized a conventional household load profile made by the German Association of Energy and Water Industries to distribute the consumption over the simulation period. This profile illustrated a common load scenario for a household during a weekend with low consumption during the night, one peak at around 11:00 and another peak at the evening around 20:00. As the loads in question are constituted by cottages, however, the consumption pattern is believed to differ quite a bit from this. Therefore, patterns of consumption for some measuring points have been examined in order to create a load profile that better represent the demand situation in question.

The available consumption data indicates that a Friday evening during the winter may be one of the most critical periods for the supply. Here, a lot of the owners arrive at the cabin, many probably at the evening between 17:00 and 19:00. Due to cold weather the cottage at this point is quite chilly, meaning that a lot of electrical heaters are used to heat the cottage quickly. Additionally, it seems reasonable to assume that many of the residents start to prepare food around 19:00-20:00. This being mostly new cottages induction ovens are common, which is known to require a lot of power. Adding the electric heating and cooking appliances to other home appliances such as TVs, refrigerator and water heaters, the power demand for each customer is thought to be large these first few hours of the weekend.

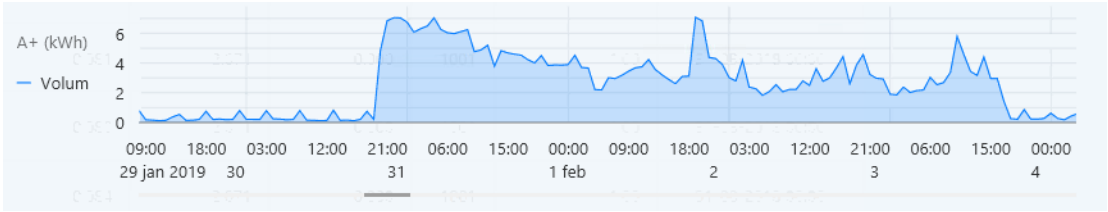

Figure 6.1: Consumption profile for a consumer in the cottage area.

Figure 6.1 show the consumption profile for one of the consumers in the area that clearly illustrate the usage pattern. It is evident that the residents has arrived somewhere between 19:00 and 20:00, as the consumption is rapidly increasing at this time. Observing the magnitude of the load, it is as a trend slowly decreasing during the initial night and the next day. Compared to the other nights, the first night has a drastically higher consumption. This is probably caused by the heating demand, which is not as large after the cottage has been heated initially. Thus, the electric heaters does not require the large amount of power. This also causes the load profile to resemble a more standard household profile after the first 24 hours, as one can discern one peak in the morning and one peak during the evening.

Following this consumption pattern, an attempt has been made to create a load profile to use at the transformer node load. Every consumer will, however, have some kind of difference to its usage pattern. Since every transformer station has a lot of customers connected to it, the aggregated load profile probably will have "smoother" transitions and a bit more spread in the consumption. It is assumed that most of the consumers experience the initial high demand period. Thus, a general focus has been on this period when developing the load profile.

Figure 6.2 show the developed load profile for Friday and Saturday. It is evident that it resembles the one shown in fig. 6.1, but some considerations has been made. During Friday night, morning and day there is not much happening, with a low base consumption caused by

e.g. water pumps and lighting. By the evening, at around 17.00, the consumption is starting to increase rapidly, and keeps increasing until reaching its peak at approximately 21.00. From this point the consumption is slowly decreasing during the late evening and night, with the demand decreasing under 0.9 p.u. around 04.30. From this point the consumption continue to decrease until about 06.00 where an increase to another peak is occurring. This is resulting in a very high demand situation for a prolonged period of time, where the demand is above 0.9 p.u. for a period of about 8 hours while the demand is above 0.8 p.u. for 9.5 hours. After the initial high demand period there occur a few peaks, where the mid day peak and evening peaks induce demand of 0.85 and 0.9 p.u. respectively.

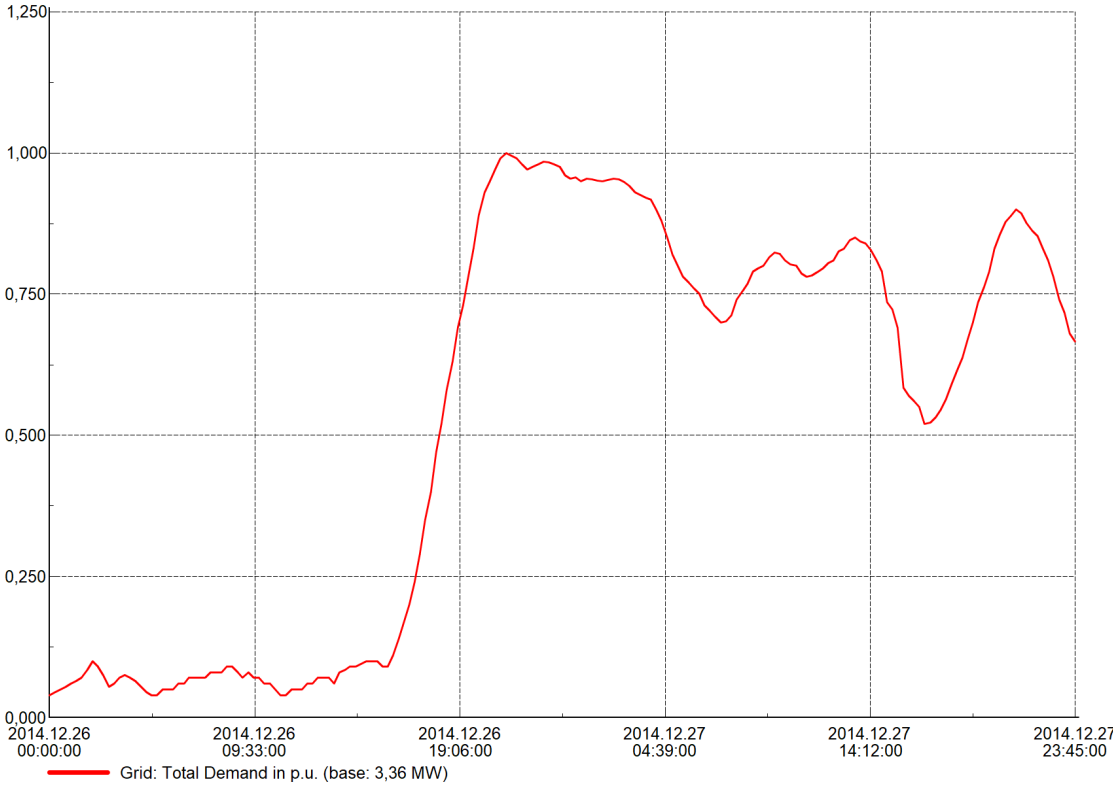

Figure 6.2: Load profile developed for use in simulations.

6.2.4 Voltage dependency

During the preliminary project [2] an evaluation of the voltage dependency for the loads was conducted. The voltage dependency is modeled by the so-called ZIP model, which is given by eq. (6.2). The parameter a_1 represent the share of the load being modeled as a constant impedance, a_2 represent the share of constant current demand, and a_3 represent the share of the load being modeled as a constant power load. [2] [27]

$$P = P_0 \left(a_1 \left(\frac{V}{V_0} \right)^2 + a_2 \left(\frac{V}{V_0} \right) + a_3 \right) \tag{6.2}$$

In short it was in [2] assumed that a large share of the demand is due to heating equipment, which without a thermostat operate with a constant impedance characteristic. Further, a

fair share of switching power electronics, in addition to the thermostatically operated heating, causes the constant power characteristic parameter to be significant. Rotating machinery, operating with the constant current characteristic, is assumed to have a limited effect on the power variation. As a result, values for the parameters of eq. (6.2) are selected as shown in table 6.1.

Table 6.1: Selected values for the parameters of voltage dependency.

Parameter	Value
a_1	0.5
a_2	0.15
a_3	0.35

6.3 Battery control system

The objective of installing a battery in the cottage area is to decrease the line loading of the supply line bottlenecks, as the lines may prove to be exposed to overloading. A peak shaving control algorithm is therefore implemented for the battery operation. In general, active power discharge is desired when the lines and cables are heavily loaded, while charging should occur when the demand is otherwise low. The battery control algorithm is gathered from the PowerFactory User Manual [28], which is initially made for a power system with a load, an external grid, a battery and a solar generation unit. Therefore the algorithm has implemented an approach to charge the battery when there is surplus power from the production. As the analyzed power system does not have solar generation, or any other form of local production, the battery as a result is unable to charge when this approach is used. Because of this significant changes has been done to the control algorithm in order to get the battery to operate as desired.

Further in this section the changes done to the battery control system from the user manual is described. For an in-depth explanation of how the control system operates, the reader is directed to [2, ch. 4.3] or [28]. The complete updated battery control algorithm can be found in appendix D.

6.3.1 Power operation mode

Equation (6.3) shows the starting point of the control system, which is measuring the power in the bottleneck line section 2 named $P_{measured}$. Since there is no local production in the system, the equation is simplified to eq. (6.4). It is seen that the measured power must be equal to the load, meaning all load demand and losses in the system. When the battery is connected the actual power flow in the line, P_{line}, may be different from $P_{measured}$ since the battery can request to be charged or discharged. When the battery is discharging $P_{battery}$ is positive, meaning that the the power in the line is reduced compared to a case without the battery. When the battery charges, however, $P_{battery}$ is negative. This increases the load demand and thus the power in the line.

$$P_{PV} + P_{load} = P_{line} - P_{battery} = P_{measured} \tag{6.3}$$

$$P_{load} = P_{line} - P_{battery} = P_{measured} \tag{6.4}$$

Unlike the case where local production is present $P_{measured}$ cannot be negative since P_{load} always will be larger than or equal to zero. The original control system utilized the change of polarity of $P_{measured}$, where the battery would discharge at negative values and charge at positive values. With $P_{measured}$ staying either just positive or just negative, according to the polarity, the battery could not be controlled to both charge and discharge throughout the period. To fix this, a change to the logic of the control system algorithm was made.

First, changes to the power operation mode, $ChargeP$, strategy was made. The new logic is shown in eq. (6.5) while table 6.2 indicates the behaviour of the three modes. Table D.1 describes the state variables and parameters of the control system.

$$\begin{aligned} 0 < P_{measured} < P_{StartStore} &\Longrightarrow ChargeP = 1 \\ P_{StartStore} < P_{measured} < P_{StartFeed} &\Longrightarrow ChargeP = 2 \\ P_{measured} > P_{StartFeed} &\Longrightarrow ChargeP = 3 \end{aligned} \tag{6.5}$$

Table 6.2: Power operation modes [2].

Statement	Battery operation mode
chargeP=1	Charging
chargeP=2	Inactive
chargeP=3	Discharging

As can be seen from eq. (6.5) the power operation mode structure now, given that $P_{StartStore}$ and $P_{StartFeed}$ are positive, enables both charge and discharge without a change of polarity by $P_{measured}$. When $P_{measured}$ is below $P_{StartStore}$ the system load demand is regarded as low, meaning that it is safe to increase the power in the bottleneck by charging the battery. Thus, $ChargeP$ is set to one and the battery is in charge mode. When $P_{measured}$ increase above $P_{StartFeed}$ the system load demand is high, meaning that it is desired to decrease the bottleneck power flow by discharging the battery. In this situation $ChargeP$ is set to three and the battery is ready to be discharged. For all values of $P_{measured}$ between $P_{StartStore}$ and $P_{StartFeed}$ the battery is set to be inactive. The principle of this power operation strategy is depicted in fig. 6.3.

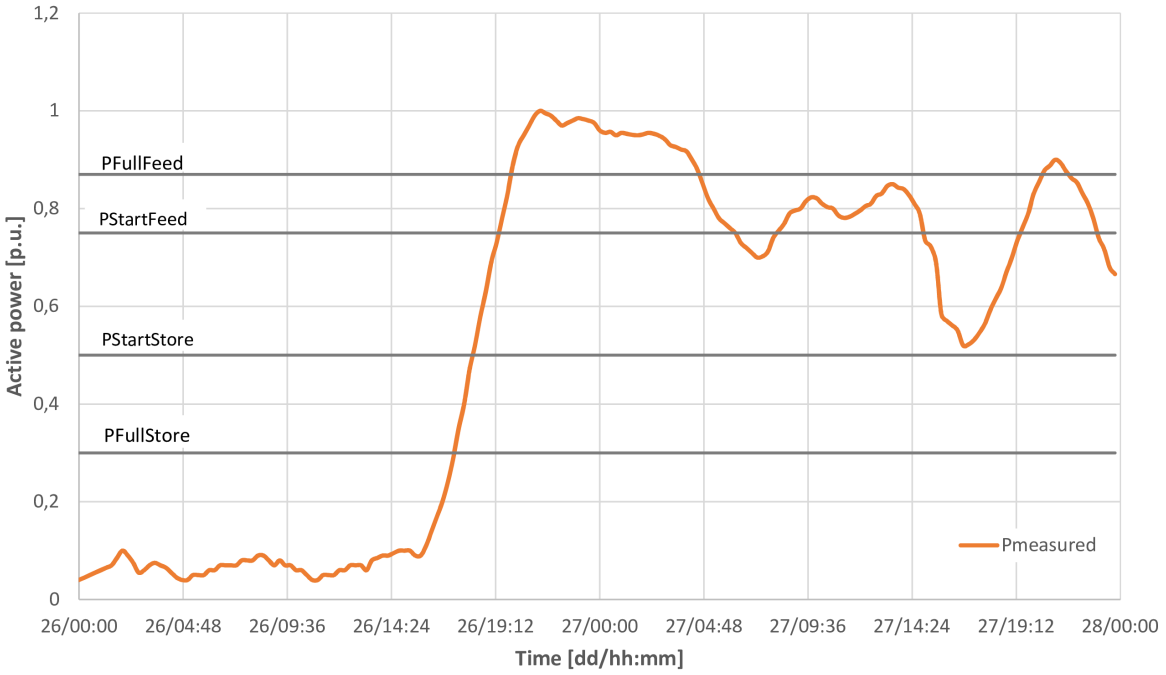

Figure 6.3: Principle of power operation for battery. Charge below PStartStore, discharge above PStartFeed.

6.3.2 Magnitude of active power

Two requirements for the strategy described in the previous paragraph to work are shown in eq. (6.6). This differs from the original control system gathered from the user manual [28]. Here, $P_{StartFeed}$ must have a lower value than $P_{FullFeed}$, while $P_{StartStore}$ must have a larger value than $P_{FullStore}$. This is done to enable a reasonable control of the amount of power to be fed or stored.

$$\begin{aligned} 0 < P_{FullStore} < P_{StartStore} \\ P_{StartFeed} < P_{FullFeed} \end{aligned} \tag{6.6}$$

For storing the battery will, as mentioned, begin charging when $P_{measured}$ drops below $P_{StartStore}$, and it will charge at nominal power when $P_{measured}$ is smaller than $P_{FullStore}$. Between $P_{FullStore}$ and $P_{StartStore}$ the charging power is reduced gradually when $P_{measured}$ is increasing according to eq. (6.7), meaning that when the system load demand is lower the battery will request more charging power.

$$P_{battery,charge} = -P_{store} \cdot \left(1 - \frac{P_{FullStore} - P_{measured}}{P_{FullStore} - P_{StartStore}}\right) \tag{6.7}$$

Discharge of the battery starts when $P_{measured}$ becomes larger than $P_{StartFeed}$, and it will discharge at rated power when $P_{measured}$ is larger than $P_{FullFeed}$. Between the thresholds for start and nominal discharge, the discharge power increases as $P_{measured}$ increases. This happens according to eq. (6.8), allowing the discharge to increase gradually as the system load demand increases.

$$P_{battery,discharge} = P_{feed} \cdot \left(1 - \frac{P_{FullFeed} - P_{measured}}{P_{FullFeed} - P_{StartFeed}}\right) \tag{6.8}$$

6.3.3 Control of reactive power

The reactive behaviour of the battery inverter is controlled in basically the same way as the active power described in section 6.3.2. It does not have its own control scheme, meaning that it uses the same power and energy operation modes, $ChargeP$ and $ChargeE$, as the active power. It also make use of the same thresholds as the active power, being $P_{StartFeed}$, $P_{FullFeed}$, $P_{StartStore}$ and $P_{FullStore}$. This means that the inverter will supply reactive power whenever the battery supply active power, and that it will draw reactive power while the battery is charging. A so-called *constant cos* ϕ control is thus implemented, following eq. (6.9). Following the same pattern as active power eqs. (6.10) and (6.11) determine the storage and feeding reactive power.

$$cos\phi = \frac{P}{\sqrt{P^2 + Q^2}} = Constant \tag{6.9}$$

$$Q_{battery,discharge} = Q_{feed} \cdot \left(1 - \frac{P_{FullFeed} - P_{measured}}{P_{FullFeed} - P_{StartFeed}}\right) \tag{6.10}$$

$$Q_{battery,charge} = -Q_{store} \cdot \left(1 - \frac{P_{FullStore} - P_{measured}}{P_{FullStore} - P_{StartStore}}\right) \tag{6.11}$$

6.4 Modeling of grid upgrade alternatives

In this section, modeling of the alternatives of sections 4.2 and 4.3 will be presented. For each alternative the change in the PowerFactory model is visualized by showing a part of the model. The complete grid model is shown in fig. A.1.

6.4.1 Alternative 2: Refurbish existing line

As mentioned in section 4.2 the existing supply line sections 1 to 6 for this alternative has to be demolished, exchanging them with a new high capacity cable. A segment of the PowerFactory model is shown in fig. 6.4, where the old supply cables and overhead lines are disconnected and replaced with new cable sections. Note that also the battery module is disconnected in this alternative.

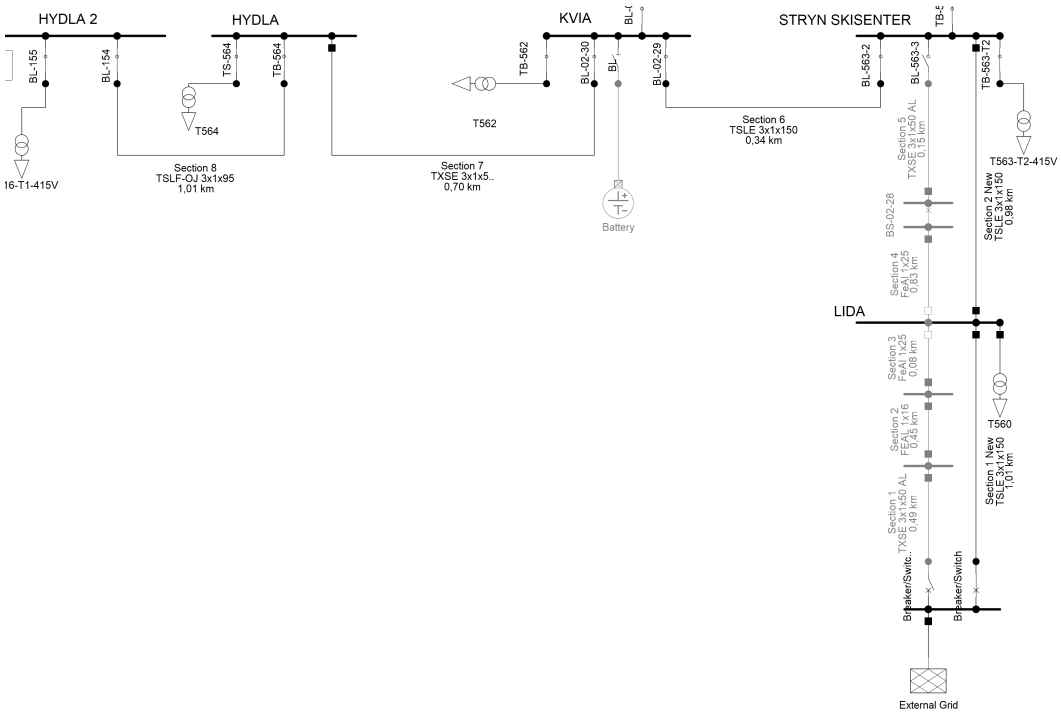

Figure 6.4: Part of the PowerFactory grid model for alternative 2.

Before refurbishment, line sections 1, 2 and 3 was a mix of cable and overhead lines. As shown in the model these are replaced with a single cable connection between the external grid and the transformer station “Lida”, which constitute to what is called “Section 1 New”. The length of this section is approximately 1 km. Figure 6.4 show that a TSLE 3x1x150 cable is installed. This will be referred to as alternative 2.1, while alternative 2.2 will utilize TSLE 3x1x240 cables instead.

For sections 4 and 5 the situation is mostly the same as for section 1 to 3, as section 4 is an overhead line and section 5 is a cable. Thus, a single cable has been connected between the transformers “Lida” and “Stryn Skisenter” which is called “Section 2 New”. Similarly to “Section 1 New” this section is about 1 km, and will be named alternative 2.1 or 2.2 depending on the chosen cable. Section 6 is about 340 meters long, and has kept its original name even though it is upgraded.

6.4.2 Alternative 3: Add new connection

When adding a new connection from an external grid to “Hydla 2” a 4.5 km cable has to be built, while all existing sections initially are unchanged. Figure 6.5 show a part of the PowerFactory model after adding the new connection path. The figure specifies a cable of 150 mm^2 cross section, which will be used for alternative 3.1. Additionally, alternative 3.2 will utilize a 240 mm^2 cable.

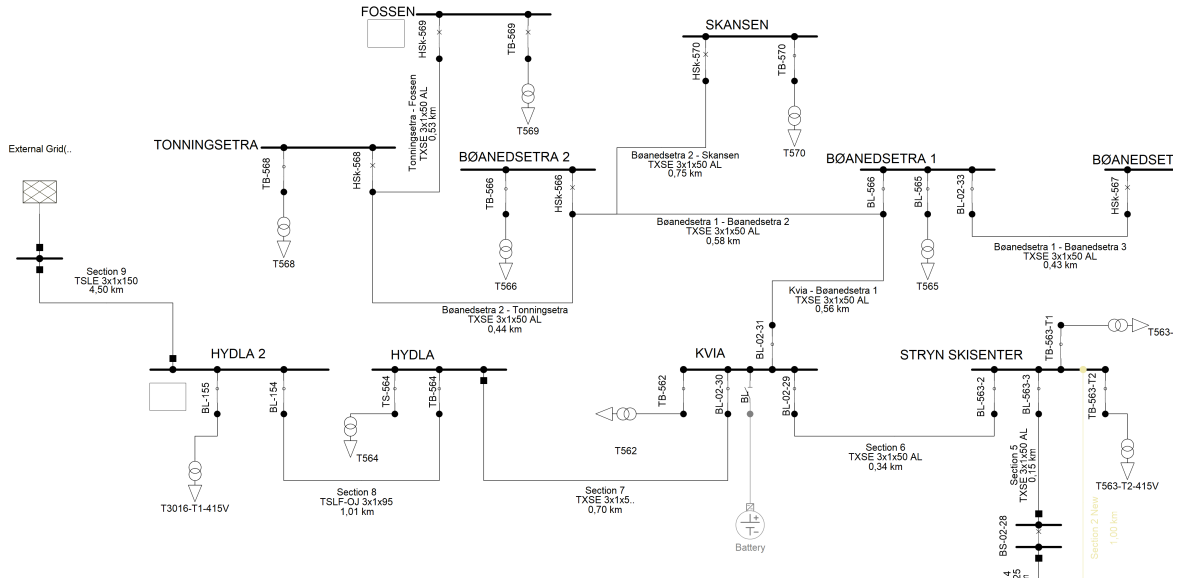

Figure 6.5: Part of the PowerFactory grid model for alternative 3.

Chapter 7

Results and discussion of technical analysis

In this chapter several simulation load scenarios are presented and their results will be displayed and analyzed. For each load scenario all alternatives presented in chapter 4 will be investigated. The chapter is divided into cases which each represent a combination of a load scenario and an alternative. Sections 7.1 and 7.2 deals with the two different load scenarios, where the first depict a forthcoming expansion of the cottage area and the second depict a large expansion that pushes the limit of the governed maximum number of cottages for the area. To provide results in the time domain quasi-dynamic simulations are run for a period of two days, Friday and Saturday, for all cases. The quasi-dynamic simulation runs a load flow analysis with a given time step throughout the simulation period. In this project the time step is chosen to be 15 minutes, which enables analysis of e.g. the time dependent battery behaviour without requiring a demanding dynamic simulation. In the analysis line sections 1 to 9 of fig. A.1 are investigated. This is because none of the line sections "above" the node "Kvia" are affected by the supply method, and the sections in that area therefore does not change any characteristics between the different alternatives. Table 7.1 give an overview of the load scenarios and cases that has been analyzed. Each case is assigned to a load scenario and a solution alternative, where the first number indicates the load scenario and the following numbers indicate the alternative[1]. The table also serve as a reminder on the basics of an alternative, and additionally gives the location where each case is presented in this chapter.

Table 7.1: Scenarios, cases and alternatives overview.

Scenario	Alternative	Content	Location
Load scenario 1		Planned expansion. Relatively low demand	Section 7.1
Case 1.1	Alternative 1	No grid upgrade	Section 7.1.1
Case 1.2.1	Alternative 2.1	Refurbishment 150 mm^2	Section 7.1.2
Case 1.2.2	Alternative 2.2	Refurbishment 240 mm^2	Section 7.1.2
Case 1.3.1	Alternative 3.1	Add connection 150 mm^2	Section 7.1.3
Case 1.3.2	Alternative 3.2	Add connection 240 mm^2	Section 7.1.3
Case 1.4	Alternative 4	Install battery	Section 7.1.4
Load scenario 2		Critical loading	Section 7.2
Case 2.1	Alternative 1	No grid upgrade	Section 7.2.1
Case 2.2.1	Alternative 2.1	Refurbishment 150 mm^2	Section 7.2.2
Case 2.2.2	Alternative 2.2	Refurbishment 240 mm^2	Section 7.2.2
Case 2.3.1	Alternative 3.1	Add connection 150 mm^2	Section 7.2.3
Case 2.3.2	Alternative 3.2	Add connection 240 mm^2	Section 7.2.3
Case 2.4	Alternative 2.4	Install battery	Section 7.2.4

[1]E.g. Case 1.2.1 equals load scenario 1 alternative 2.1.

7.1 Load scenario 1

The first load scenario reflects case 3 of [2]. This deals with a planned expansion of the existing cottage area, such that the total number of customers becomes about 500. Each customer have a peak load demand corresponding to the one discussed in section 6.2.1, and follows the load profile presented in section 6.2.3. This expansion represent specific construction plans to include 139 new cottages, in addition to 38 older ones that is being connected to the grid. For simplicity, however, the entire demand increase is added to the node "Hydla 2" where the construction of the new cottages will take place. The peak load for each node in this situation is shown in table C.1. [2]

7.1.1 Case 1.1: No grid upgrade

This case describe the power system behaviour when no action is done, meaning that no existing components are removed or new ones added. It therefore represents the existing grid situation, and the viability of this alternative after the planned expansion will therefore be inspected. The results are shown in figs. 7.1 to 7.3. Figure 7.1 show the active and reactive power in line section 2 which is the line with the lowest capacity. As all load nodes are assumed to follow the same load profile, the active power is resembling the load curve shown in fig. 6.2. This results in low active power during the first 15 hours, before the demand increases steeply. The maximum active power in the line occurs at 21:15 Friday evening, and amounts to a total of 3.34 MW. From this point onward the active power slowly decreases during the night until two peaks occur during the next morning and midday at 2.75 and 2.84 MW respectively. After experiencing a dip in the demand another peak occurs during Saturday evening, this one at 3 MW.

The reactive power in line section 2 appear to follow mostly the same curvature as the active power. During the initial low demand period it is observed that the reactive power is negative. This indicates that reactive power is carried out of the cottage area, into the external grid, a phenomenon that is discussed further in section 7.3. When the load demand increases, the reactive power fed from the external grid through section 2 also increases. This is a result of the inductive power factor of 0.95 for each load node, which indicates that the supplied reactive power to the loads increase as the active power demand increases. At peak demand, the reactive power fed from the external grid through section 2 is 0.981 MVAr.

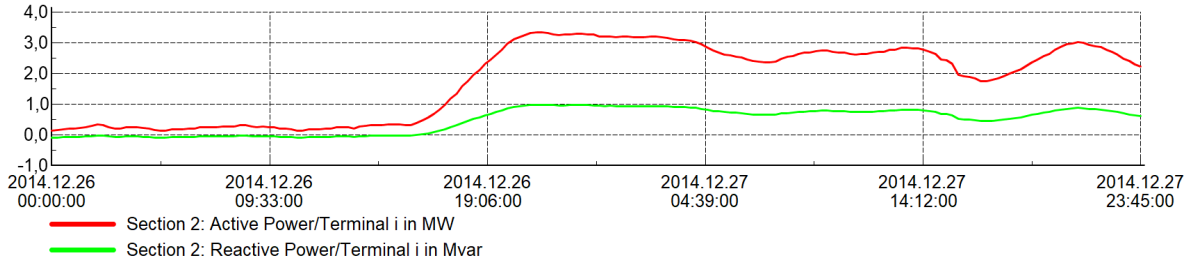

Figure 7.1: Scenario 1 Alt. 1: Active and reactive power in section 2.

Figure 7.2 show the loading of sections 1 to 8 for this alternative. By observing the figure it is evident that section 2 is the one that carries the highest share of current related to its

thermal capacity, meaning that this section got the lowest current capacity and thus is the highest loaded. The section is loaded 53.6% at the peak demand, while also sections 1, 5 and 6 are loaded nearly at 50%. Figure 7.3 show the power losses in each of the sections. As a result of the 0.83 km length of section 4 this line has the largest individual loss despite having a higher capacity, and thus lower loading, than line sections 1, 2, 5 and 6. At peak demand the power losses in section 4 is 15 kW. The second largest individual loss is observed to be in section 2, at 0.45 km, which induce a loss of 12.7 kW. In total the power losses in sections 1 to 8 amount to 48.9 kW.

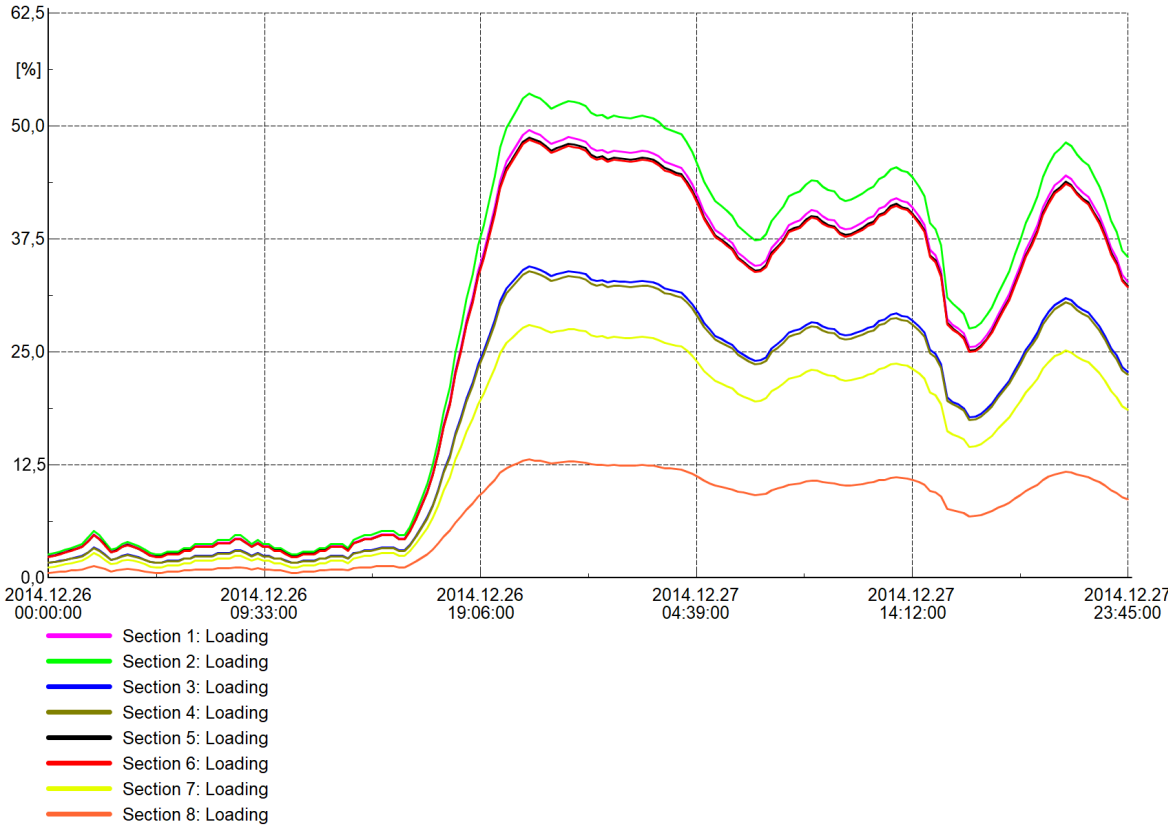

Figure 7.2: Scenario 1 Alt. 1: Loading of sections 1 to 8.

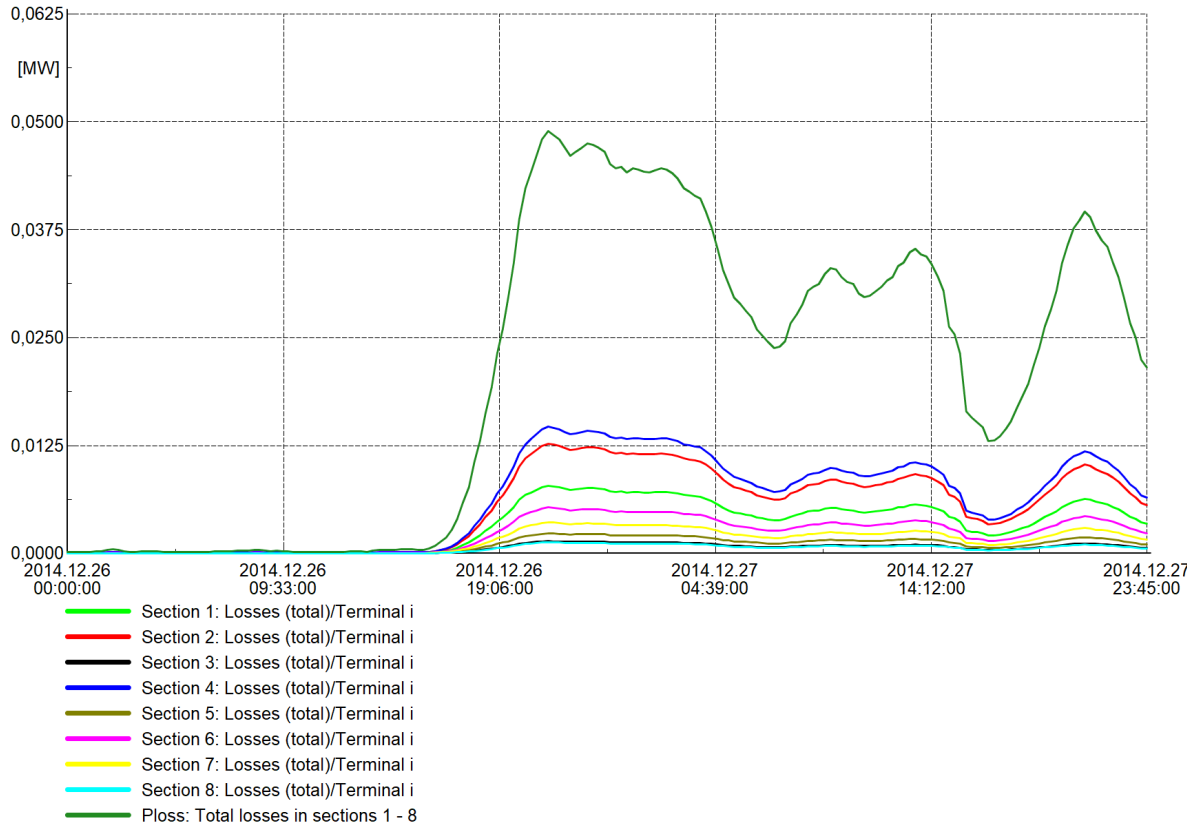

Figure 7.3: Scenario 1 Alt. 1: Power losses in sections 1 to 8.

7.1.2 Case 1.2: Refurbish existing connection

In this section the power system is analyzed after an reinforcement has been conducted as described in section 4.2. The PowerFactory modeling for this alternative has been presented in section 6.4.1. The simulation has been run with two different cable cross-sections, 150 mm^2 and 240 mm^2, to analyze the effect of changing the cable capacity. First the results for alternative 2.1, which utilize 150 mm^2 cables, are presented. Then the results when 240 mm^2 are used, i.e. alternative 2.2, are shown. As described in section 6.4.1 the initial cable coming into the area from the external grid now is called “Section 1 New”. Therefore the active and reactive power is referred to this section.

Case 1.2.1: 150 mm^2

Similarly to the first case, the load demand is in this case met by supplying power from the external grid through the supply grid. As there still is one source, the active and reactive power in “Section 1 New” shown in fig. 7.4 is relatively similar to what was observed in case 1.1. The active power still follows the demand determined by the load profile closely, but minor differences compared to case 1.1 can be observed. The active power is now 3.352 MW at peak demand, while the reactive power amount to 0.904 MVAr. This reactive power is significantly lower than what was found in section 7.1.1, and is caused by the the characteristics of the cables, which behaves as a reactive source. This is discussed further in section 7.3 and causes the necessary imported reactive power from the external grid to decrease.

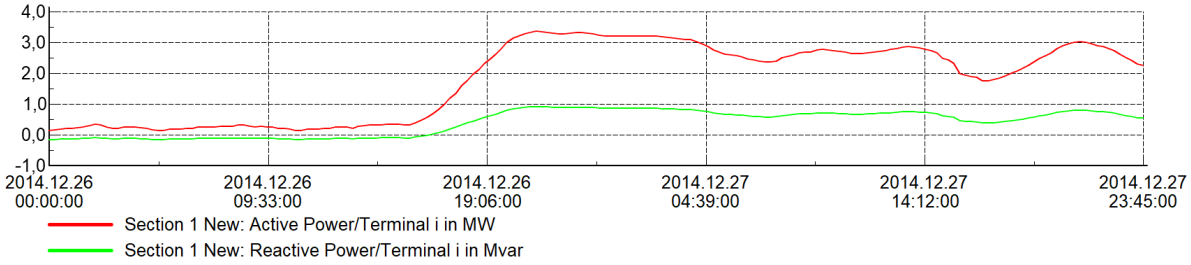

Figure 7.4: Scenario 1 Alt. 2.1: Active and reactive power in "Section 1 New".

Figure 7.5 show the loading of the two new cable sections, and sections 6 to 8, when 150 mm^2 cables are built. This cable has a thermal rating of 355 A which is significantly higher than the overhead lines and cables that were used in the first alternative, as can be seen in tables A.1 and A.2. As a result, all cables in "Section 1 New", "Section 2 New" and section 6 are loaded fairly equally at about 25% during the peak demand. Section 7 has not been refurbished, thus still consist of a 50 mm^2 cable, and therefore got a loading of around 28% despite the reduced power flow in this section. The losses in each section is presented in fig. 7.6, where it is evident that the losses has been reduced significantly compared to case 1.1. The total power losses in the sections from the external grid to "Hydla 2" now are 16.6 kW at peak loading, a reduction of 32.2 kW. Sections "1 New" and "2 New" now are the ones who incur the largest losses, at 5.2 kW and 4.9 kW respectively.

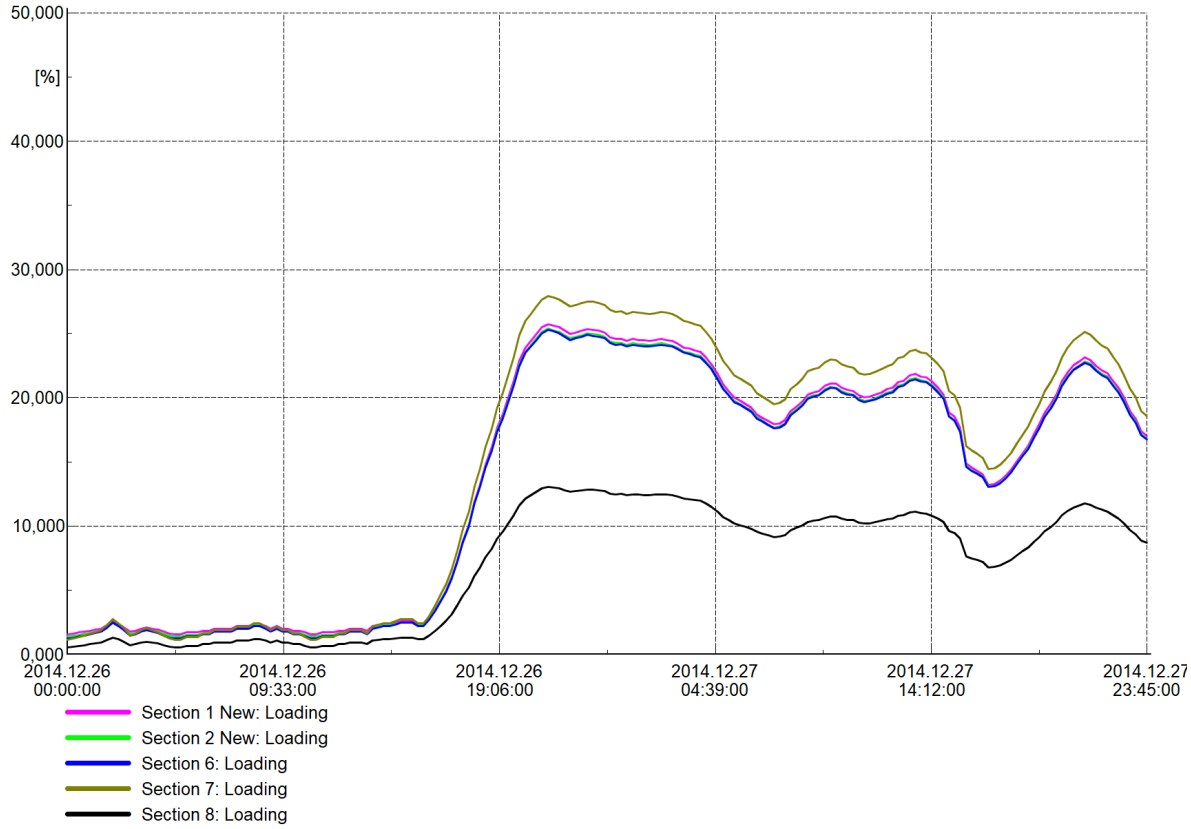

Figure 7.5: Scenario 1 Alt. 2.1: Loading of sections 1-8

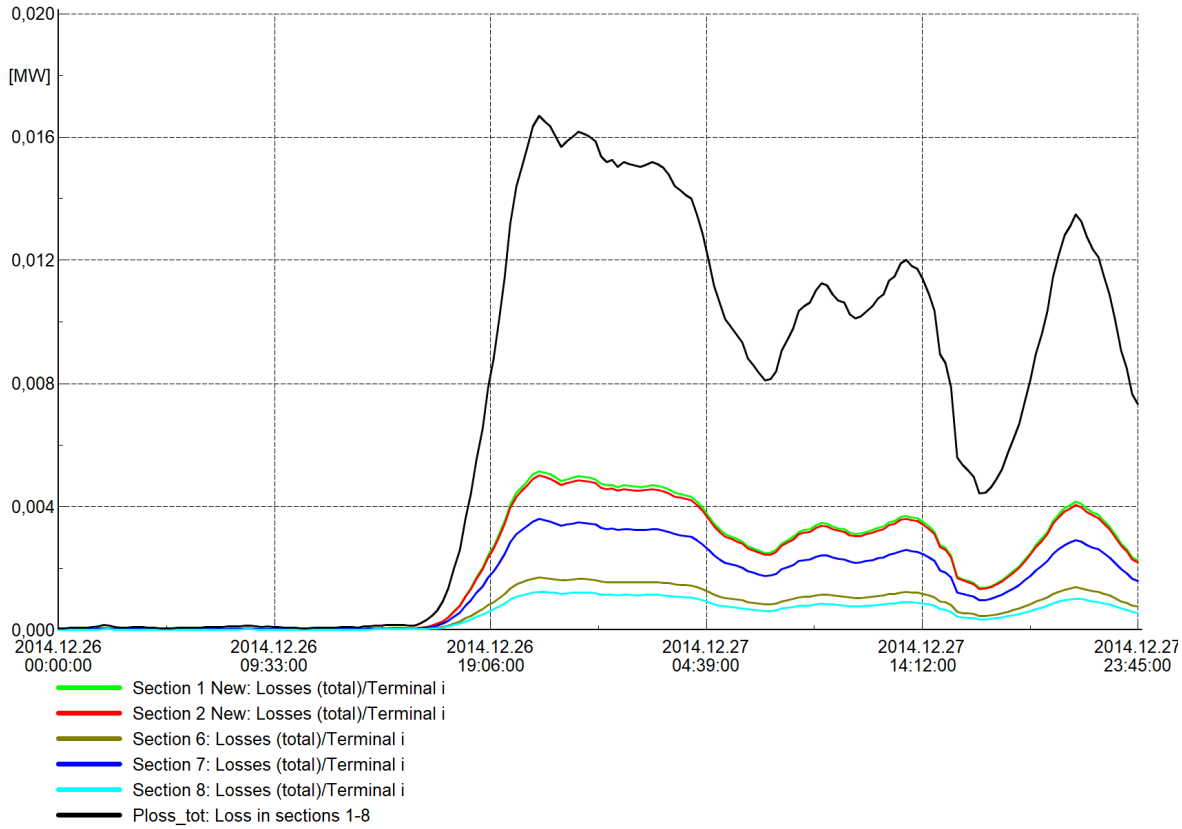

Figure 7.6: Scenario 1 Alt. 2.1: Power losses in sections 1 to 8.

As a result of lower resistance in the new supply connection in this alternative, the losses in the system has decreased compared to case 1.1. The external grid has to supply the load and losses in the system at all time points. Since the load is kept equal, it is reasonable to believe that the active power supplied by the external grid would decrease given that the losses are reduced. It has, however, been observed that the active power going into the grid in fact has increased from 3.348 MW to 3.352 MW after upgrading the cables. This is of course a minor increase but since the loss reduction is significant, the power should have decreased similarly. The reason for this phenomenon to occur is related to the voltage dependency of the loads, which is introduced in section 6.2.4. To examine the behaviour the node "Hydla 2" is looked into. Figures 7.7 and 7.8 show the voltages for cases 1.1 and 1.2.1. From these figures it is observed that the voltage at the investigated node is 0.984 p.u. at peak demand in the first alternative, while the voltage is 0.993 p.u. in the second alternative. Equation (6.2) show the ZIP model which determines how the active power load demand varies with varying voltage. The parameters used in the ZIP model are presented in table 6.1. An a_1 of 0.5 indicates that 50% of the rated power demand is modeled as a constant impedance, meaning that it varies with the square of the voltage change. 15% is modeled as a constant current load, meaning that it changes linearly with the voltage change. The remaining 35% is modeled as constant power, meaning that it is voltage independent. By using these parameters in eq. (6.2), inserting the rated power peak power demand of 1.3 MW at "Hydla 2" and the per unit voltage, the power demand in each of the cases are found. In case 1.1, where the grid connection is not upgraded, the real peak power demand is found to be 1.276 MW at the node. For case 1.2.1, where lower losses causes the voltage to be nearer 1 p.u., the actual peak power is found to be 1.290 MW.

The difference is not huge, but it explains why the active power coming into the area is larger when alternative 2 is deployed than when alternative 1 is used.

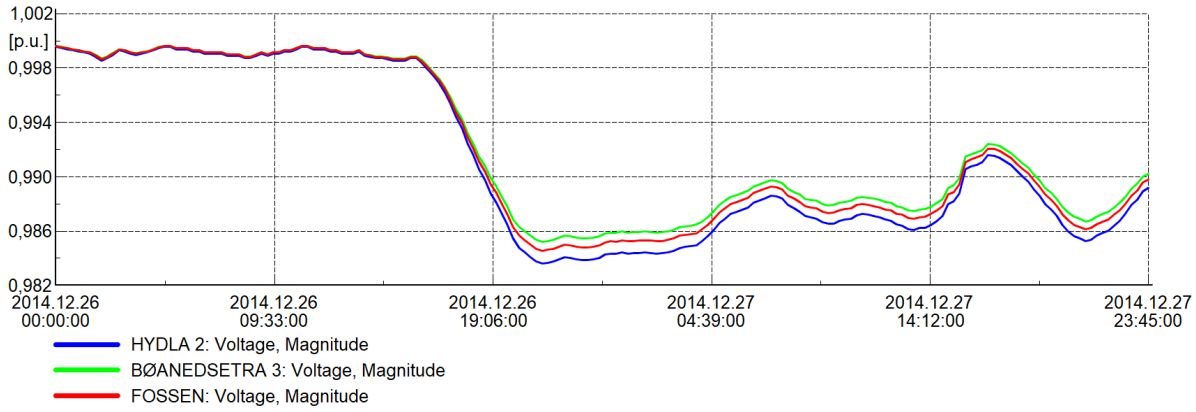

Figure 7.7: Scenario 1 Alt. 1: Voltage.

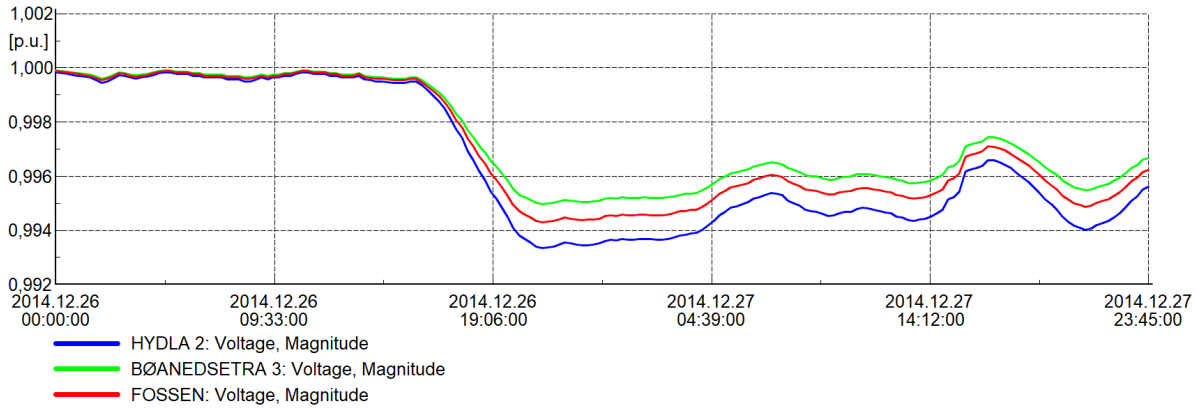

Figure 7.8: Scenario 1 Alt. 2.1: Voltage.

Case 1.2.2: 240 mm^2

The effect of upgrading the cables to 240 mm^2 will now be investigated, thus the focus are put on comparing the results with case 1.2.1. Figures 7.9 to 7.11 show the results when running the simulation with 240 mm^2 cables at sections “1 New,” “2 New,” and 6. Similarly to case 1.2.1, the active power coming into the area is 3.352 MW at the peak demand. The reactive power, however, is lowered further in this case. At peak demand it is now 0.885 MVAr, a reduction from 0.904 MVAr. This indicates that the reactive power production of the cables has increased. As can be observed in fig. 7.10, the loading of section 7 still is the largest with 28%. This is to be expected since no change has been done to this section. The loading of the upgraded sections are now between 19 and 20%, a reduction of 5 percentage points compared to case 1.2.1. As expected also the losses has been reduced with the total loss now being 11.97 kW, a reduction of 28% compared to the earlier case. Inspecting the individual sections of fig. 7.11 it is found that section 7 now is the one inducing the largest power loss with 3.60 kW at peak load. The losses of sections ”1 and 2 New” now are 3.15 kW and 2.97 kW respectively.

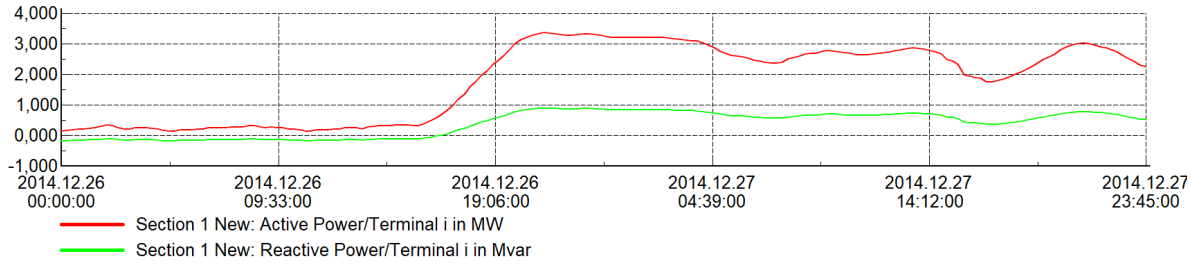

Figure 7.9: Scenario 1 Alt. 2.2: Active and reactive power in "Section 1 New".

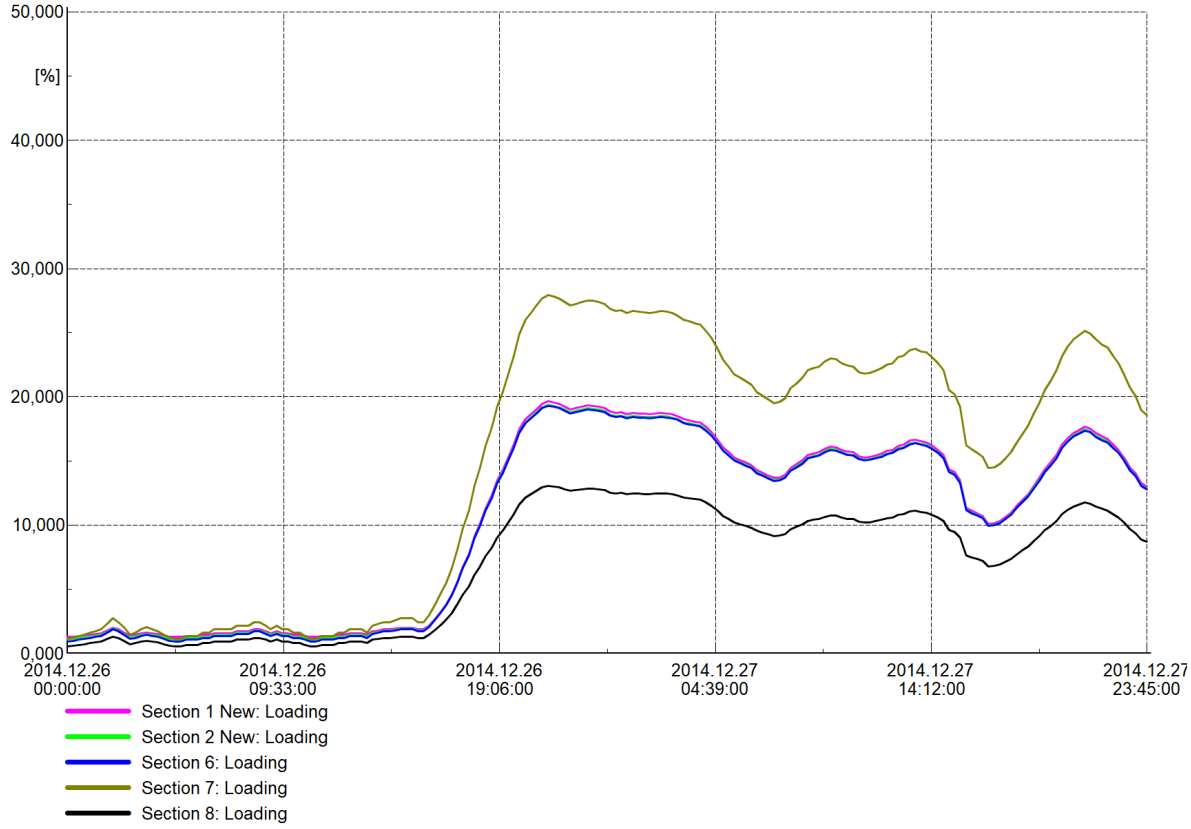

Figure 7.10: Scenario 1 Alt. 2.2: Loading of sections 1 to 8.

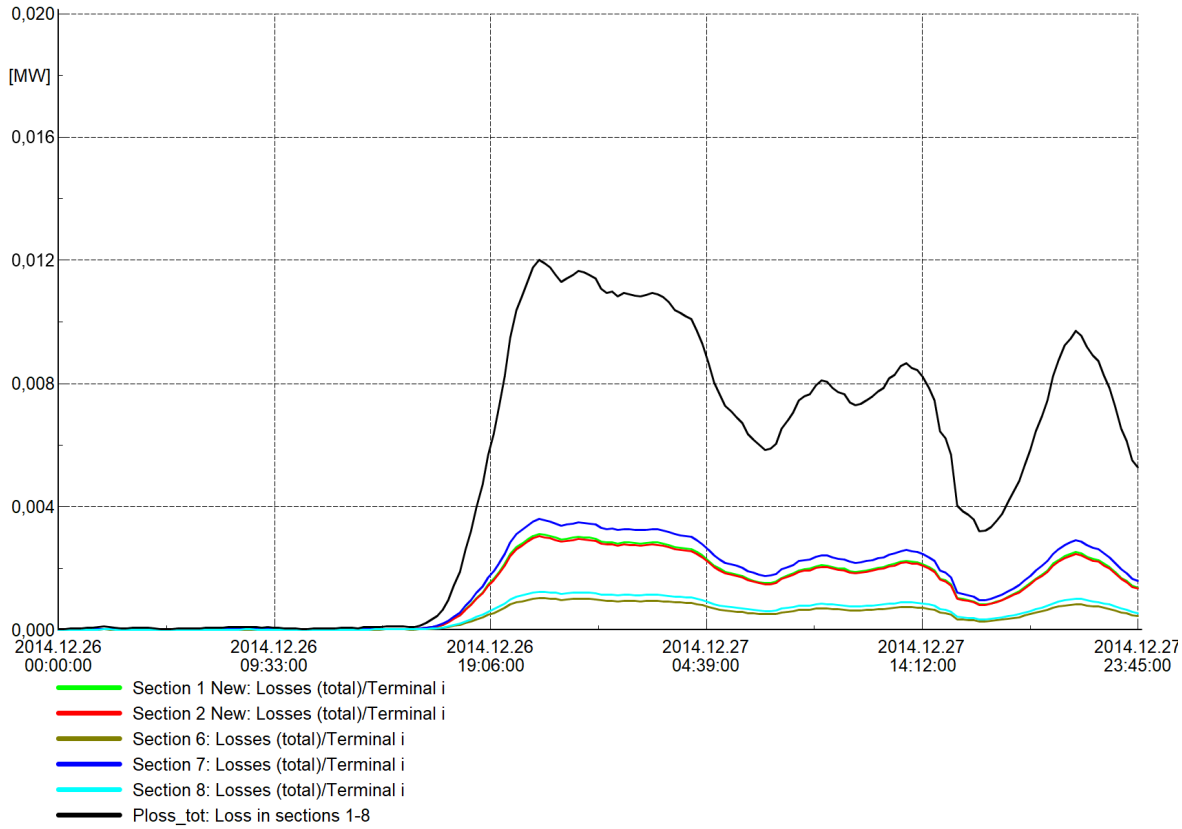

Figure 7.11: Scenario 1 Alt. 2.2: Power losses in sections 1 to 8.

7.1.3 Case 1.3: Add new connection

In this section the power system is analyzed after deploying alternative 3, meaning that an additional cable has been connected to the node "Hydla 2", as described in section 4.3. The PowerFactory modeling for this alternative has been presented in section 6.4.2. The simulation has been run with two different cable cross-sections, 150 mm^2 and 240 mm^2, to analyze the effect of changing the capacity. Figures 7.12 to 7.15 show the results when utilizing 150 mm^2 cables, while figs. 7.16 to 7.19 present the results when 240 mm^2 are used. The power coming into the grid can now be fed from two different connections. Therefore, the power will be measured at line sections 2 and 9.

Case 1.3.1: 150 mm^2

First, the results when using a TSLE 3x1x150 cable are investigated. Figure 7.12 show the active power in sections 2 and 9. As both the external grids are set to operate as a slack bus, the total power coming into the grid should cover the load demand plus losses in the system. As a result, section 9 is providing 2 MW of active power, while section 2 provides 1.35 MW at peak demand. The reactive power is shown in fig. 7.13 and indicates that in this case, also, reactive power is carried out of the area and into the external grid during the low demand period. Further discussion of this will be presented in section 7.3. At the maximum load situation section 9 is providing a total of 0.56 MVAr, while section 2 provides 0.26 MVar. Despite the fact that section 9 provides both the most active and reactive power, the section

is loaded at 15.7% while section 2 is loaded at 21.1%. Also sections 1, 5 and 6 are loaded more heavily than the new connection, indicating that the new cable has a beneficial current carrying capacity. When looking at the power losses of fig. 7.15 it is clear that section 9 incur the largest losses. For a cable of 4.5 km, however, the losses seem quite small at 8.4 kW at peak loading. Losses in the rest of the sections are in the magnitude of 2 kW and below, making the total loss 15.5 kW.

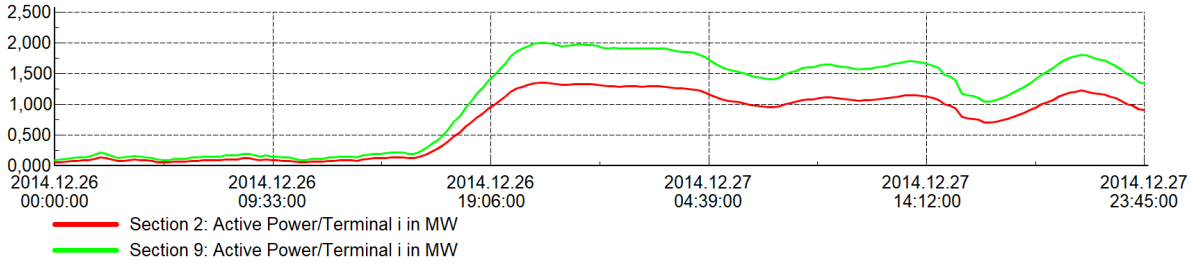

Figure 7.12: Scenario 1 Alt. 3.1: Active power in sections 2 and 9.

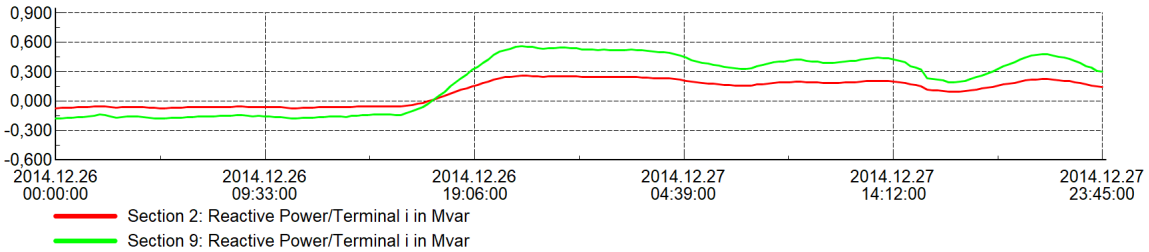

Figure 7.13: Scenario 1 Alt. 3.1: Reactive power in sections 2 and 9.

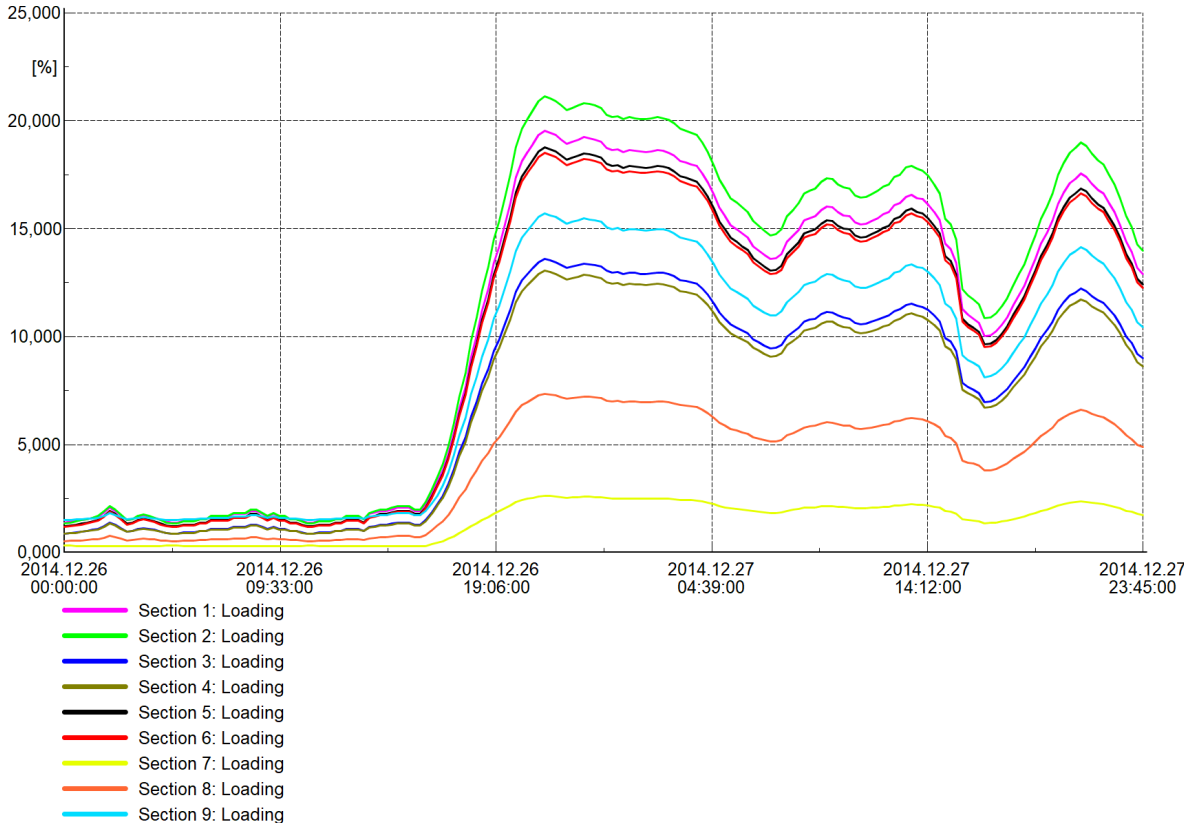

Figure 7.14: Scenario 1 Alt. 3.1: Loading of sections 1 to 9.

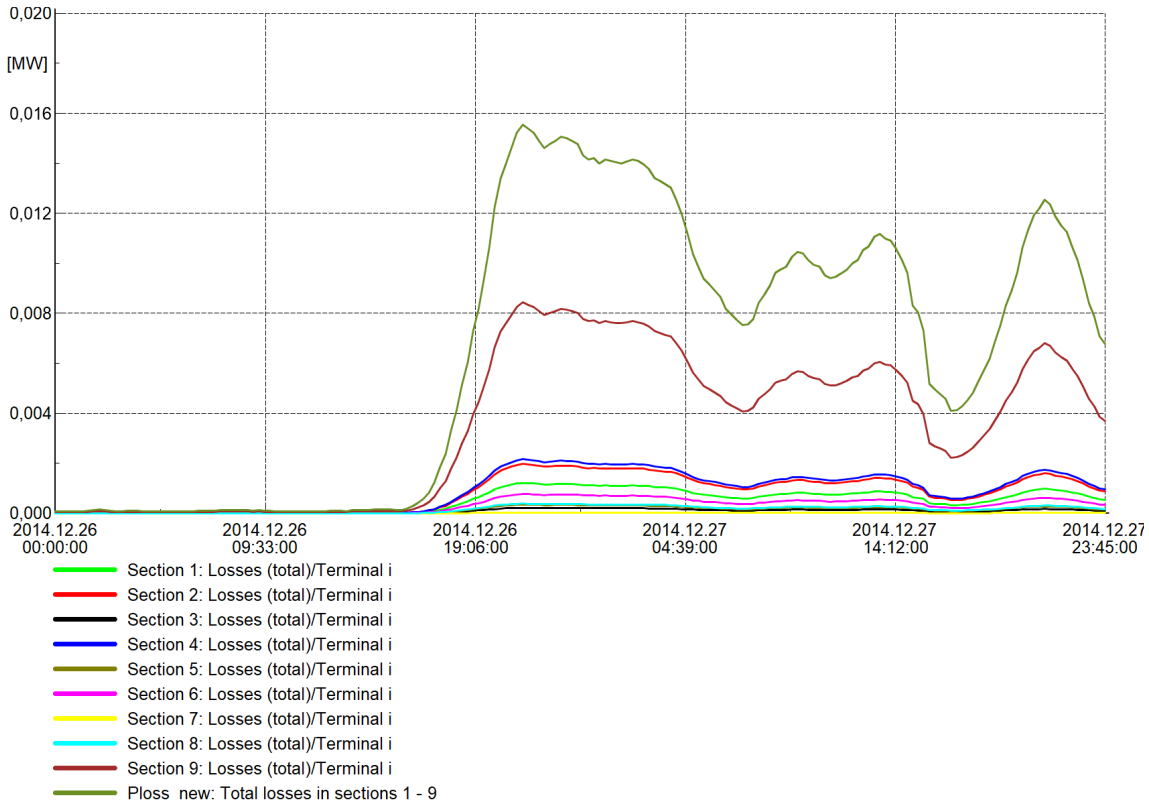

Figure 7.15: Scenario 1 Alt. 3.1: Power losses in sections 1 to 9.

Case 1.3.2: 240 mm^2

The effect of upgrading the cables to 240 mm^2, alternative 3.2, will now be investigated, thus the focus are put on comparing the results with case 1.3.1. Figure 7.16 show the active power of sections 2 and 9 when a cable with cross section 240 mm^2 has been constructed. The overall profile looks similar to the previous case, but the increased capacity of cable section 9 now causes it to supply 2.19 MW at the maximum compared to 2 MW for alternative 3.1. This has allowed the active power of section 2 to be reduced to 1.16 MW.

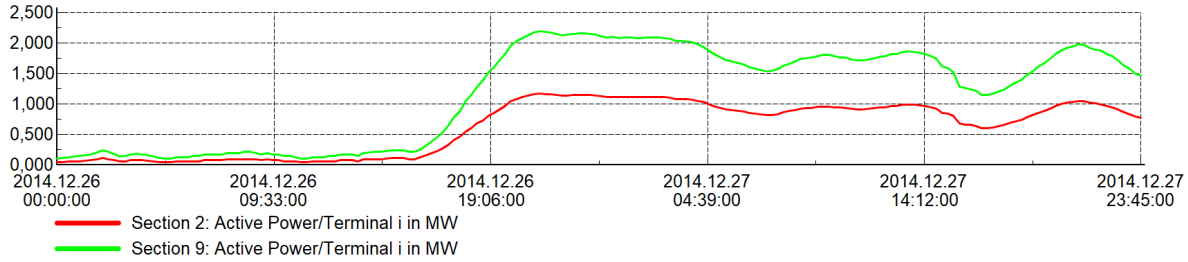

Figure 7.16: Scenario 1 Alt. 3.2: Active power.

Figure 7.17 now indicates that a larger share of the reactive power is provided through section 9. It is now providing 0.65 MVAr at peak demand, an increase from 0.56 MVAr for alternative 3.1. As a result section 2 now provides a maximum of 0.13 MVAr.

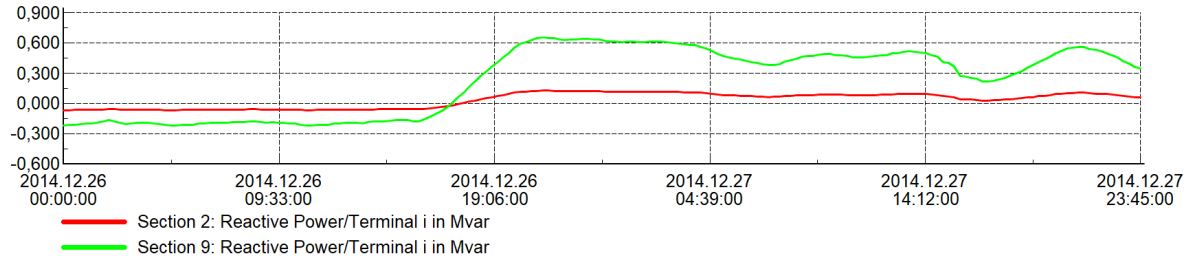

Figure 7.17: Scenario 1 Alt. 3.2: Reactive power.

In total the change of cable type has decreased the loading of section 2 to 18% at its maximum, while also the loading of section 9 is lowered to 13.2%. The increased cable capacity has caused the total losses to be decreased to 11.8 kW, as can be observed in fig. 7.19. Section 9 still induce the greatest losses, which now are restricted to 6.2 kW.

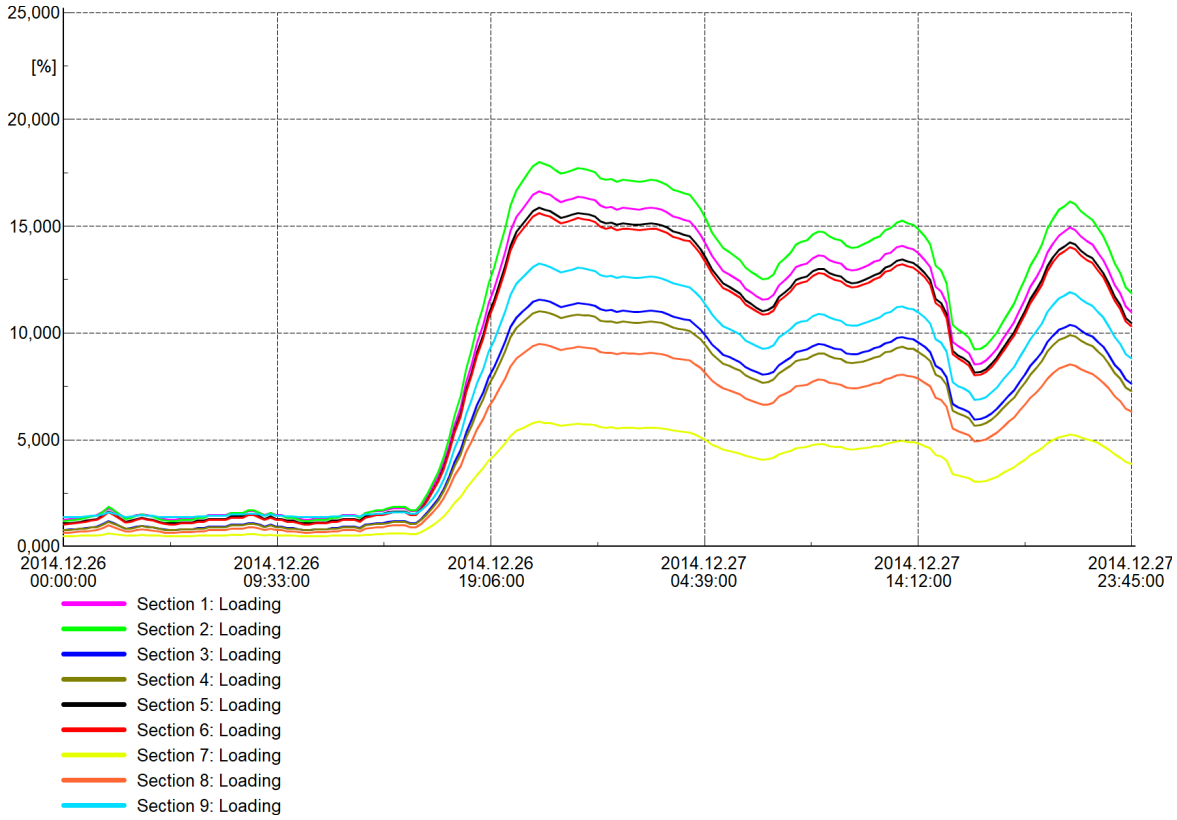

Figure 7.18: Scenario 1 Alt. 3.2: Loading of sections 1 to 9.

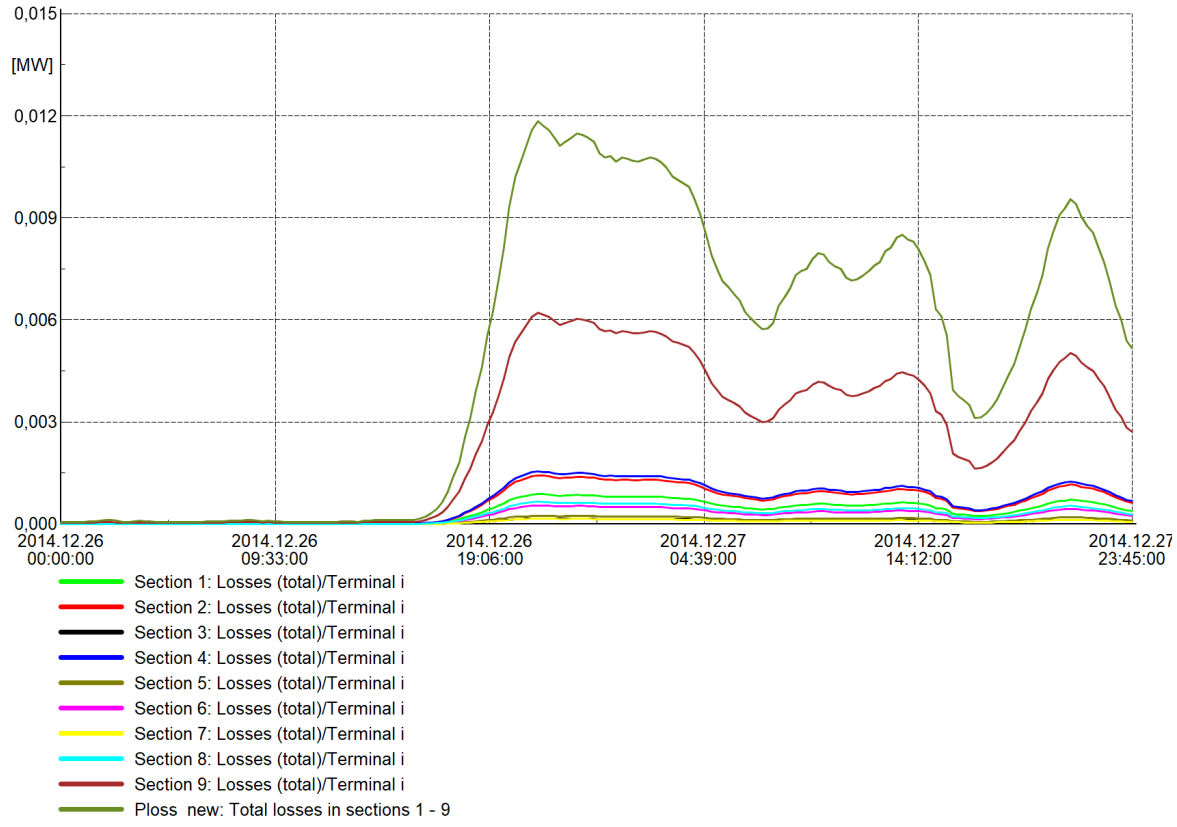

Figure 7.19: Scenario 1 Alt. 3.2: Power losses in sections 1 to 9.

7.1.4 Case 1.4: Install battery

In this section the effect of installing a battery at the node "Kvia" will be investigated. This installation point was chosen because the battery should contribute to lowering the loading of the most heavily loaded sections. As seen in section 7.1.1, line sections 1 to 6 are loaded the most heavily when no action is taken. As section 6 ends at "Kvia" all these sections will benefit when the battery contributes. E.g. installing the battery at the node "Lida" would only benefit sections 1 to 3, as the power in sections 3 to 6 would be equal to a case without battery. [2]

As the loading of section 2 in this load scenario is not critical, it is not an intuitive task to choose battery parameters. As will be shown in chapter 9 the battery solution for this case will be significantly more expensive than doing nothing to the grid, or even replacing the existing lines with new cables. Therefore, it do not make sense to try calculating the economically optimal battery parameters, and the battery therefore has to be dimensioned in regards to some other criterion. As an alternative, an attempt was made to find what battery parameters must be used in order to solve the problem in question. It is, however, not entirely clear what the problem in this load situation actually is. The supply lines are not critically loaded so the battery is not needed to avoid thermal overloading, which in fact is the intent of the battery installation and is what it is controlled to do. A remaining question could be to investigate if a BESS could reduce the power losses incurred for the supply. To have a starting point of the simulation a rated battery discharge power of 1 MW is chosen. Due to the prolonged high demand period of approximately 8 hours, as discussed in section 6.2.3, a large energy capacity is needed to sustain the rated power for the entire high demand period. By trial and error, a capacity of 9.5 MWh is chosen in the simulation. The maximum and minimum thresholds for the SOC is set to 90% and 10%, resulting in a DOD of 80% and a usable capacity of 7.6 MWh. Utilizing lithium-ion batteries from 10 to 90% SOC is a common strategy in several management systems, in order to prolong the battery life while still using a fair share of the available capacity [2] [29] [24]. All battery parameters are shown in table 7.2. The results of the simulation when running the QDSL battery model with these parameters are shown in figs. 7.20 to 7.25.

Table 7.2: Battery parameters for load scenario 1 alternative 4.

Parameter	Unit	Value
Eini	MWh	9.5
SOCini	%	50
SOCmin	%	10
SOCmax	%	90
Pstore	MW	1
Qstore	MVAr	0.05
PStartStore	MW	2.499
PFullStore	MW	1.5
Pfeed	MW	1
Qfeed	MVAr	0.05
PStartFeed	MW	2.5
PFullFeed	MW	3.5
orientation	-	-1

Figure 7.20 show $P_{measured}$, which represent the active power demand, and the active power provided through section 2. It is recommended to view this in relation to figs. 7.21 and 7.22, who show the active power being fed and drawn, and the state of charge of the battery. During the initial hours of the simulation it is observed that the battery is charging at 1 MW, since the battery active power is negative. This causes the power of section 2 to supply the battery charging power in addition to the minimal load demand in the area. After approximately four hours the SOC has reached its maximal allowed value at 90%, meaning that the battery no longer will charge. The battery then stays inactive during the remaining low demand period, as section 2 provides whatever power is needed at each point. When the measured power reaches $P_{StartFeed}$, the threshold for starting to discharge, at 2.7 MW the battery active power indeed indicates that the battery is feeding power into the grid. As $P_{measured}$ is increasing the discharged power ramps in order to keep the power flow through section 2 at 2.7 MW. The battery is allowed to start charging when the demand drop below 2.7 MW, but the charging will never cause the section 2 power to exceed the threshold. Charging occur during the night after the first high demand period, where $P_{measured}$ is slightly below $P_{StartStore}$. Thereafter the demand increases above the threshold once again, causing the battery to discharge. The SOC during this discharge period almost reaches SOC_{min}, before charging is allowed in the subsequent valley which increase the SOC to approximately 35%. This way, the battery is also able to shave the last peak of Saturday. As a result, the import from the external grid is kept constant at 2.7 MW, while the battery is taking care of the variations in the load.

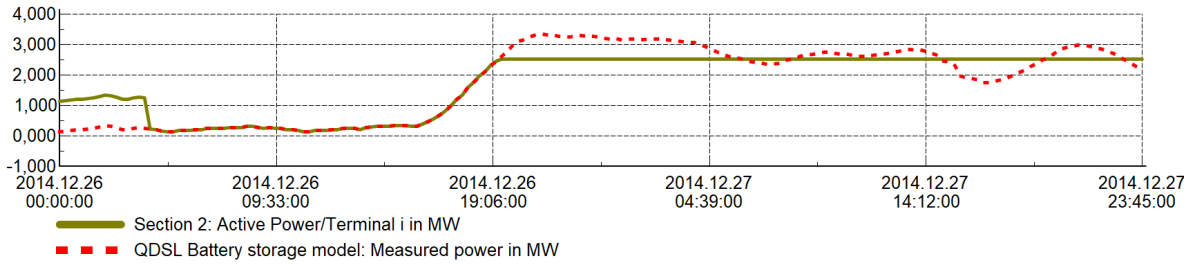

Figure 7.20: Scenario 1 Alt. 4: Active power in section 2.

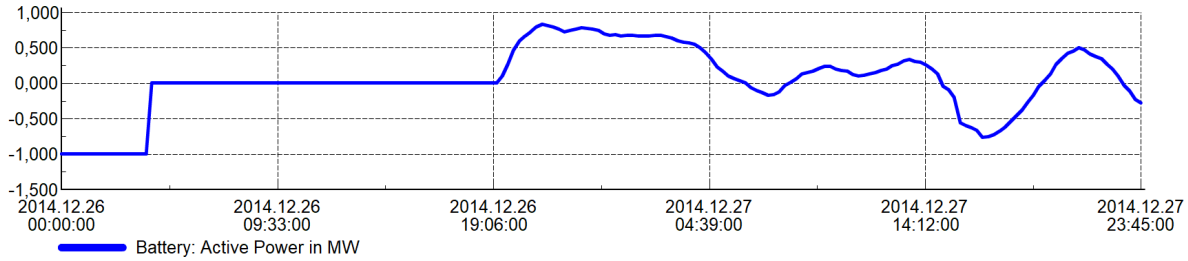

Figure 7.21: Scenario 1 Alt. 4: Active power of battery.

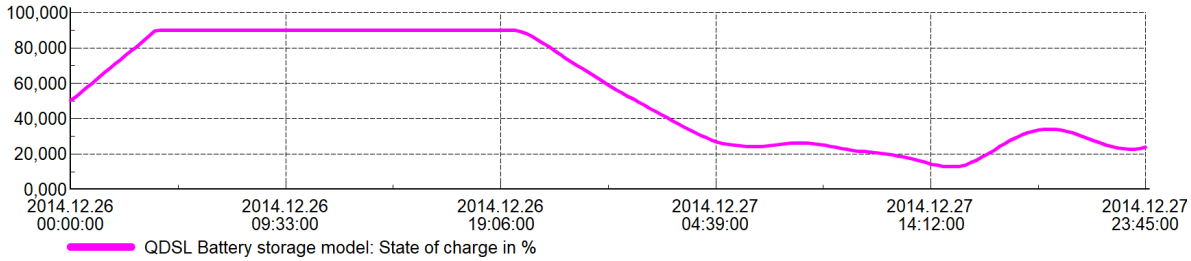

Figure 7.22: Scenario 1 Alt. 4: State of charge of battery.

Figure 7.23 show the active and reactive power of the battery, in addition to $cos\ \phi$. The figure illustrates the working principle of the battery control system in relation to the reactive power drawn and fed, as described in section 6.3.3. As the reactive power is controlled by the active power thresholds the two follow the same profile, meaning that they always will draw and feed with the same percentage of their respective ratings. Looking e.g. at the maximum discharge point the active power is 0.829 MW while the reactive power is 0.041 MVAr. With ratings of 1 MW and 0.05 MVAr respectively, both are feeding 82.9% of their rated power. This means that the battery is operating with a constant $cos\ \phi$, whose value is determined by eq. (6.9). By inserting the earlier specified values the power factor of the battery is found to be 0.9988 with the chosen parameters. The constant power factor is further illustrated in fig. 7.23 where it is observed to have a constant positive value for feeding and constant negative value for storing. Because of the low rating for feeding of reactive power, the battery can only diminish a small amount of the reactive power drawn from the external grid. At peak demand section 2 supply 0.975 MVAr, which is a reduction from case 1.1 approximately equal to the battery Q_{feed} rating.

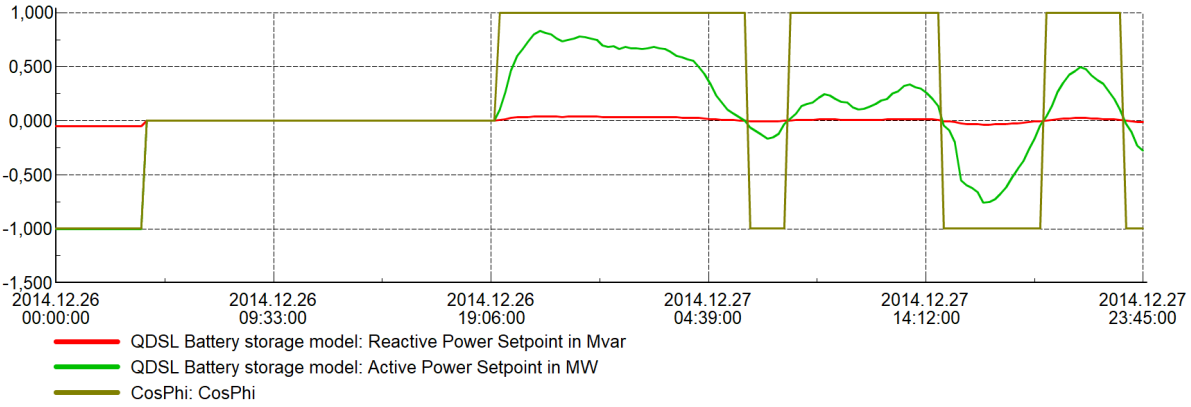

Figure 7.23: Scenario 1 Alt. 4: Active and reactive power of battery.

The loading of sections 1 to 8 is shown in fig. 7.24. It is evident that the loading of sections 1 to 6 are increased during the period where the battery is charging. As the battery starts to discharge, and for the remaining simulation period, the loading of these sections are kept fairly constant. This should be the desired result as the active power supplied by the external grid is constant during this period. The small variations that are occurring are caused by the varying reactive power that is changing proportionally with the active load demand. In total, this causes the loading of section 2 to be 41% at the maximum, while sections 1, 5 and 6 all are loaded around 37%.

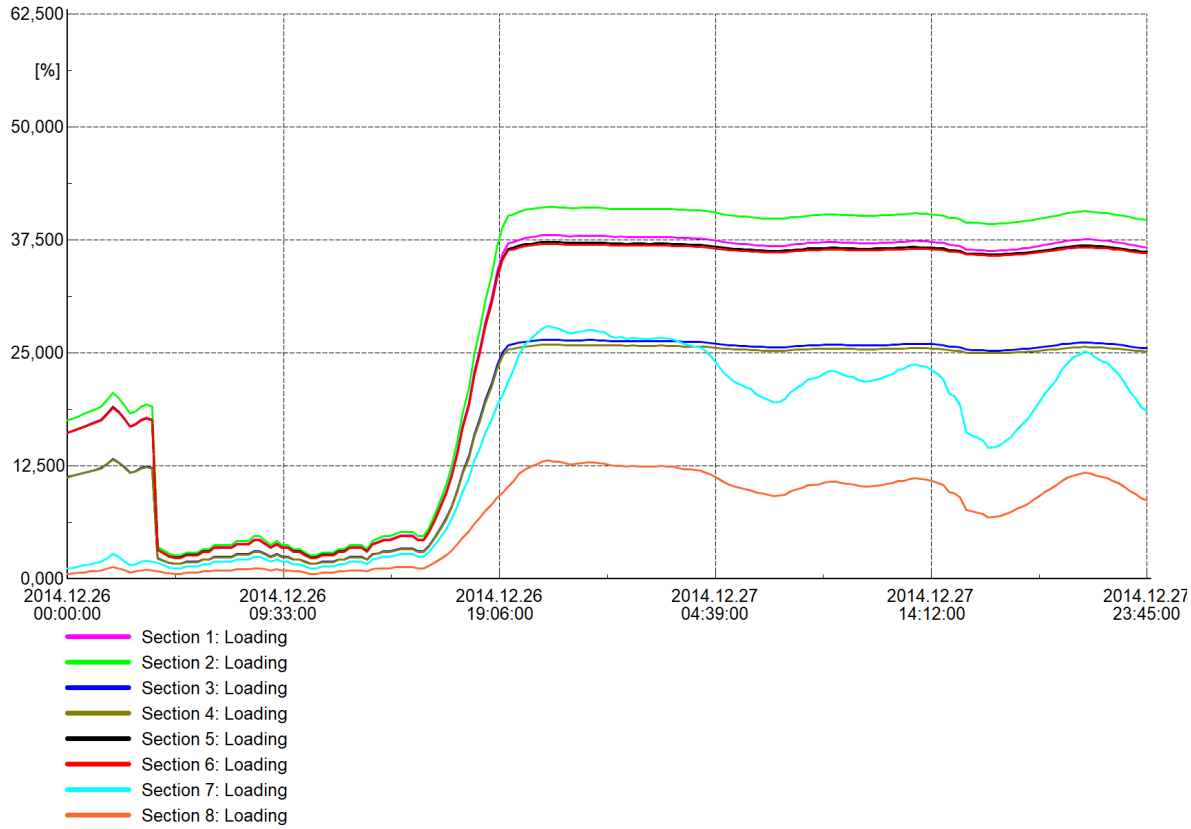

Figure 7.24: Scenario 1 Alt. 4: Loading of sections 1 to 8.

Figure 7.25 show the power losses in sections 1 to 8, losses in the battery and the total losses when running the simulation with the battery installed. The losses in the individual line sections are restricted to 8.5 kW at the maximum, which occur in section 4, while section 2 induce a loss of 7.5 kW. It seems, as such, that the battery has successfully reduced the losses in the supply lines. This is, however, countered by the loss in the battery itself, which is modeled with a 97.5% one-way efficiency [30]. At maximum discharge a loss of 21 kW is therefore generated, causing the total system loss to be 51 kW. This is in fact more than what was observed in case 1.1. Additionally, charging the battery during the low demand period also incur losses. As a result it can be concluded that a battery of this size cannot reduce the maximum power losses in the modeled load scenario, despite reducing the line loading during peak hours.

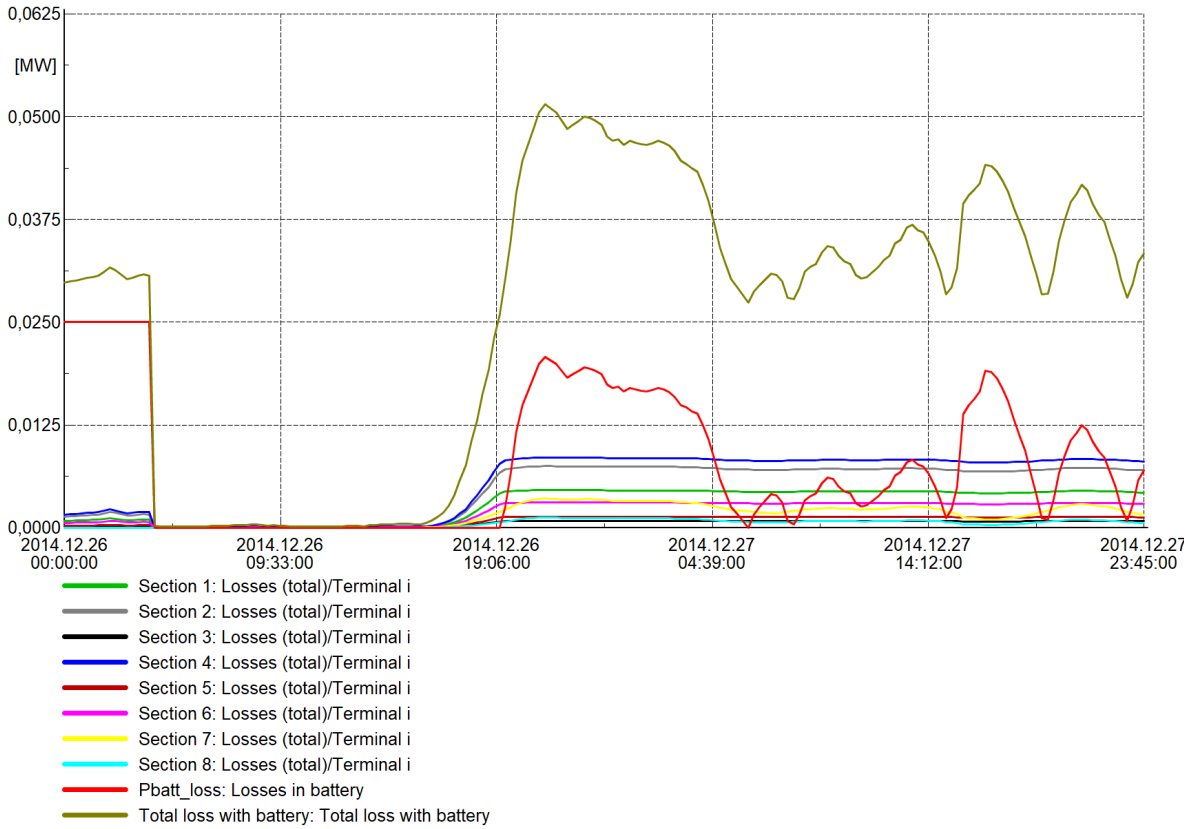

Figure 7.25: Scenario 1 Alt. 4: Loss in system.

7.2 Load scenario 2

This load scenario will investigate a situation where the existing supply connection to the external grid is critically loaded. This situation is relevant as the area is regulated for an approximate total of 1000 cottages, which is a significant increase comparing to the existing 350 cottages [5]. To emulate this situation an additional demand of 2.7 MW is added to "Hydla 2" compared to the first load scenario, making the total load at the node 4 MW. With the estimated average peak active power of about 7 kW, as described in section 6.2.1, this correspond to approximately 600 new cottages compared with the existing situation, up to a total of about 900 customers. The load at each node is presented in table C.2. Similarly to what was done in section 7.1, all solution alternatives will be presented for this scenario. Results and analyses of the simulations for each alternative will be presented in sections 7.2.1 to 7.2.4.

7.2.1 Case 2.1: No grid upgrade

This case deals with the load scenario by utilizing the existing grid to supply the cottage area, i.e. solution alternative 1. The viability of this alternative will be considered by presenting and discussing the simulation results. Figures 7.26 to 7.28 show the active and reactive power, the section loading and the power losses for this alternative.

Observing the active power of line section 2 in fig. 7.26 the bottleneck line now supply 6 MW during the maximal demand, which is occurring Friday evening at 21:15. Similarly to case 1.1, the reactive power of the section follow the same curvature as the active power. Due to the elevated demand, however, a peak of 1.91 MVAr is now supplied by section 2.

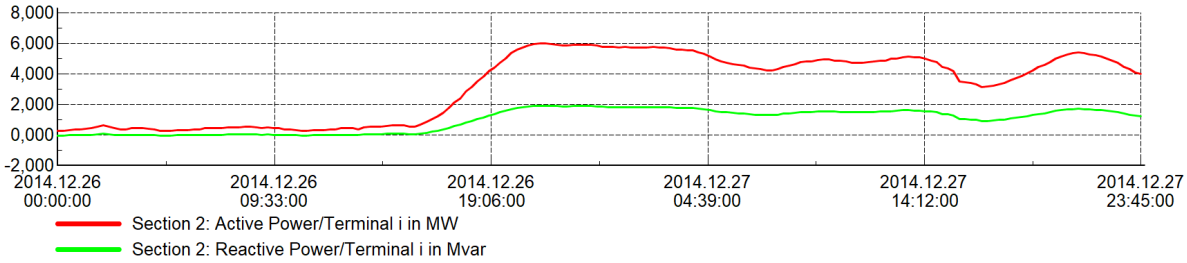

Figure 7.26: Scenario 2 Alt. 1: Active and reactive power in section 2.

The significant consumption increase has had a serious impact on the loading of the lines supplying the area, as seen in fig. 7.27. Section 2 has a loading that is exceeding 97%, while sections 1, 5 and 6 has a loading close to 90%. Section 8 is the only one loaded below 50%, while the remaining sections experience between 60% and 70% loading. It is clear that the sections above 90% are critically loaded, as only a small demand increase or change of conditions can cause the thermal boundary to be violated.

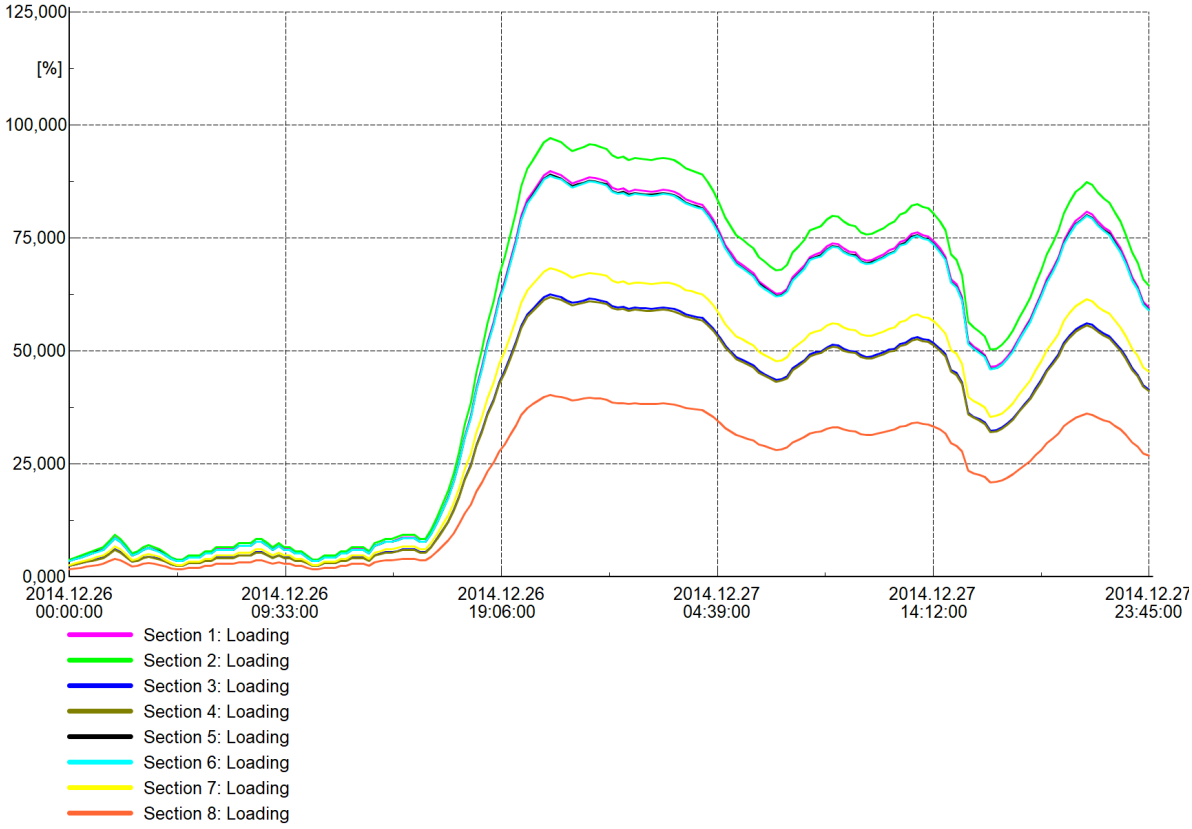

Figure 7.27: Scenario 2 Alt. 1: Loading of sections 1 to 8.

The increased load has also affected the power losses in the supply greatly. These are presented

in fig. 7.28. Equally to case 1.1 section 4 is observed incur the largest loss, at a maximum of 49 kW, while section 2 cause a power loss of 42 kW. The total losses in sections 1 through 8 are now 179 kW, which is an increase with a factor 3.65 compared to case 1.1.

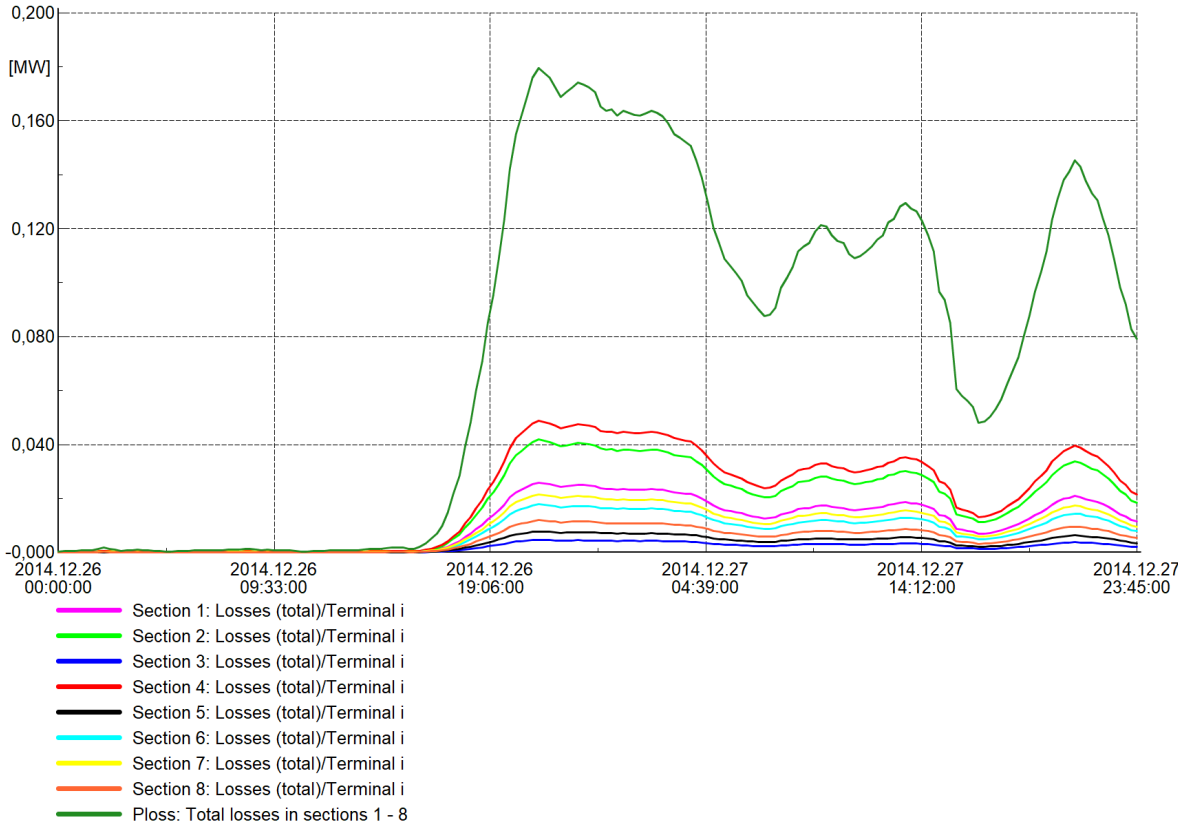

Figure 7.28: Scenario 2 Alt. 1: Power losses in sections 1 to 8.

7.2.2 Case 2.2: Refurbish existing connection

This case will investigate the supply situation of the critical load scenario when sections 1 to 6 are removed and replaced with higher capacity underground cables, as described in section 4.2. The modeling is conducted as presented in section 6.4.1. Similarly to what was done in section 7.1.2 the simulations has been run with two different cable types, TSLE 3x1x150 (alternative 2.1) and TSLE 3x1x240 (alternative 2.2), whose parameters are appended in table A.1.

Case 2.2.1: 150 mm^2

First, results will be presented and analyzed for the alternative where TSLE 3x1x150 cables are used. By analyzing "Section 1 New" the exchange of power with the external grid can be found. Figure 7.29 show the active and reactive power for this section. For this configuration it is observed that the power coming into the grid is slightly above 6 MW at the maximum, a small increase compared to what was found in case 2.1. This is, once again, caused by the voltage dependency of the load. As the voltage drop for this case is smaller than for the previous alternative the maximum demand is larger, as was discussed in section 7.1.2. The

maximal drawn reactive power from the external grid is for this case 1.816 MVAr, which is a reduction of about 0.1 MVAr compared to case 2.1. This is caused by production of reactive power in the cables which have replaced the overhead lines, and will be discussed further in section 7.3.

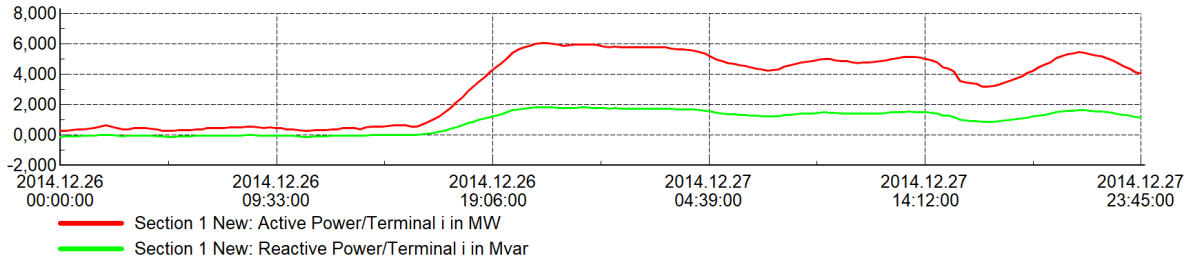

Figure 7.29: Scenario 2 Alt. 2.1: Active and reactive power in "Section 1 New".

Looking at the loading of each section in fig. 7.30 it is obvious that the general loading of the supply has been reduced. "Section 1 New", "Section 2 New" and section 6, which carry the largest current, now are all loaded slightly above 46%. This is a great reduction in comparison to the sections which they have replaced. Section 7, however, has not been replaced. Thus this section now is the one having the largest magnitude of loading at 68%.

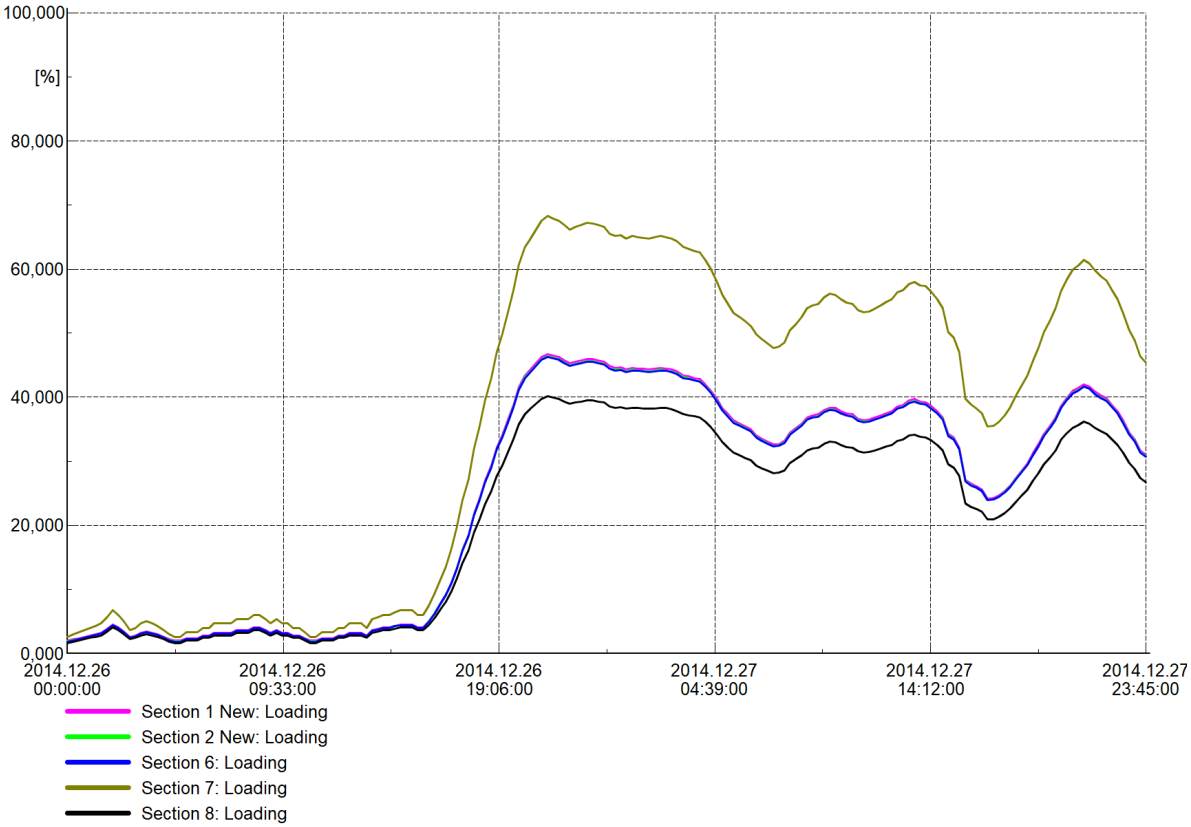

Figure 7.30: Scenario 2 Alt. 2.1: Loading of sections 1 to 8.

Having replaced the supply connection with new cables, the resistance of the grid is significantly reduced. This has caused section 7, which has not been replaced, to incur the largest

power loss at 21 kW. “Section 1 New”and “Section 2 New”, which both are about 1 km, now give rise to 17 kW and 16 kW losses respectively. In total, sections from the external grid to “Hydla 2” now experience a power loss of 72.4 kW. This is a major reduction compared case 2.1, as over 100 kW has been abated.

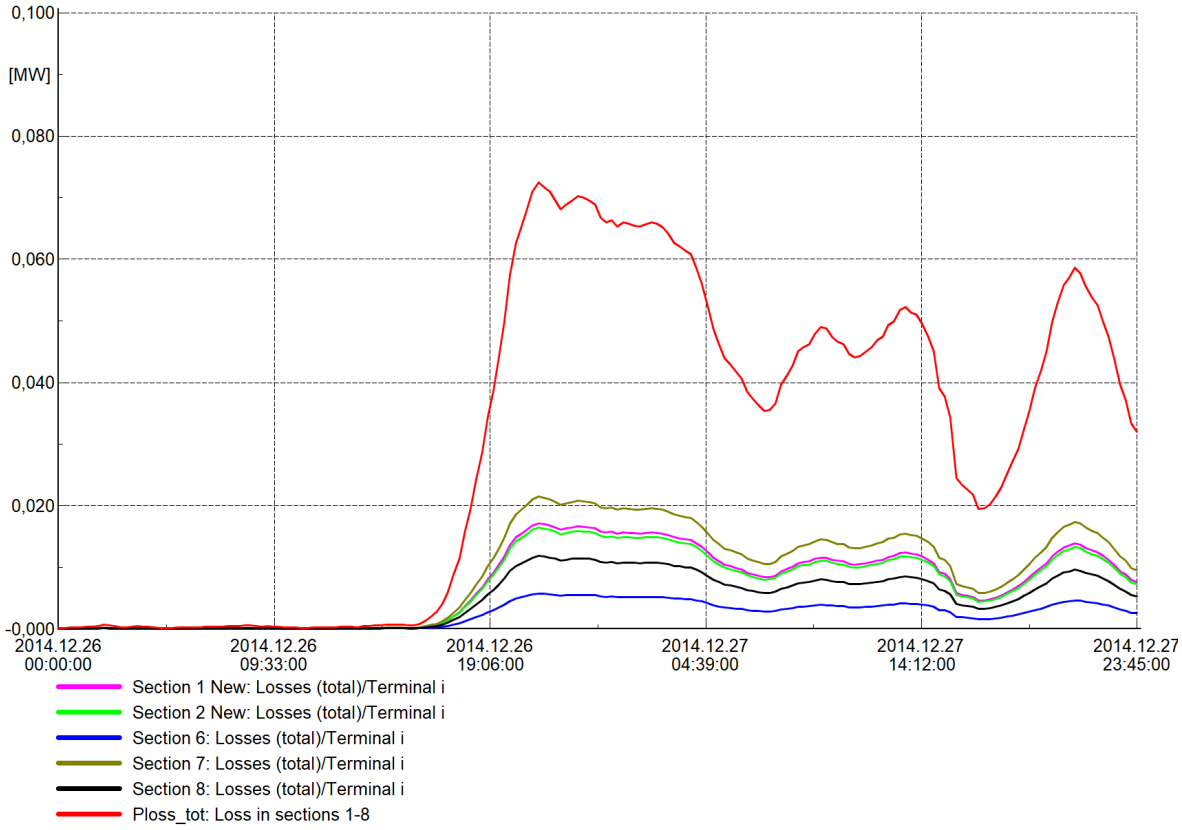

Figure 7.31: Scenario 2 Alt. 2.1: Power losses in sections 1 to 8.

Case 2.2.2: 240 mm^2

Now the same load scenario as in the previous case is simulated, but instead alternative 2.2 is conducted meaning that 240 mm^2 cables are used as replacement for the old supply. The results will be compared to those of alternative 2.1 from case 2.2.1, in order to investigate the impact of having a greater cross-section. Observing fig. 7.32 the active power coming into the area is exactly the same as in the last case, with a peak of 6.043 MW. The peak reactive power has, however, decreased slightly as a result of the new cables, and is now 1.796 MVAr. This is caused by the elevated susceptance of the new cables.

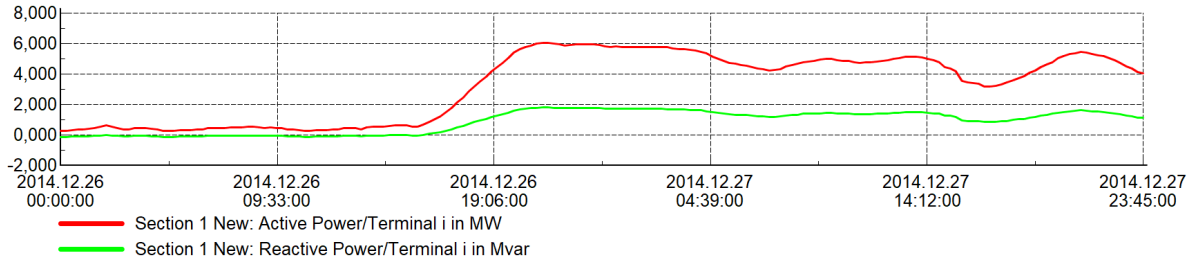

Figure 7.32: Scenario 2 Alt 2.2: Active and reactive power in "Section 1 New".

Figure 7.33 show the loading of each section. It is evident that the loading of the upgraded sections, "Section 1 New", "Section 2 New" and section 6, is reduced. In case 2.2.1 the loading was about 46%, while it now is approximately 36%. The loading of the remaining sections is unchanged from the previous case. Table A.1 indicates that the cables now should have a reduced power loss as a result of decreased resistance. This is also the case, as seen in fig. 7.34, as losses in the three upgraded sections now are 10 kW, 10 kW and 3.5 kW. Losses in sections 7 and 8 remain unchanged, making the maximum total loss 57 kW.

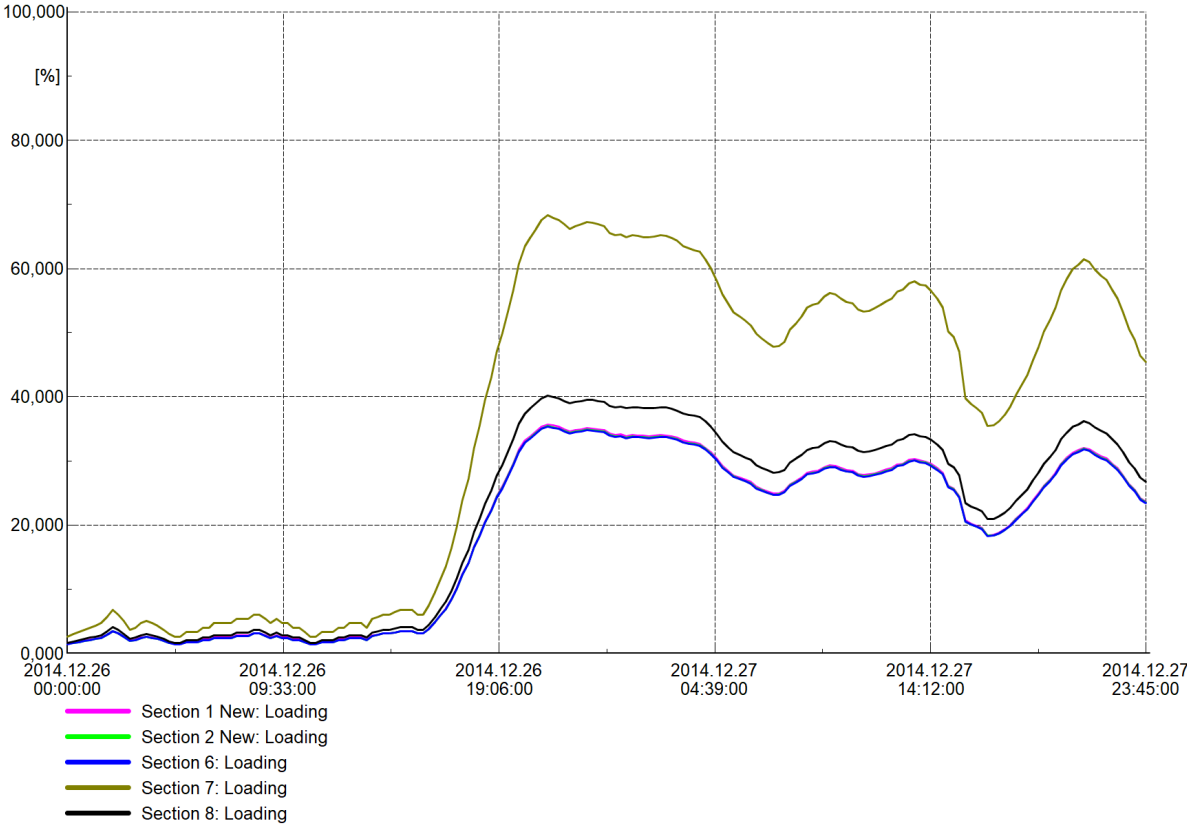

Figure 7.33: Scenario 2 Alt 2.2: Loading of sections 1 to 8.

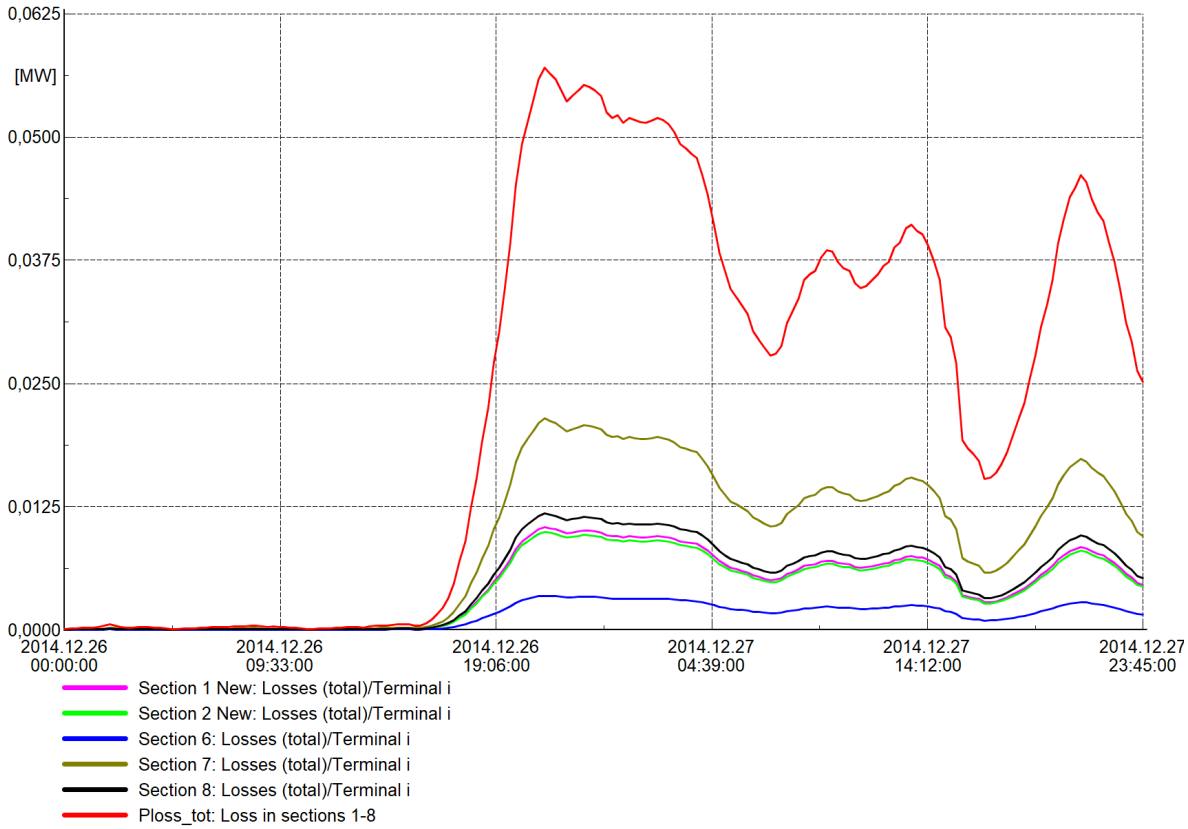

Figure 7.34: Scenario 2 Alt 2.2: Power losses in sections 1 to 8.

7.2.3 Case 2.3: Add new connection

Now the effect of adding an additional supply connection, instead of replacing the existing connection, will be analyzed for load scenario 2. The extra cable connection will be added to the node "Hydla 2", as is described in sections 4.3 and 6.4.2. Also for this case, the simulation has been conducted with two different cable cross-sections. Alternative 3.1, with the 150 mm^2 cable, is analyzed in case 2.3.1, while case 2.3.2 deals with the 240 mm^2 cable of alternative 3.2.

Case 2.3.1: 150 mm^2

First, the system is analyzed when using 150 mm^2 cables. Figure 7.35 show the active power in sections 2 and 9, which amount to 2.145 MW and 3.897 MW respectively at the peak demand. Thus, the two external grids in total supply 6.042 MW, which is basically the same as in case 2.2.1. In regards to the reactive power shown in fig. 7.36, it is observed that section 9 definitively is supplying most of the reactive power. This section provides a maximum of 1.314 MVAr, while section 2 provides 0.407 MVAr.

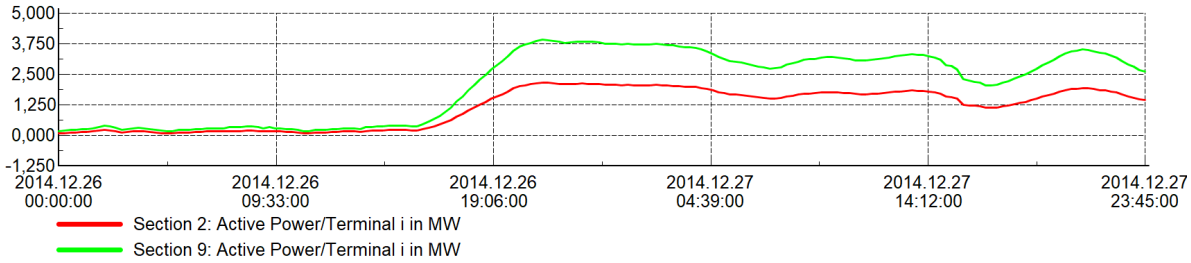

Figure 7.35: Scenario 2 Alt. 3.1: Active power in sections 2 and 9.

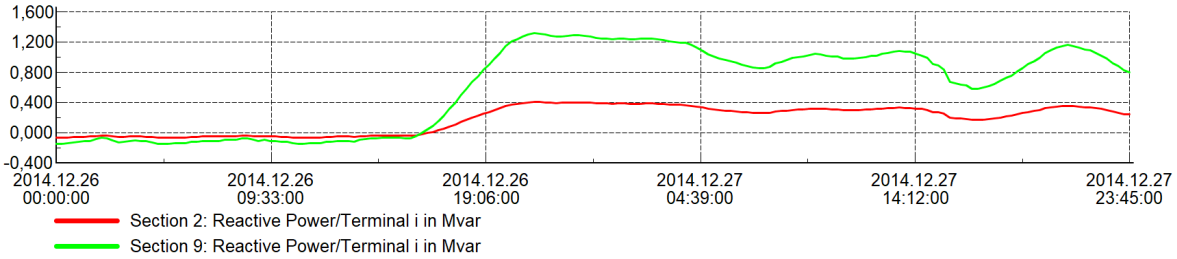

Figure 7.36: Scenario 2 Alt. 3.1: Reactive power in sections 2 and 9.

Figure 7.37 show the loading of sections 1 to 9 for this load scenario. Section 2 is the most heavily loaded at 33.6%, while sections 1, 5, 6 and 9 follows at approximately 30%. The relatively low loading indicates that the grid is very well suited for this load situation and is able to supply an even heavier load increase. Because of the relatively long cable from the external grid to “Hydla 2”, section 9 clearly incur the largest losses as can be observed in fig. 7.38. The section experience losses of 33 kW, while all other sections have maximum losses under 6 kW. In total the supply grid give rise to 50 kW losses for this alternative.

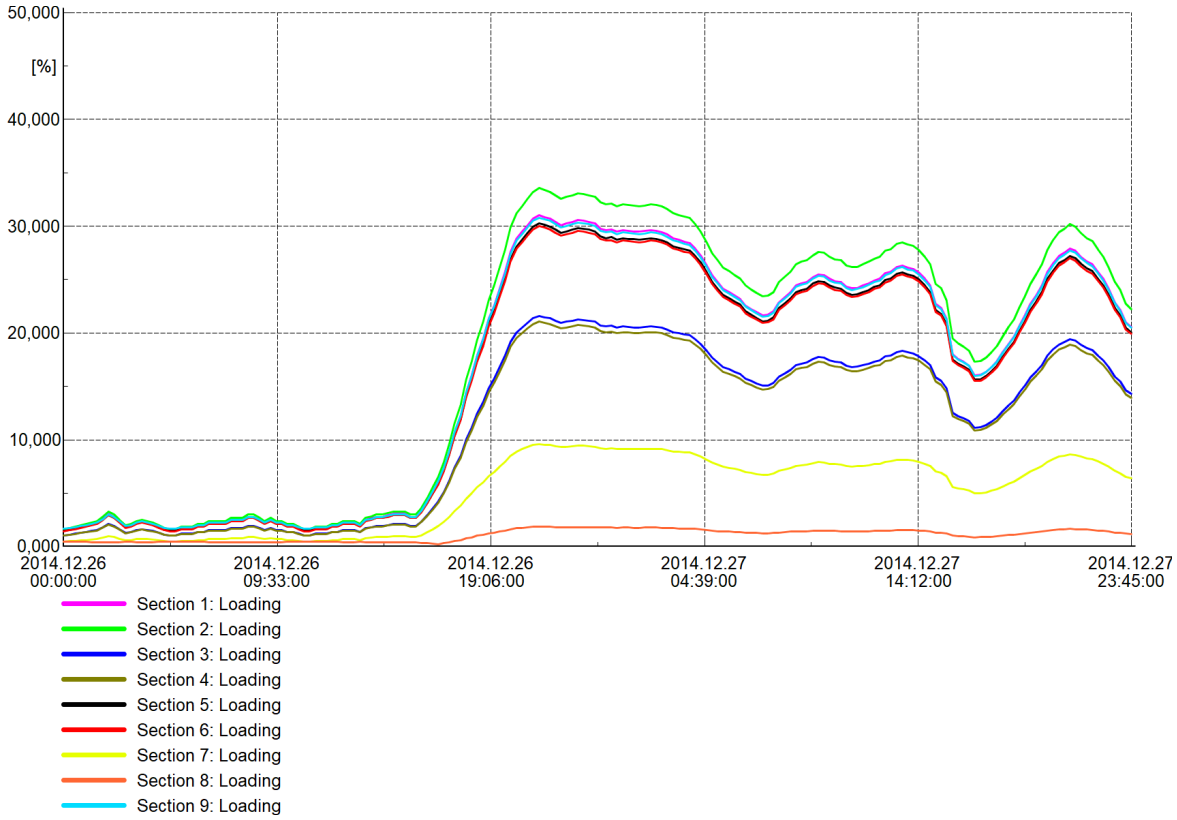

Figure 7.37: Scenario 2 Alt. 3.1: Loading of sections 1 to 8.

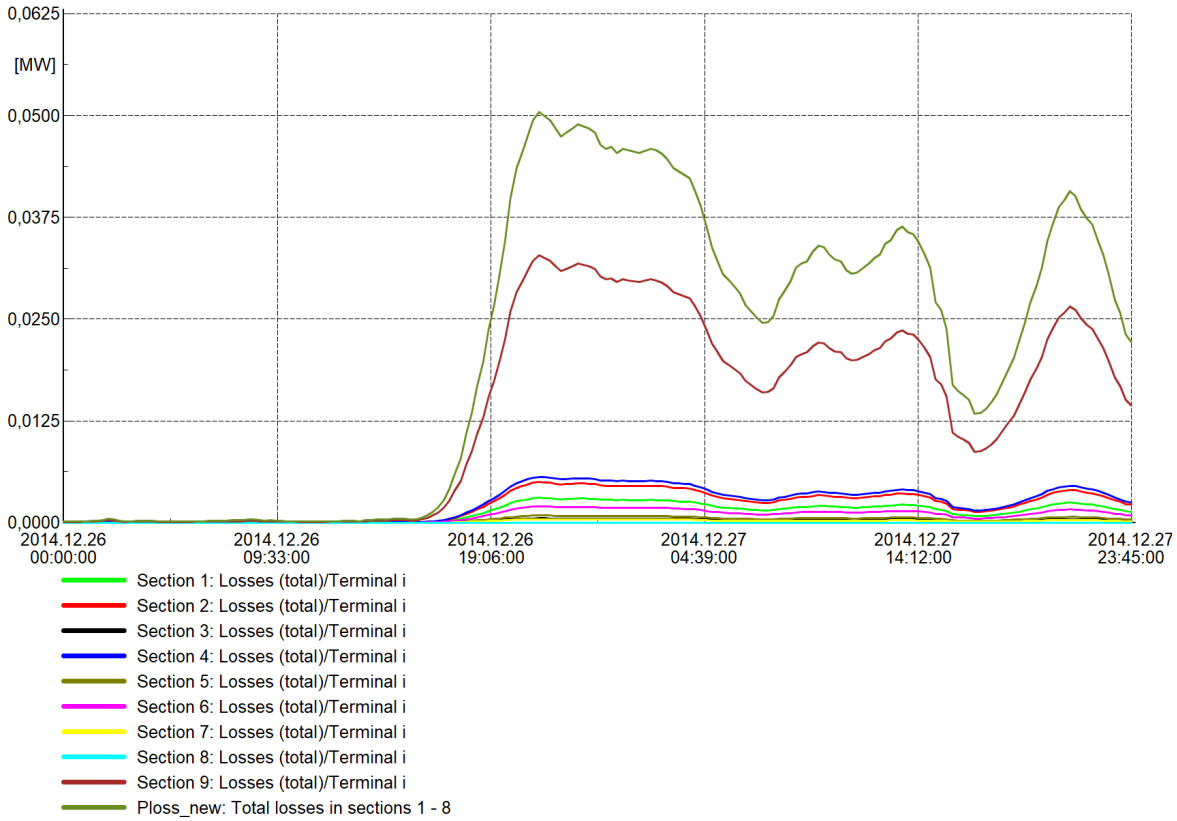

Figure 7.38: Scenario 2 Alt. 3.1: Power losses in sections 1 to 8.

Case 2.3.2: 240 mm^2

Figures 7.39 and 7.40 show the active and reactive power of sections 2 and 9 when the new connection is built with 240 mm^2 cables. In this case section 9 provides even more of the total power than in case 2.3.1 with 4.26 MW, while section 2 provides 1.79 MW. The same is observed in regards to the reactive power where section 9 supply 1.547 MVAr at peak demand, while section 2 provides 0.138 MVAr. The total demand for reactive power from the external grid during the peak load has therefore decreased as a result of the increased susceptance of the cable.

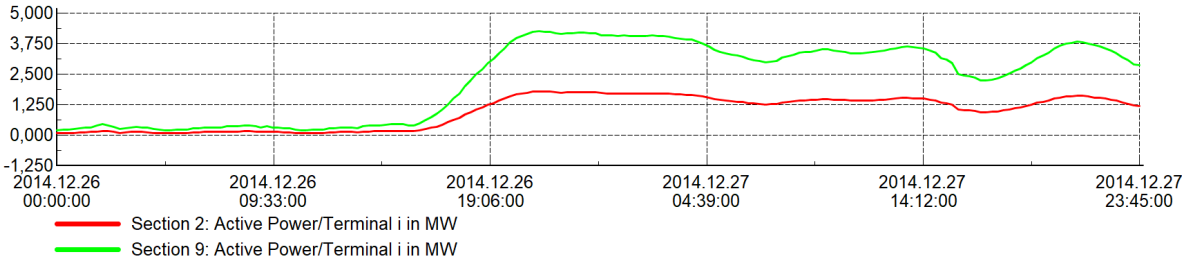

Figure 7.39: Scenario 2 Alt. 3.2: Active power in sections 2 and 9.

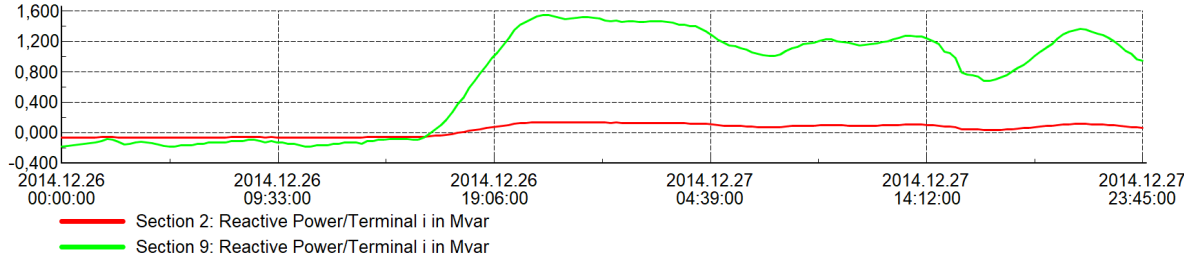

Figure 7.40: Scenario 2 Alt. 3.2: Reactive power in sections 2 and 9.

Figure 7.41 show the loading of sections 1 to 9, which for this alternative generally is low. Section 2 once again experience the greatest loading of 27.5%, despite section 9 providing the majority of power. Section 9 is, nevertheless, loaded slightly lower at 26%. Thanks to its length section 9 still definitively have the largest power losses with 24 kW according to fig. 7.42. As all other sections have losses smaller than 4 kW, the total loss of the supply now is restricted to a maximum of 36 kW.

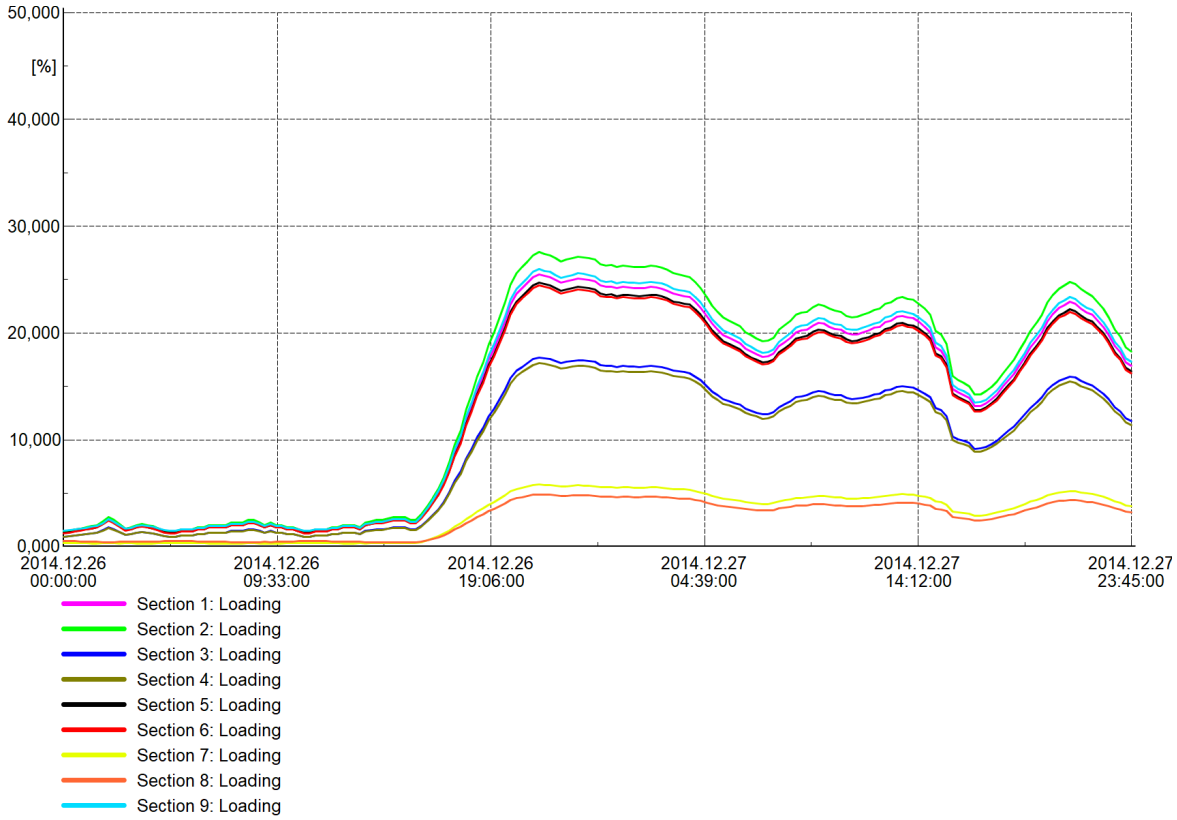

Figure 7.41: Scenario 2 Alt. 3.2: Loading of sections 1 to 9.

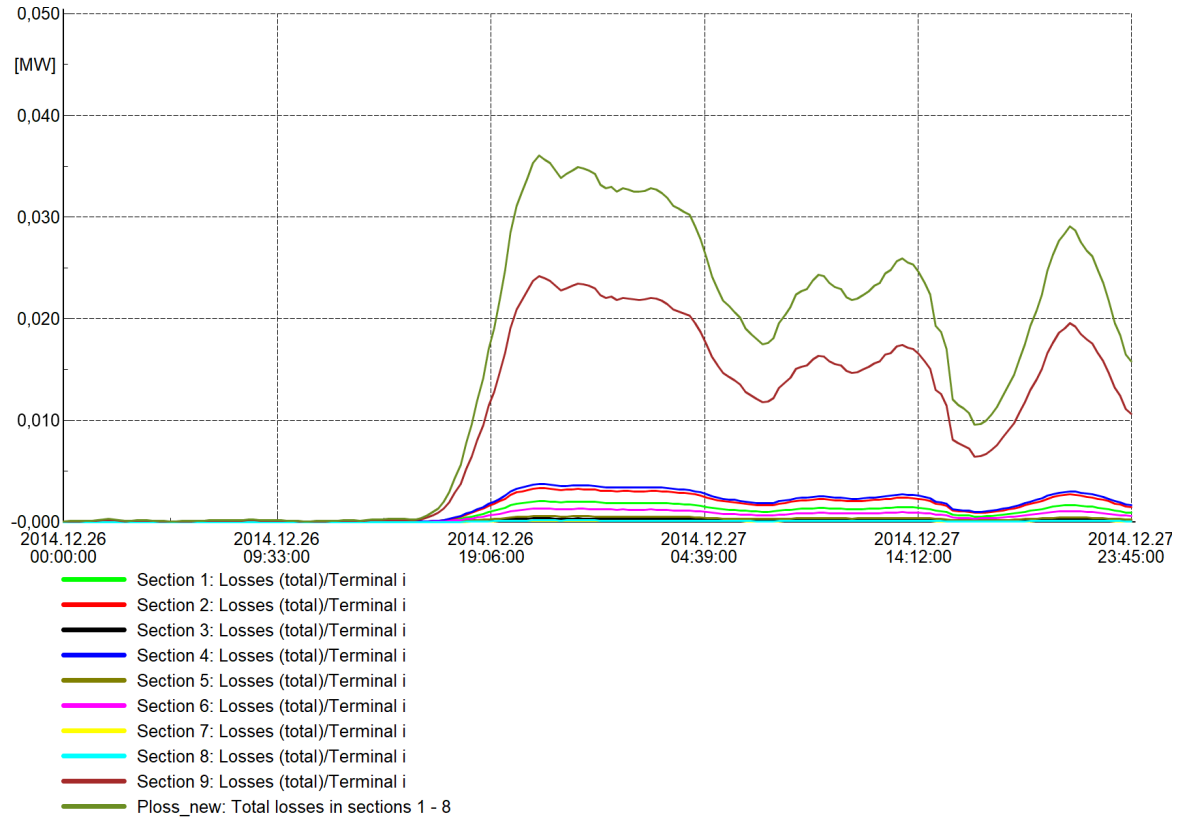

Figure 7.42: Scenario 2 Alt. 3.2: Power losses in sections 1 to 9.

7.2.4 Case 2.4: Install battery

As the supply line sections are critically loaded in this load scenario, an attempt has been made to find battery parameters that can diminish the import from the external grid such that the lines no longer are loaded critically. Suitable parameters and thresholds were found through observing the results of several simulations, which led to the battery parameters shown in table 7.3. The rated active power has been increased to 1.2 MW to be able to restrict the maximum loading of section 2 to 80%. Therefore, $P_{StartFeed}$ is set to 4.8 MW while charging is allowed below this value. To sustain discharge during the high demand period the energy capacity has been slightly increased compared to the first load scenario, as it now is set to 10 MWh. Similarly to case 1.4 the DOD is set to 80% by setting SOC_{min} at 10% and SOC_{max} at 90%, which are common values for stationary lithium-ion batteries [29] [24].

Table 7.3: Battery parameters for load scenario 2 Alt. 4.

Parameter	Unit	Value
Eini	MWh	10
SOCini	%	50
SOCmin	%	10
SOCmax	%	90
Pstore	MW	1
Qstore	MVAr	0.05
PStartStore	MW	4.79
PFullStore	MW	3.79
Pfeed	MW	1.2
Qfeed	MVAr	0.05
PStartFeed	MW	4.8
PFullFeed	MW	6
orientation	-	-1

Figures 7.43 and 7.44 show $P_{measured}$ and active power for the battery, in addition to the active power flow in section 2. The state of charge during the simulation period is shown in fig. 7.45. As the initial SOC is set to 50% the battery is charged to SOC_{max} during the initial low demand period. It is further on inactive until the demand increases rapidly Friday evening. When $P_{measured}$ reaches 4.8 MW the battery is starting to discharge, and ramps its power in order to keep the active power flow in section 2 to 4.8 MW. The 10 MWh capacity allows the battery to keep the discharge until $P_{measured}$ falls below the feeding threshold. At this point, the SOC is tangent to its minimum value of 10% before the battery is allowed to charge.

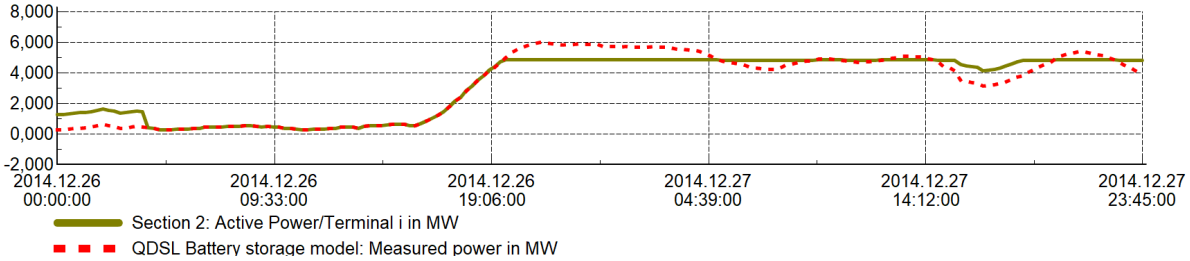

Figure 7.43: Scenario 2 Alt. 4: Active power in section 2.

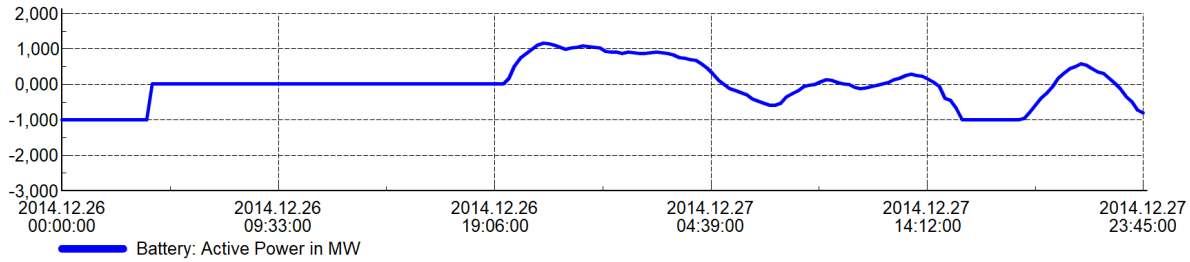

Figure 7.44: Scenario 2 Alt. 4: Active power of battery.

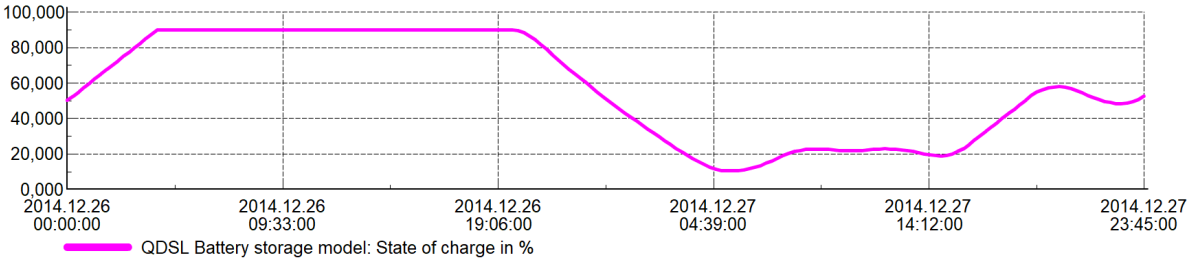

Figure 7.45: Scenario 2 Alt. 4: State of charge of battery.

Figure 7.46 illustrates the active and reactive power of the battery, and the resulting constant $cos\ \phi$ of the operation. As is described in section 6.3.3 the reactive power is controlled by the active power thresholds. Therefore a constant $cos\ \phi$ is observed, which for charge is 0.9988 and for discharge is 0.9991 given by eq. (6.9). The power factor for charge is the same as in case 1.4, but for discharge the power factor has increased. This is because the rated discharge active power has increased to 1.2 MW while the discharge reactive power remains unchanged.

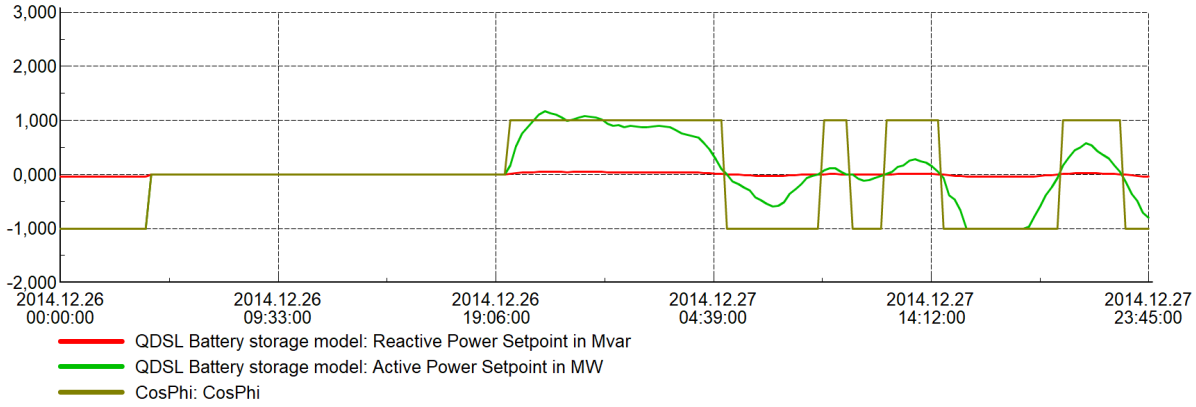

Figure 7.46: Scenario 2 Alt. 4: Active and reactive power of battery.

Figure 7.47 show the loading of sections 1 to 8 where it is obvious that the supply sections now experience a leveled load, instead of the much more varying loading in the base case. Section 2 is still the most heavily loaded at 79.6% while sections 1, 5 and 6 supply between 72.5% and 73.5% of their capacity. Section 7 is still unaffected by the installation, and thus also is quite heavily loaded. Losses in the supply grid are shown in fig. 7.48, which indicates that the total loss is much higher in this alternative than if the cables are refurbished. The total loss is 160 kW which is only approximately 20 kW less than in case 2.1. At the peak demand section 4 is the one incurring the greatest loss, while section 2 follows. These line sections, due to their level loading, have an almost constant power loss. The battery, however, has a much more varying loss. At maximum demand the battery is a source of 29 kW power loss. All in all, installing the battery has removed the critical strain on the line sections by utilizing its peak-shaving characteristics. Additionally, the battery has contributed to reducing the system losses compared to case 2.1. The losses are, however, reduced more by both alternative 2 and 3.

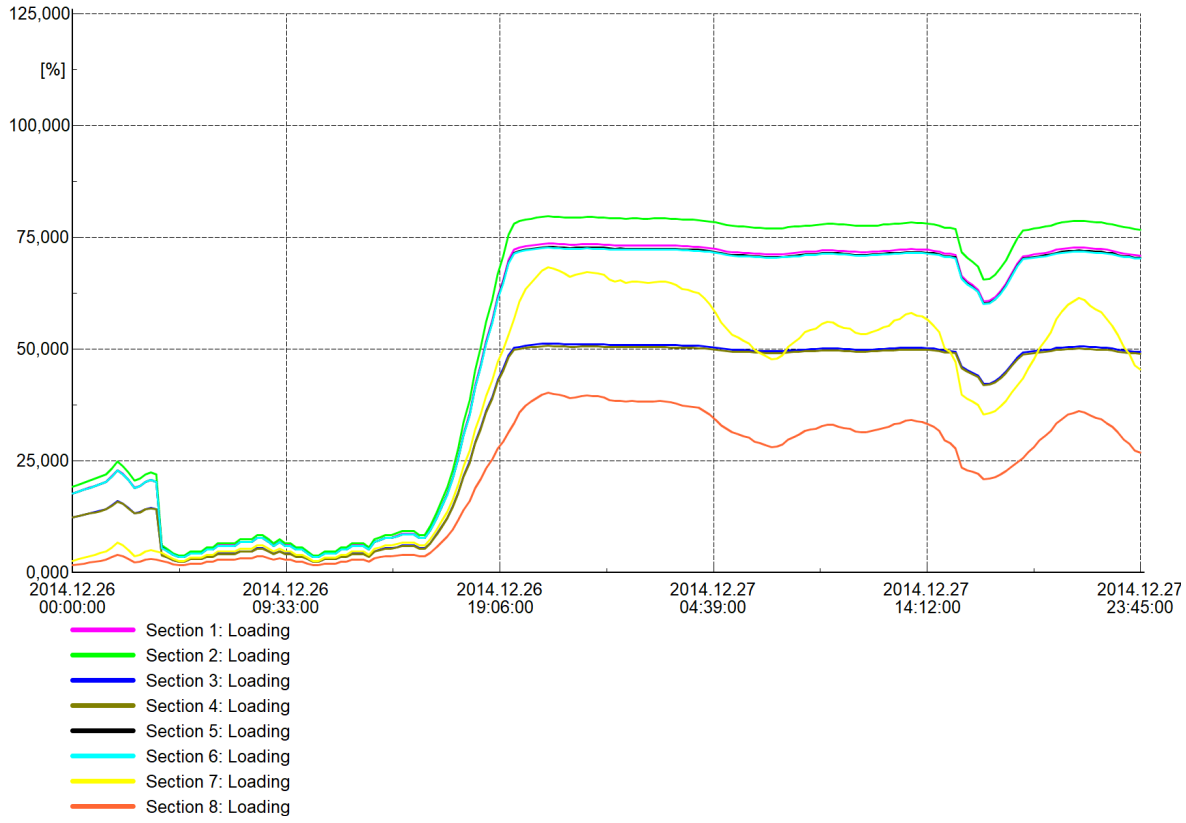

Figure 7.47: Scenario 2 Alt. 4: Loading of sections 1 to 8.

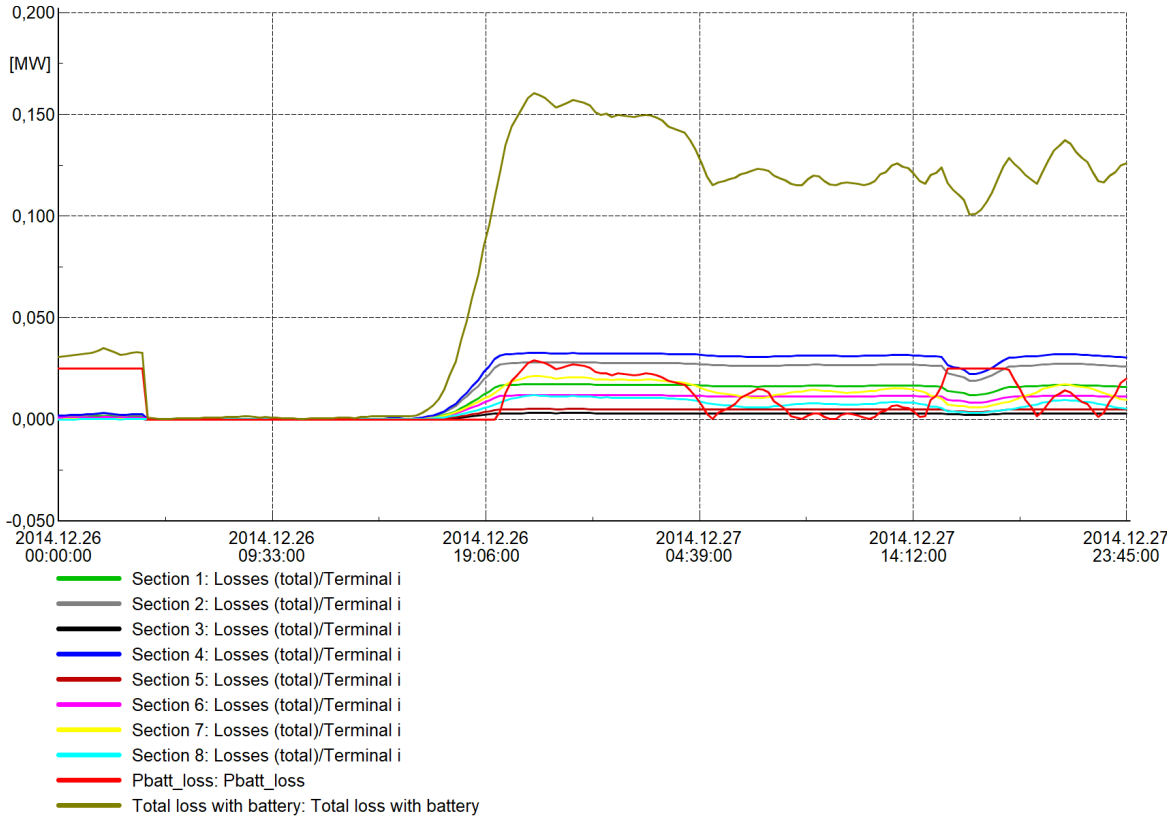

Figure 7.48: Scenario 1 Alt. 4: Loss in sections 1 to 8 and in battery.

7.3 Reactive power in cable system

In many of the simulations presented in this chapter, it has been observed that reactive power has been carried out of the system during low demand periods, into the external grid, despite the fact that there is no active power production in the area. In this section, which is in its entirety based on [27] and [31], this phenomenon will be discussed. Figure 7.49 show a per phase equivalent for the medium length line model.

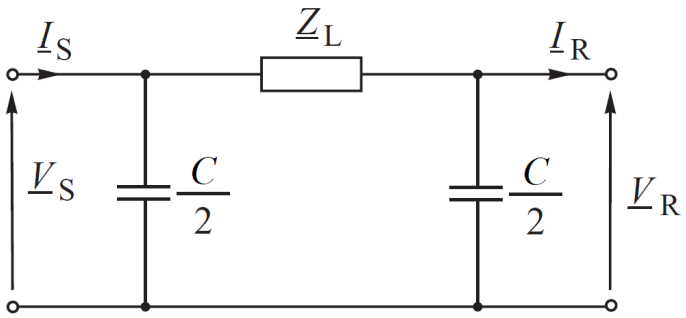

Figure 7.49: π-equivalent for medium length line model [27].

In general the reactive line loss due to active power flow can be positive or negative, such that the line can generate or consume reactive power. The line capacitance causes the line to generate reactive power, as shown in eq. (7.1). The generated reactive power also depends on the voltage, but since the voltage normally has relatively small variations the production is rather constant.

$$Q_{prod} = \frac{V_{LL}^2}{X_c} = \omega \cdot C_d \cdot V_{LL}^2 = B \cdot V_{LL}^2 \tag{7.1}$$

V_{LL} of eq. (7.1) is the line-to-line voltage, the capacitive reactance of the line is given by

$$X_C = \frac{1}{\omega C_d},$$

and B is the susceptance given by

$$B = \omega C_d$$

The net reactive power loss has, however, also an inductive component which determines the amount of reactive power consumed in the line. This is strongly dependent on the loading of the line, and is given by eq. (7.2) where X_L is the inductive reactance and I is the line current.

$$Q_{cons} = 3 \cdot X_L \cdot I^2 \tag{7.2}$$

The net reactive power is as a result determined by eq. (7.3).

$$Q_{net} = Q_{prod} - Q_{cons} = \omega C_d \cdot V_{LL}^2 - 3X_L \cdot I^2 \tag{7.3}$$

When the loading of the line is low, meaning that the current is low, the consumed reactive power in the line is small. The line may then have a positive net reactive power, meaning that it is a reactive source. This may occur in both overhead lines and cables but due to the much larger capacitance of underground cables, as shown in table A.1, the reactive production of cables is larger. E.g. in cases 1.2.1 and 1.2.2 the reactive power export from the area during the low demand period was increased when the overhead line supply was replaced with cable sections, which is a result of the increased capacitance of the cables. The capacitance also increases when increasing the cable cross-section. This is illustrated in the two mentioned cases as well, as a larger reactive production is observed for case 1.2.2 than in case 1.2.1. As a result of the increased production in the new cables of alternatives 2 and 3, a lower reactive power demand from the external grid was observed during the high demand periods than for alternative 1.

When the generated and consumed reactive power is equal, the reactive power loss is zero. This occurs when the active power being supplied is equal to what is called the surge impedance loading (SIL) given by eq. (7.4)

$$P_{SIL} = \frac{V_{LL}^2}{Z_c} = \frac{V_{LL}^2}{\sqrt{\frac{L}{C}}}, \tag{7.4}$$

where the denominator is the surge impedance which is found by setting Q_{prod}=Q_{cons} as shown in eq. (7.5).

$$\begin{aligned} 3 \cdot \frac{V_{ph}^2}{X_C} &= 3 \cdot I^2 X_L \\ \implies \frac{V_{ph}^2}{I^2} &= X_L \cdot X_C \\ &= \frac{2\pi f \cdot L}{2\pi f \cdot C} \\ \implies Z_c &= \frac{V_{ph}}{I} = \sqrt{\frac{L}{C}} \end{aligned} \tag{7.5}$$

Figure 7.50 show examples of the net reactive power of a line as a function of its active load for various voltage ratings. It is observed that when P_R equals P_{SIL}, e.g. the loading is equal to the surge impedance loading, the net reactive power is zero. When the ratio is below one, meaning that P_R is smaller than P_{SIL}, Q_{net} is capacitive meaning that reactive power is generated. Oppositely, when $P_R > P_{SIL}$, the net reactive power is inductive and the line consumes reactive power.

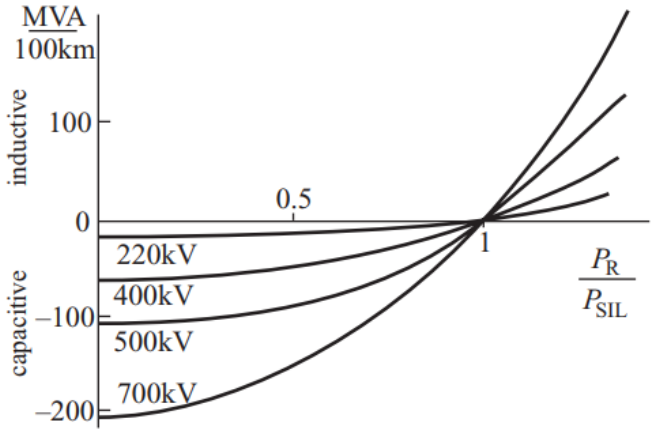

Figure 7.50: Net reactive power of a line as a function of its active power [27].

Chapter 8

Method for economic analysis

In this chapter, the method and approach for the economic analysis will be introduced and discussed. This includes discussions on choices made regarding relevant cost elements used in the analysis. Cost elements of great importance that will be taken into account are the investment cost, cost of electrical losses and operation and maintenance costs. These are all presented generally in chapter 3, while they in this chapter will be discussed more specifically in relation to the project. For elements that are relevant for several solution alternatives, the choice of specific values will also be discussed. Further on the choice of battery technology is discussed, and market and literature surveys of appropriate battery energy storage systems are presented.

As mentioned in chapter 3, a socioeconomic analysis of grid upgrades should compare the costs and benefits for relevant alternatives. Additionally, it is a requirement that the analysis is technologically independent. This implies that no specific action should be preferred over another because of its technology if the analysis show that both solutions could solve the problem in question. Preferably all benefits and disadvantages should be included in the economic analysis, meaning that the action with the best socioeconomic profitability always should be chosen. In practice, however, it is difficult to reflect all costs and benefits in the economic assessment. Therefore, there might occur factors that not are reflected in the socioeconomic analysis which could change the conclusions found.

8.1 Analysis period

The analysis period chosen for the socioeconomic assessment of the grid upgrade scenarios has been set to 30 years. Upgrades in the grid incur large initial investment while the benefit is gathered over an extended period of time. Setting the analysis period to 30 years allow the economic assessment to take these benefits into account. Furthermore, all investments are assumed to be done in the initial year of the analysis period, which applies to both investments in cables and of the BESS. Additionally, it is assumed that the equipment does not have any salvage value at the end of the analysis period. Another simplification that has been done is that the battery lifetime is assumed to be 30 years, such that it does not need reinvestment. In many projects battery degradation would cause the need for this, but for the intended application the amount of yearly cycles is relatively small. Therefore the physical life should be extended, and is thus for the purpose of this analysis assumed to be 30 years.

8.2 Cost elements

8.2.1 Investment cost

The investment cost of each alternative has been estimated on the basis of SINTEF Energy's "Planleggingsbok for kraftnett", where [32] present costs for equipment in the low and high voltage distribution system. Additionally, however, the distribution system operator has provided estimates of costs based on their experience from similar construction cases. As mentioned in chapter 4 it is desired that, if new supply lines are built, they are built as cable connections. Therefore, costs for overhead lines are not thoroughly assessed. Table B.1 show the costs provided in [32] for cables at the 24 kV level, while table B.2 show the elements included in these costs. These cable costs for the different cross sections will be utilized in the analysis to find the most reasonable design.

When constructing a cable connection, however, the cable cost is not the only major contributor to the expense. The costs of digging trenches can amount to a large cost, but varies highly depending on location and ground conditions. The digging cost does not, however, depend on the cable cross-section. The trench costs given in [32] are shown in table B.3, and are divided into three location types. These are "city area", "suburb" and "countryside". Additionally, there occur costs for pipes and grounding at 62 543 NOK/km and 44 833 NOK/km respectively. All these costs are based on surveys that DSOs in Norway has answered, meaning that they provide an average estimated cost for the three location types. The relevant cable paths to the cottage area clearly would be categorized as "countryside". A definition of countryside will however vary depending on where in the country the DSO is located, and the difficulty of digging will have huge local differences. As digging cost clearly is highly depending on the ground conditions, it seems reasonable to utilize local knowledge from the DSO to estimate more correct digging costs for the area.

The cost elements included in the trench digging estimates are shown in table B.4. After discussing these with the DSO an estimated cost for the given area has been suggested. In the DSOs experience from similar cases, the digging and especially blasting costs are significantly higher than those listed in table B.3. The area consists of rough, hilly terrain with typically a shallow soil layer. Therefore, probably a lot more than the 20 meters of blasting given in table B.4 is needed to construct one kilometer of cable trench. As a result, the DSO estimate a trench cost of 600 000 to 800 000 NOK/km for the relevant paths of both alternative 2 and alternative 3. The analysis for each alternative will therefore be conducted with investment cost for trenches of 700 000 NOK/km. [33]

8.2.2 Cost of losses

The cost of losses in the system is calculated on the basis of eq. (3.3). k_p and k_{weq} are equal for all alternatives and their values are shown in table B.5, which are gathered directly from [8]. Furthermore, the maximum power loss ΔP_{max} for each case is found by simulation in PowerFactory as presented in chapter 7. This power loss is assumed to be constant during the analysis period, and the simulated values are therefore utilized in the calculations. The power loss of interest in the analysis is that of sections 1 to 9 of fig. A.1, as this loss will change between the simulation alternatives. As no changes are done either to the load or the grid from the node "Kvia" to any of the end points "Fossen", "Skansen" or "Bøanedsetra 3",

the losses arising in these cables do not change. Therefore the cost of losses in these cables is assumed equal for all alternatives, and is therefore not included in the analysis.

The last parameter of eq. (3.3), the utilization time for electrical losses, is challenging to obtain analytically. To find this one has to integrate the power losses over the entire year. Since this project mostly deals with the worst-case scenario, demand during other parts of the year is not studied. Finding the integrated loss of the one-day load profile is possible, but doing so for the maximum demand day does not represent the consumption pattern e.g. in a low-demand summer day. By assuming the loss during the worst-case scenario as the daily loss one would find a too large value for the loss over the year. Because of this, it is common practice to use an estimated utilization time for electrical losses as it then is sufficient to only simulate the worst-case scenario.

There has earlier been done studies to estimate the utilization time for electrical losses, T_t, for different consumer groups. For example, [34] utilized a program developed by SINTEF to estimate T_t for a range of load types, ranging from office buildings and hotels to single-family houses. Values for the utilization time of losses for cottages has, however, not been investigated. As the consumption pattern of cottages differs greatly compared to other consumer groups, with a large demand during weekends and holidays, it has been concluded that none of the given load types represent cottage consumers well.

Feilberg [35] inform that the utilization time for electrical losses for a cottage will depend highly on whether or not water and sewage are installed. When water and sewage are present it increases the energy demand because the cottage then needs to be heated through the whole year. Thus, an annual consumption of 8000 kWh with water and sewage and 2000-3000 kWh without is assumed. Data given by [35] states that the average peak power demand both with and without water and sewage is around 7 kW for a cottage, which coincides well with what was found in section 6.2.1 and shown in table A.6. Based on this, a utilization time of losses for a cottage with water and sewage could be estimated to slightly above 1000 hours. As described in chapter 2 most of the cottages in the area are large and newly built, almost mimicking a residential house, and clearly have water and sewage installed. As a result, a utilization time for electrical losses of 1000 hours is used in the calculations.

Using the aforementioned values and parameters for each case, the annual cost of losses has been found by inserting them into eq. (3.3). Then the cost of losses for each year has been discounted to year 0 by using the interest rate of 5.82% as given in section 3.1.5. By summing the discounted cost for all years in the analysis period, the total capitalized present value for the cost of losses is found.

The transformer losses are mostly neglected in the analysis. This is based on the fact that there are small differences of the drawn power at each transformer between the alternatives, meaning that the loss difference also is small. For alternative 4, however, an extra transformer is needed to connect the inverter to the 22 kV busbar which not is necessary for the three other alternatives. Therefore, this transformer will induce slightly increased losses which are not shown in the simulations of chapter 7. The cost of these losses will be added to alternative 4 by using the load and no-load losses for the 1250 kVA transformer given in table 8.3. The load losses of the transformer are added to the loss in the rest of the system, and thus included in eq. (3.3). The same is the case with the losses occurring in the battery. This is possible because the utilization time for losses of the battery is assumed to be similar to the one for the total system. When looking at the system as a whole, which has to be done when calculating

the cost of losses this way, the variability of the losses is similar, regardless of the battery being installed or not [36]. This results in the utilization time for losses being independent of the battery, meaning that 1000 hours is used also for the losses originating from the battery and additional transformer. The no-load losses of the transformer, however, have a utilization time for losses of 8760 hours, and are therefore calculated separately.

8.2.3 Cost of operation and maintenance

The cost of operation and maintenance (O&M) are not a very large expense for the DSO in the analyzed area. For the existing overhead lines, the cost mostly consists of forest clearing around the line. This cost is estimated at 100 000 NOK every fifth year for line segments 2 and 4, which in total has a length of around 1.3 km. For cable sections there are no specified O&M costs, meaning that this expense only will be relevant for the reinforcement alternatives which do not remove the existing overhead lines. [18]

For the case where a battery has been installed some O&M cost could be expected. These will be discussed further in section 8.3.

8.2.4 Cost of energy not supplied

Historically the existing supply line has experienced very few outages according to [33], meaning that the cost of energy not supplied generally has been low. Thus, there are few available data who can be used in the socioeconomic analysis. Potential outages in the cottage area could e.g. be because of threes falling over the overhead line. The reinforcement alternatives may have a varying impact on the probability of an outage. When the entire supply is underground cables there are few reasons for the supply to fail. That would then be caused by a fail in the external supply, meaning that an outage in the area not could have been avoided whatever the supply method. By installing a battery there exist an opportunity for the area to be supplied single-handedly by the battery. This requires the battery output power to be able to match the load demand in the area, which may be possible in some cases. This is would, however, only be an option during short outages while the demand is relatively low. Therefore, the overall difference of CENS between the existing supply with and without a battery is assumed to be small. Replacing the existing overhead lines with cables could provide some benefit in this context, but due to the lack of data about outages in the relevant area the cost of energy not supplied is neglected in the case of this project.

8.3 Battery technology and cost

In this section the selection of battery technology is discussed, and required features of the BESS are introduced. Further, market and literature studies of available BESS-solutions that are appropriate for the purpose is introduced. The survey results are used to estimate the cost of installing an energy storage system, which further is used in the socioeconomic analysis of chapter 9.

A study of different battery technologies have been done in [2], and table 8.1 show a comparison of characteristics for the battery technologies that have been studied in the report. The table

summarizes some of the typical values of important parameters for the technologies, while pros and cons for each technology are highlighted as green and red respectively. The key takeaways discussed in [2] will be presented in the next paragraph.

Table 8.1: Comparison of typical parameter values of battery technologies [2]. Based on [37].

Technology	Spec. energy [Wh/kg]	DOD [%]	Eff. [%]	Cycle life	Maturity	Hazard	Other
Lead-acid	30-50	max. 50	60-90	1000	Very high	No	[1]
NaS	200	50-90	75-90	2 500 - 5 000	Medium	Fire	[2]
Lithium-ion	250	80	85-95	5 000 - 10 000	High	Fire	
Flow	10-20	100	70-80	Above 15 000	Low	No	[3]

Lead-acid batteries are the most mature battery technology, and is known to have a low investment cost. Its depth of discharge and energy density is, however, low. Also the cycle life of approximately 1000 cycles is poor, meaning that lead acid batteries probably cannot operate over many years without replacement. Sodium-sulphur (NaS) is another well-proven technology which have seen use in grid scale operation. NaS has great energy density and efficiency, while the cycle life also is satisfactory. The operating temperature is the major drawback at around 300-350°C, causing the operation to be difficult and posing a great hazard if faults occur. Due to this, the technology has not seen a great deal of usage the past years. Flow batteries have low specific energy and need some degree of maintenance. The upsides of this technology are its great depth of discharge of 100% and its very long lifetime of over 15 000 cycles. The technology is, however, presently quite early in its development, meaning that there are few projects in grid-scale operation that can prove its long-term performance.

Usage of lithium-ion batteries in large scale applications has in the last couple of years grown immensely. Rapid growth of EV manufacturing and sales has caused the lithium-ion battery price to plummet, making them viable for some stationary applications. This technology got an outstanding efficiency of about 95% round trip, in addition to a very high power and energy density making it preferable in portable applications such as EVs. Its cycle life is fairly good at 5 000 - 10 000 cycles depending on the depth of discharge. The focus on and decreasing price of the lithium-ion technology has made it the dominant force for grid applications the last couple of years. At the end of 2016 lithium-ion represent more than 80% of the installed power and energy capacity for grid applications in the U.S. Thus, there are a lot of MW-scale projects in stationary use which can be utilized as a reference for the intended operation. A lot of these project are mostly intended for power quality measures such as frequency and voltage regulation, requiring high power and short duration. For long discharge times, which is the goal in this case, the technology may prove to be expensive. As a lot of lithium-ion cells has to be stacked and managed individually to achieve the required energy capacity, the price is increasing for these type of applications. [2]

To sum up, all these technologies are able to fulfill the requirements for the intended operation, but flow and lithium-ion batteries seem to be the most provident. As will be discussed in the next section, however, the requirement of a turnkey solution limits the selection basically to only including lithium-ion products. As such, presently there seem to be little incentive to choose one of the other technologies.

[1] Thermal management.
[2] High temperature.
[3] Maintenance.

8.3.1 Market survey

Gathering the cost of installing a battery energy storage system proved to be a difficult task for the purpose of this project. Though there are a plethora of manufacturers who supply such systems none of which has been investigated got openly available prices for large scale systems. As a result, an attempt has been made to contact some of the manufacturers to inquire prices for turnkey solutions.

Such a solution, which includes everything needed for the system to operate, is a must for the DSO who has limited to none experience with designing a battery system. Therefore, the focus has been on so-called containerized energy storage systems. These systems typically include batteries, inverter, monitoring, a battery management and control system, fire detection and suppression, and HVAC equipment providing heating, ventilation and air conditioning. In short, such a containerized solution should provide everything needed for the battery energy storage system to function, while a transformer is required to connect it to the 22 kV grid.

As mentioned earlier there are many different manufacturers that assemble containerized energy storage solutions. These are located around the globe and ranges from huge well-known conglomerates such as LG [38], BYD [39], SAFT (TOTAL) [40] and Mitsubishi [41] to smaller companies dedicated to the task such as PBES [42], Autarsys [43] and HRESYS [44]. All these manufacturers assemble turnkey solutions where power and energy capacities varies greatly. Each of them provides different container sizes, often ranging from 12-ft to 53-ft, which affect the number of battery modules the container can accommodate. Also for a given container size the power and energy capacity varies greatly across the manufacturers, which often also have several configurations for each container size. It has therefore been a challenging task to navigate the market for containerized solutions. Due to the extensive desired discharge time, the focus has been to find configurations that pack a large energy capacity while keeping the output power relatively low. Gathering price information has shown to be challenging for the purpose of this master's thesis. Many manufacturers have been contacted, including but not limited to those mentioned earlier in this paragraph, but most of them have been unwilling to provide economic data for their products due to confidentiality concerns.

Three honorable exceptions did, however, reply with estimates for some configurations. One of them, who are kept anonymous of confidentiality reasons, have given an indicative price of a 1.2 MW/2.5 MWh container utilizing lithium-ion batteries, and the additional price for a matching DC/AC bidirectional inverter. Another manufacturer, BYD, could not provide cost data due to confidentiality, but has given some industry standard ranges to utilize in the analysis [29]. These costs do not represent prices for any of the products BYD offers, and is merely an indicative estimation for the industry as a whole. The third and last manufacturer that has provided feedback on the inquiry is the Chinese company HRESYS. They provide fully equipped battery containers, but without the required inverter. Their containerized BESS is priced at 260 to 280 $/kWh, which has to be added to the cost of a suitably sized inverter [45]. The maximum given energy capacity of their 40-foot container is 3.1 MWh [24]. The same manufacturer also provided the price for a lead-acid battery, which could serve as a reference [45]. These batteries are not containerized, and as such a battery storage system has to be built from scratch with the modules. All the provided estimations are converted to cost in $/kWh and presented in table 8.2, which show investment costs for an installed energy storage system ready to operate but not the cost of connecting it to the grid. The BESS configuration is also stated in the table as it specifies the discharge duration, proving to

be an important parameter when providing the per-energy-unit cost, which will be examined in section 8.3.2. For each cost estimate there are also different cost elements included in the given value. Therefore a comment is inserted to indicate what the given price is including.

Table 8.2: Investment cost for containerized lithium-ion energy storage.

Cost [$/kWh]	Configuration	Comment
446	1MW/2.5MWh	Without instal. labor, grid connection and EMS
325	500kW/1MWh	Without instal. labor and grid connection/transformer
581	1MW/1MWh	Fully installed, everything incl. for LV-side. No transformer
353	1MW/3.1MWh	Without instal. labor and grid connection/transformer.
190	-	Lead-acid without BMS, instal., housing or grid connection

The BESS is assumed to have an output DC voltage in the range 700-800 V. To connect it to the 22 kV distribution grid, the output voltage need to be increased to the correct voltage level. By deploying a specialized DC/AC inverter it may be possible to increase the voltage directly to the 22 kV level. Due to the limitations present for this project this opportunity has not been investigated, as the initial feeling is that this solution would incur large investment costs. It seems therefore reasonable to assume that the DSO need to install a transformer between the DC/AC bidirectional inverter and the 22 kV busbar. The price of three transformers with different ratings have been gathered[1] and is listed together with P_k and P_0 losses in table 8.3, but only the 1250 kVA one will be utilized further [46].

Table 8.3: Investment cost of transformer [46].

Rating [kVA]	Cost [$]	P_0 [W]	P_k[W]
1000	15 502	1 230	8 430
1250	19 368	1 260	10 580
1600	21 544	1 520	12 870

8.3.2 Literature survey

In addition to surveying potential specific products in the market as described in the previous section, publications regarding the cost of batteries has been studied. This way the estimates of some renowned research facilities can be compared to the figures given by the manufacturers. All the information will then be used to find a suitable approximation for the price of a battery storage system, which then will be used in the economic analysis.

Bloomberg NEF operates with a price of 209 $/kWh (2017 USD) in [47] for lithium-ion batteries, as depicted in fig. 8.1. The forecasted battery price is also depicted in the figure with a reduction to 70 $/kWh in 2030, which is a reduction of 67% from today. Looking at the historical prices a reduction of 79% is seen from 2010 to 2017. The price plummeting has been driven by the large-scale deployment of electric vehicles, which is also the reason for further price reduction as manufacturing capacity is rapidly increasing.

[1] Converted from NOK to USD with a rate of 1 USD=8.7 NOK

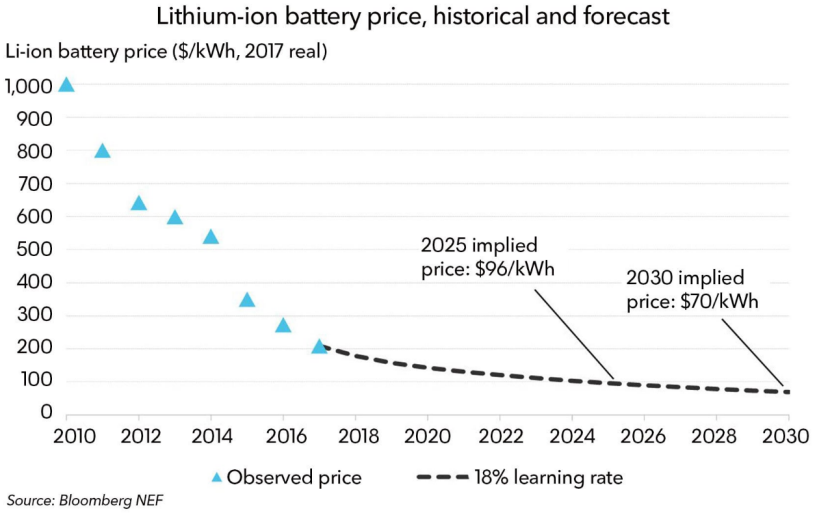

Figure 8.1: Historical and forecasted lithium-ion battery price [47].

It has to be noted, however, that the given cost in the previous paragraph includes only the battery module. As have been discussed earlier there is a lot of equipment and software necessary to have an operational battery energy storage system. A study that takes all factors into account and estimates the total system cost is presented by NREL in [48]. One of the key takeaways is shown in fig. 8.2 where the cost per kWh is presented for utility-scale containerized lithium-ion battery storage. The cost is based on a 60 MW system and the figure depict the cost for several discharge durations from 0.5 hours to four hours, meaning 30 MWh to 240 MWh energy capacity. The per-energy-unit battery cost is set to be constant at 209 $/kWh which is the same as was found in [47]. It is observed that the BESS price per kWh clearly is lowest when the discharge duration is prolonged, as the cost is 380 $/kWh for a four-hour system and 895 $/kWh for a 0.5-hour system. This may be caused by the fact that some of the non-battery related costs are independent of the energy capacity. Looking e.g. at the given inverter cost it amounts to $4.2 million for all duration alternatives. Spreading the inverter cost over many more kWh thus will reduce the per-energy-unit cost. Other cost elements, such as e.g. the installation labor cost, does not have this characteristic as the total labor cost clearly increases as more containers have to be installed. The installed capacity does, however, increase more than the cost increase, causing the $/kWh cost to decrease. As a result, the battery cost in the four-hour system accounts for 55% of the total cost, while it only accounts for 23% in the 0.5-hour system. [48]

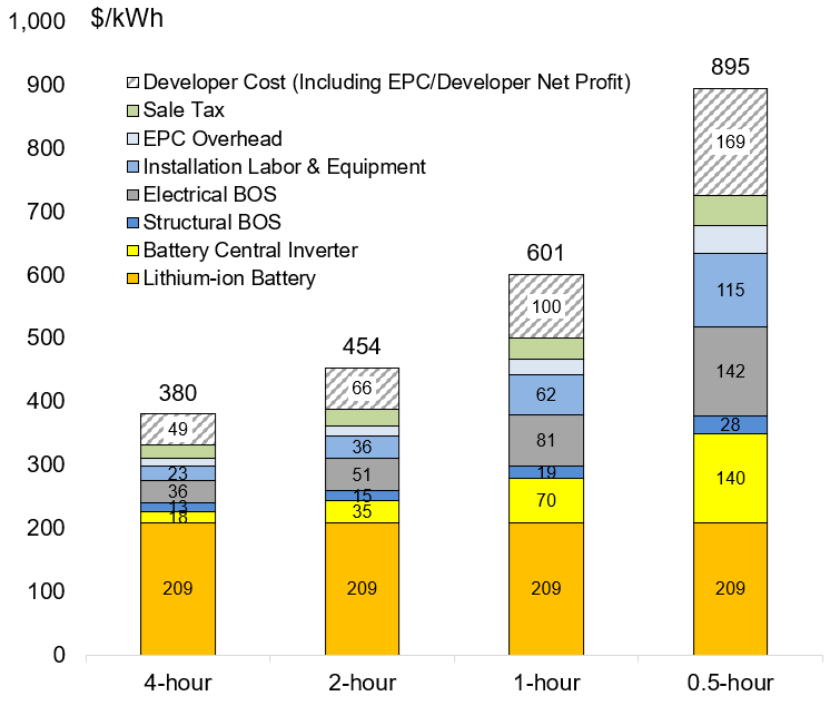

Figure 8.2: Lithium-ion battery storage cost for durations 0.5 to 4 hours [48].

As seen in chapter 7 it is in this project desired to have a large energy capacity, while huge output power is not needed. Therefore, it is reasonable to refer to the long-duration costs given in fig. 8.2. The costs of table 8.2 are given for rated discharge durations of 2-3 hours, and all are in the same order of magnitude as what is given in [48] for this discharge duration. As the discharge duration of this project surpasses 4 hours, with peak shaving periods of 8-10 hours, it may be possible to utilize the economics of scale to further decrease the per kWh cost of the installed BESS and as such obtain a better cost estimation for this area of application. To do this a regression analysis has been done based on fig. 8.2 and data given in [48], and this is used to extrapolate the cost for an eight-hour discharge system.

First, the cost of each model component is calculated in the 60 MW system for all of the discharge durations. The battery cost per kWh is assumed constant and is as such left out of this calculation. The same is done to the EPC overhead and the sale tax, as these are given as percentages of the other components in [48]. The calculated cost elements are visualized as a function the discharge duration, and a second-order polynomial regression is then applied to each of the components. Figure 8.3 show the result of this visualization together with the regression that has been extended one period, meaning that it represents the eight-hour discharge case. Figure E.1 show the same figure with the equations for each of the components. These equations are used to find the total cost for each element in the eight-hour 60 MW system. Furthermore, the per-energy-unit cost for each component is found by dividing the total cost by the energy capacity of 480 MWh. Table 8.4 present the total and per-energy-unit costs for the eight-hour system.

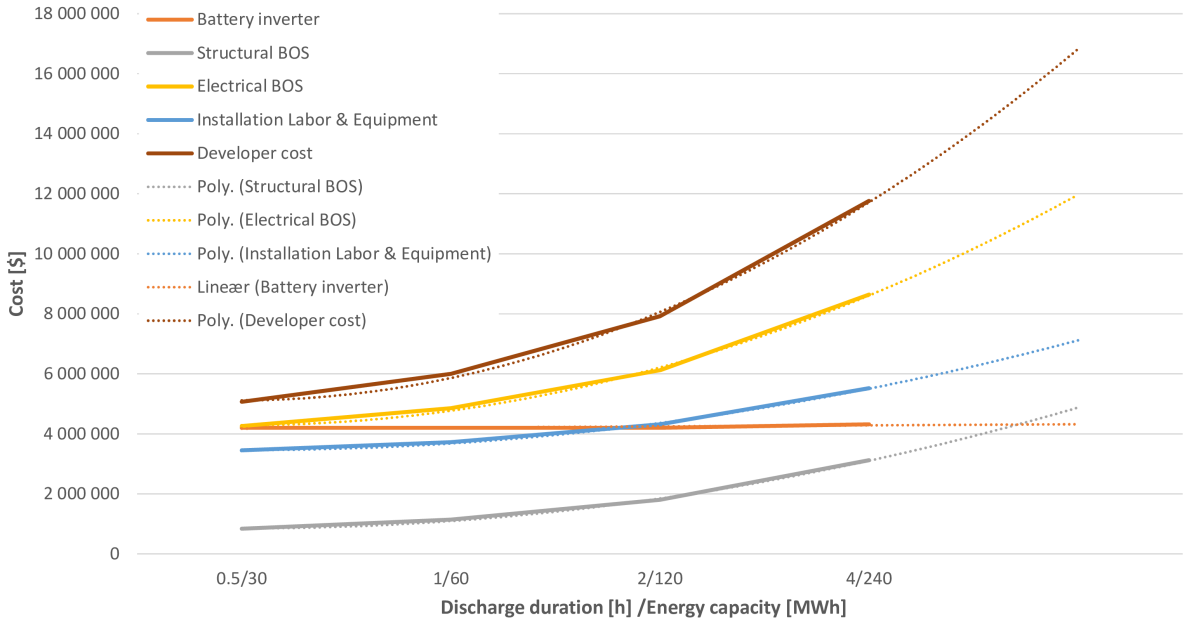

Figure 8.3: BESS component cost regression. Based on values from [48].

Table 8.4: Total cost of lithium-ion energy storage system. Based on values from [48].

Component	Total cost 480 MWh [M$]	per-energy-unit cost [$/kWh]
Lithium-ion battery	100.32	209.0
Battery Inverter	4.20	8.8
Structural BOS	4.88	10.2
Electrical BOS	11.97	24.9
Installation Labor & Equipment	7.12	14.8
EPC overhead	-	8.0
Sals tax	-	20.0
Developer cost	16.82	35.0
Total	158.75	331.0

Figure 8.4 show the resulting battery storage cost for an eight-hour system together with the values of 0.5, 1, 2 and 4 hour systems from fig. 8.2. Even if the results are calculated through the use of a 60 MW system, the cost per kWh should be applicable also for other system sizes. The cost of 331 $/kWh could therefore be utilized in all system configurations with eight hours rated discharge such as e.g. 200 kW/1600kWh, 1 MW/8MWh or 5 MW/40MWh.

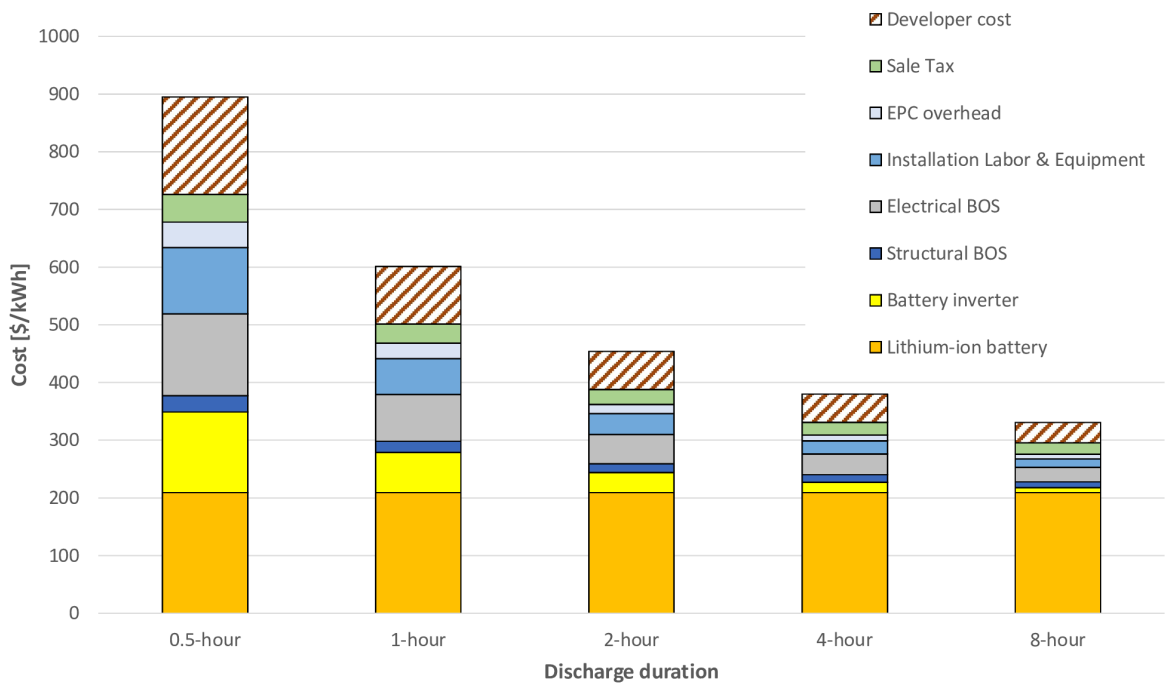

Figure 8.4: Lithium-ion battery storage cost for durations 0.5 to 8 hours. Based on values from [48].

8.3.3 Battery investment cost selection

As discussed in sections 8.3.1 and 8.3.2, there are many different parameters influencing the per-energy-unit cost of a battery energy storage system installation. Some are more difficult to quantify than others, and some may have huge local variations throughout the world. As the market survey revealed there are many opportunities when configuring the system, and each manufacturer operate with different sizes and ways to specify their prices. As a result, the collected cost data varies greatly. Knowing what the variation is caused by is difficult as both configuration and the provided services in the product differ between each manufacturer. The literature study revealed that the discharge duration has a large impact on the cost per kWh, which is an especially important finding for the intended area of application as the desired discharge period is very long. The base for the cost given in the literature and by the manufacturers seems, however, to bee quite similar. Looking e.g. at the value including all costs for the 1 MW/1 MWh system from table 8.2 it is relatively similar to the one-hour discharge duration cost given in fig. 8.2, at 581 $/kWh and 601 $/kWh respectively. This may indicate that the data basis for the regression analysis conducted in the previous section does replicate the market survey costs relatively well. As a result the eight-hour estimation of fig. 8.4, 331 $/kWh, is used in the economic analysis.

8.3.4 Additional cost

In addition to the initial capital cost, there are other cost elements related to the BESS that will be present during the analysis period. The need for maintenance is typically low for lithium-ion batteries, but some monitoring and periodic inspections may be necessary [49].

Thus, maintenance costs are typically low and are therefore neglected. Additionally, the air conditioning, fire suppression and monitoring systems require some ancillary power to operate. These systems should usually not require a lot of power, and since it is hard to estimate the costs related to this it will be neglected. To control the system behaviour an energy management system must be utilized. Therefore the DSO need to invest in such a system that fit their needs, if it is not already included when buying the containerized solution. An industry standard service fee for an AI automation management system is estimated to 20 000 $/MW annually by [29]. As the benchmark cost of [48] includes the energy management system in the "Electrical BOS" component, the cost for this is not added as an annual operational cost.

Chapter 9

Results and discussion of economic analysis

This chapter will present results of the economic assessment that has been conducted for each of the relevant solution alternatives presented in chapter 4. The results are obtained through the methods and considerations presented in chapter 8, and is based on the simulation results obtained in chapter 7. The results will be presented in the same manner as in the technical analysis, where section 9.1 includes all alternatives in load scenario 1 and section 9.2 deals with all alternatives for the second load scenario. The investment cost for alternatives 1, 2 and 3 will be equal between the load scenarios, but the cost of losses will highly depend upon the scenario. The results for each alternative will be presented and shortly commented. After all alternatives are presented for each load scenario their economic viability is compared and discussed in section 9.3. Some important prerequisites and assumptions that previously have been presented are summarized in table 9.1.

Table 9.1: Prerequisites for the economic analysis.

Element	Assumption
Calculation interest rate	5.82%
Analysis period	30 years
Physical life BESS	30 years
Salvage value of cables	0 NOK
CENS	0 NOK
BESS cost	331 $/kWh
Conversion rate	1 $=8.7 NOK
Utilization time for electrical losses	1000 h
Cable cost	See table B.1
Trench digging cost	0.7 MNOK/km

9.1 Load scenario 1

This section will present the cost of each alternative in the case of load scenario 1, which has been analyzed in section 7.1.

9.1.1 Case 1.1: No grid upgrade

In this case, no investments are done in the grid, as the technical lifetime of the existing components surpass the analysis period. As a result, cost of losses and O&M are relevant in this alternative. Table 9.2 show the total present value during the analysis period.

The results show that the total cost of supplying the area during the analysis period with the existing grid is 0.97 MNOK. The cost of power losses due to the 48.9 kW loss in the relevant sections (1 to 8) amount to 0.64 MNOK, while the maintenance cost equals 0.33 MNOK.

Table 9.2: Case 1.1: Total discounted costs.

Element	Cost [Million NOK]
Investment	0
Loss	0.64
O&M	0.33
SUM	0.97

9.1.2 Case 1.2: Refurbish existing connection

Here the cost of refurbishing the supply with a cable connection is found, and the resulting O&M and loss costs are established. Corresponding to the technical analysis done in section 7.1.2 the total costs are found for cables of cross-sections 150 and 240 mm^2. Since the existing lines and cables have to be removed, an additional cost of 0.1 MNOK/km occur. Tables 9.3 and 9.4 show the total discounted cost for alternative 2.1 and 2.2.

Table 9.3: Case 1.2.1: Present value of future costs.

Element	Cost [Million NOK]
Investment	2.75
Loss	0.22
O&M	0
SUM	2.97

The results show that the total investment cost when replacing section 1 to 6 with a 150 mm^2 cable is 2.75 MNOK. The maximum power loss of 16.6 kW incur a present value cost of losses of 0.22 MNOK during the analysis period, while the O&M costs are zero as mentioned in chapter 8 since the entire grid consist of underground cables. This results in a total discounted cost of 2.97 MNOK.

Table 9.4: Case 1.2.2: Present value of future costs.

Element	Cost [Million NOK]
Investment	2.86
Loss	0.16
O&M	0
SUM	3.02

For a 240 mm^2 cable the investment cost is increased to 2.86 MNOK. Decreasing the power loss to 12.0 kW, however, has lowered the present value cost of losses to 0.16 MNOK. The O&M cost is still zero, making the total discounted cost of this alternative 3.02 MNOK.

9.1.3 Case 1.3: Add new connection

Here the cost of adding a new connection to the external grid from the node "Hydla 2" is calculated, and the resulting O&M and loss costs are established. Corresponding to the technical analysis done in section 7.1.3 the total cost are found for cables of cross sections 150 and 240 mm^2. Tables 9.5 and 9.6 show the total present value for the two alternatives.

Table 9.5: Case 1.3.1: Present value of future costs.

Element	Cost [Million NOK]
Investment	4.84
Loss	0.20
O&M	0.33
SUM	5.37

The results show that the total investment cost when adding another supply connection of an TSLE 3x1x150 cable, while keeping the existing supply connection as it is, amounts to 4.84 MNOK. The maximum power loss of 15.5 kW give rise to present value costs of 0.20 MNOK during the analysis period, while the O&M costs are 0.33 MNOK. This results in a total present value of 5.37 MNOK.

Table 9.6: Case 1.3.2: Present value of future costs.

Element	Cost [Million NOK]
Investment	5.06
Loss	0.15
O&M	0.33
SUM	5.54

For the 4.5 km TSLE 3x1x240 cable, the investment cost increases to 5.06 MNOK. The power loss has been decreased to 11.8 kW, which has limited the present value of the cost of losses to 0.15 MNOK. The O&M cost is the same, as nothing is done to the existing overhead line, at 0.33 MNOK. The present value of the alternative is therefore 5.54 MNOK.

9.1.4 Case 1.4: Install battery

In this section, the cost of installing a 9.5 MWh battery energy storage system, rated for eight hours discharge, is found. Table 9.7 show the present value cost of the alternative when the investment is done at the start of the analysis period. The per-energy-unit cost of 331 \$/kWh is used, and converted to NOK by a rate of 8.7.

Table 9.7: Case 1.4: Present value of future costs.

Element	Cost [Million NOK]
Investment	27.53
Loss	0.83
O&M	0.33
SUM	28.69

Because of the huge necessary capacity of the battery the investment cost of the BESS is 27.36 MNOK, while an additional 0.17 MNOK is due to the transformer investment cost. The transformer loading loss of 8.43 kW is added to the maximum power loss of 51 kW found in the simulation, in total accounting for a cost of 0.78 MNOK during the analysis period. The transformer no-load losses incur a cost of 0.05, making the total discounted cost of losses 0.83 MNOK. The O&M cost for the battery is as stated in chapter 8 neglected, but since the overhead line in this case is present some O&M cost occurs.

9.2 Load scenario 2

This section presents the results of the economic analysis which has been conducted on the basis of the technical analysis of section 7.2, dealing with the critical demand of load scenario 2.

9.2.1 Case 2.1: No grid upgrade

In this case no investments are done in the grid, which leads to it having a critical loading as shown in section 7.2.1. As a result, only cost of losses and O&M are relevant in this alternative. Table 9.8 show the total discounted cost during the analysis period.

The calculations show that the elevated power losses give rise to a large cost of losses, which amount to a present value of 2.34 MNOK for the entire analysis period. The O&M cost is unchanged, meaning that the total present value for this alternative is 2.67 MNOK.

Table 9.8: Case 2.1: Present value of future costs.

Element	Cost [Million NOK]
Investment	0
Loss	2.34
O&M	0.33
SUM	2.67

9.2.2 Case 2.2: Refurbish existing connection

Here the alternative of refurbishing the supply connection is investigated on the basis of the results found in section 7.2.2. According to the DSO, a cost of 0.1 MNOK/km should be added for removing the existing components. As is done in the technical analysis, two different cable

cross sections are examined. Tables 9.9 and 9.10 show the present value for 150 and 240 mm^2 cables respectively.

Table 9.9: Case 2.2.1: Present value of future costs.

Element	Cost [Million NOK]
Investment	2.75
Loss	0.95
O&M	0
SUM	3.7

The investment cost of this alternative is the same as in case 1.2.1, i.e. 2.75 MNOK. The maximum power loss has, however, greatly increased. The 72.4 kW loss now gives a present value cost of 0.95 MNOK during the analysis period, while the O&M costs are zero. This results in total discounted cost of 3.7 MNOK.

Table 9.10: Case 2.2.2: Present value of future costs.

Element	Cost [Million NOK]
Investment	2.86
Loss	0.75
O&M	0
SUM	3.61

For the TSLE 3x1x240 cable the investment cost is increased to 2.86 MNOK. Decreasing the power loss to 54.0 kW, however, has lowered the present value of the cost of losses to 0.75 MNOK. The O&M cost is still zero, making the total discounted cost of this alternative 3.61 MNOK.

9.2.3 Case 2.3: Add new connection

This section deals with the case where a new cable connection to the external grid is built. The total cost is found for cables of cross-sections 150 and 240 mm^2, where tables 9.11 and 9.12 show the total discounted cost for alternative 3.1 and 3.2 respectively.

Table 9.11: Case 2.3.1: Present value of future costs.

Element	Cost [Million NOK]
Investment	4.84
Loss	0.65
O&M	0.33
SUM	5.83

Table 9.11 show that the total discounted cost of the new 150 mm^2 cable connection is 5.83 MNOK. The investment and O&M costs have not changed compared to case 1.3.1, while the increased loss causes the present value cost of losses to be 0.65 MNOK.

Table 9.12: Case 2.3.2: Present value of future costs.

Element	Cost [Million NOK]
Investment	5.06
Loss	0.47
O&M	0.33
SUM	5.86

For the TSLE 3x1x240 cable an investment cost of 5.06 MNOK still arises, while the power loss of 36 kW causes a present value cost of losses of 0.47 MNOK. O&M cost is the same as in all alternatives including the overhead line sections at 0.33 MNOK, causing the present value of the alternative to be 5.86 MNOK.

9.2.4 Case 2.4: Install battery

As established in section 7.2.4 a BESS rated 1.2 MW/10MWh is now needed to be able to diminish the critical loading of the supply connection. The results of the present value calculation are presented in table 9.13, where a per-energy-unit cost of 331 $/kWh still is utilized.

Table 9.13: Case 2.4: Present value of future costs.

Element	Cost [Million NOK]
Investment	28.97
Loss	2.26
O&M	0.33
SUM	31.55

The necessary energy capacity results in an investment cost of 28.80 MNOK for the BESS in this case, while the transformer cost of 0.17 MNOK results in a total investment of 28.97 MNOK. The maximum power loss of 160 kW, plus transformer power loss of 8.43 kW, give rise to a cost of losses at 2.20 MNOK, while the transformer no-load loss incurs another 0.05 MNOK. O&M costs are 0.33 MNOK, similarly to every alternative that includes the overhead line sections.

9.3 Overview and discussion of economic viability

In this section an overview of the results from the economic analysis is given, and the results are compared and discussed. Table 9.14 show the total discounted cost of each alternative for the two load scenarios. The alternatives are referred to chapter 4, which also describe the basics of each alternative.

Table 9.14: Result overview of economic analysis.

Alternative	Cost load scenario 1 [MNOK]	Cost load scenario 2 [MNOK]
1	0.97	2.67[1]
2.1	2.97	3.70
2.2	3.02	3.61
3.1	5.37	5.83
3.2	5.54	5.86
4	28.69	31.55

9.3.1 Load scenario 1

By observing table 9.14 it is evident that alternative 1 is the most economically desirable option for the first load scenario, with the existing assumptions and constraints. For this alternative, which is studied in case 1.1, no initial investment is conducted, meaning that all costs are caused by losses, operation or maintenance. For alternative 1 to be viable, however, there are some assumptions that need to hold as no action is done to the existing grid. First, the physical life of the grid connection is assumed to surpass the analysis period. This implies that their physical condition must continue to be adequate, meaning that the overhead lines and underground cables must be able to provide the necessary power throughout the analysis period. The thermal capacity of the lines is also assumed to be good enough for this load scenario, which according to the simulations of chapter 7 should be the case. Additional assessment on the benefit of decreasing the probability of faults, by replacing the existing connection or adding another connection with cables, should also be conducted and taken into account in the evaluation.

It is worth noting that the first load scenario replicates the load situation arising because of an imminent expansion of the cottage area. The load is assumed to be constant which is probably not going to be the case, as more expansions should be expected during the 30 year analysis period. The second cheapest alternative, alternative 2.1, is 2 MNOK more expensive than the cheapest. The reinforcement reduces the cost of losses with 66%, but this is not enough to compensate for the extensive investment that has to be done. By installing 240 mm^2 cables instead the cost of losses are further reduced with 10 percentage points, a total reduction of 76% compared to alternative 1. The investment cost of this cable type has, however, increased more than the loss reduction incur, such that alternative 2.2 in total is slightly more expensive than alternative 2.1.

For both variations of alternative 3, the increased length of connecting to the external grid has greatly increased the investment cost compared to alternative 2. Even though the cost of tearing down the existing equipment is removed, keeping the overhead lines do in fact incur larger costs than this through its need for maintenance. The cost of losses for each variation of alternatives 2 and 3 are relatively similar, meaning that one or the other is not strongly preferred in that sense. In total there seem to be no incentive to choose alternative 3 instead of alternative 2. Some effects do not, however, show its cost or benefit through the economic analysis. For example, a value has not been put on the benefit of having redundancy in the

[1]Not technically feasible.

supply. Additionally, the grid outside of the analyzed area may be affected in different ways for each alternative. Thus if a techno-economical analysis is conducted for a larger area of the DSO grid, the results for the alternatives could change diametrically due to additional costs and benefits being relevant.

When it comes to the battery energy storage system it showed for this load scenario to be more than 29 times more expensive than the cheapest alternative. As was discovered in section 7.1.4 the installation of the battery did in fact increase the losses of the supply for this load scenario, as the battery gave rise to more losses than was removed from the lines. As a result, the cost of losses are marginally higher for alternative 4 than for alternative 1. As the maintenance cost of the overhead line sections still are present the O&M costs of alternative 1 and 4 are equal. The difference then is the huge investment cost of the BESS which is over 27 MNOK, due to the large capacity needed for the long discharge period. One benefit that not is calculated is the possibility of supplying the cottage area with the battery in islanded mode, in the event of an outage of the grid connection. It is, however, unrealistic that this or any other external factors could compensate for the huge investment a battery is incurring.

When the system boundary is set as it is in this project, the techno-economic analysis of this load scenario clearly show that no action should be done to the supply of the cottage area.

9.3.2 Load scenario 2

Similarly to the first scenario it is observed from table 9.14 that alternative 1 is the most economically appealing. As shown in section 7.2.1, however, this load scenario causes the supply to be critically loaded, meaning that the alternative is not technically possible. This means that the course of action has to be chosen from alternatives 2, 3 or 4.

Alternative 2 with the 240 mm^2 cable show to be the most cost efficient with a total present value of all future costs of 3.61 MNOK, which include 2.86 MNOK in investment and 0.75 MNOK cost of losses. The increased power in the cables has made alternative 2.2 more beneficial than alternative 2.1, as the cost of losses in the latter now is 0.95 MNOK. As a result, the elevated investment cost of 240 mm^2 pays off throughout the analysis period, with a present value cost that is 0.09 MNOK less than for alternative 2.1. Regarding alternative 3 the situation is similar to what was observed in the first load scenario. Because of the distance to the external grid, this alternative still is significantly more expensive than both variations of alternative 2. Once again other factors outside of the scope for this project may indicate that having an additional connection to the cottage area compensates for the increased investment, but these will not be elaborated on further. Worth noting is that the 240 mm^2 variation of alternative 3 is only 0.03 MNOK more expensive than the 150 mm^2 variation, which is a significant decrease from 0.17 MNOK in load scenario 1.

For alternative 4, where a 10 MWh BESS is installed, the present value cost given in table 9.14 for the entire analysis period is 31.55 MNOK. This is approximately 8.5 times more than the cheapest possible alternative. As 0.5 MWh more is needed in this case compared to the first load scenario, an investment cost increase of almost 1.5 MNOK is observed. The cost of losses has also increased with approximately the same amount, but in this load scenario the battery is able to decrease the maximum power loss compared to alternative 1. The reduction from 179 kW to 160 kW decreases the cost of power loss during the analysis period with about 0.25

MNOK. Nevertheless, installing BESS is still a clearly more expensive solution than replacing or adding cables in the analyzed grid area.

9.3.3 Cable dimensioning

In the two previous sections there has been observed a difference regarding which cable is the most profitable. For load scenario 1 the 150 mm^2 cable creates the cheapest variation for both alternative 2 and 3. For load scenario 2, on the other hand, 240 mm^2 is the cheapest for alternative 2, while 150 mm^2 is marginally cheaper for alternative 3. While the investment cost is constant between the load scenarios, the increased load demand causes higher losses in the cables. As the smallest cable have a higher resistance, its power loss increases more than for the larger cross-section cable. As a result, the difference of investment cost is made up for by the difference in cost of losses. Figure 9.1 show the investment cost, cost of losses and the total cost of an arbitrary line as a function of its cross-section, when the load and length are kept constant. The figure is used as an illustration, and the values are not related to the analyzed system in this thesis.

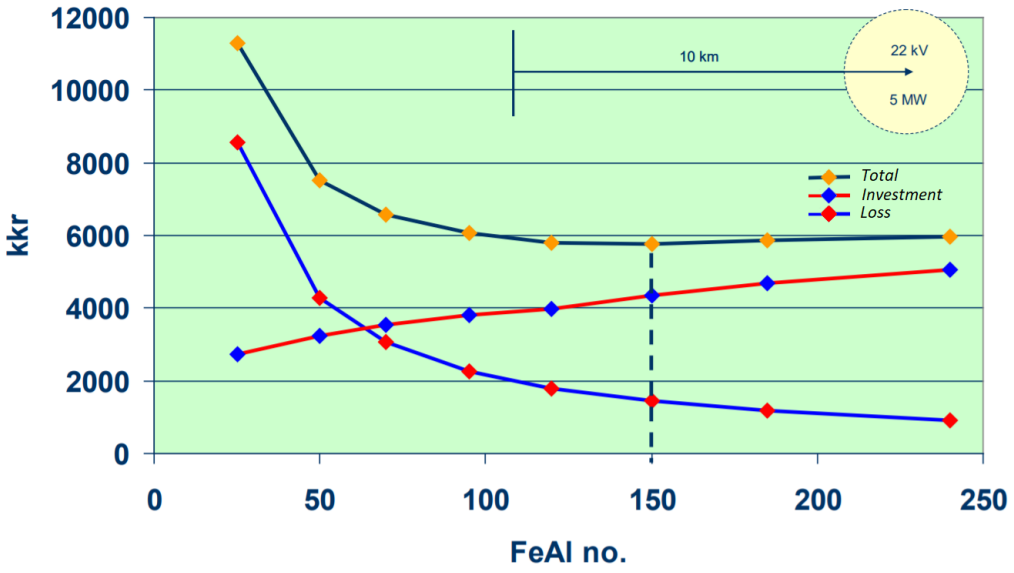

Figure 9.1: Line cost as a function of cross-section with constant load [50].

Observing the figure it is seen that the investment cost is increasing nearly linearly, while the cost of losses starts very high at small cross sections before it rapidly decreases. The rate of decrease then slows down, and it seems that the cost of losses approximately decreases at the same rate as the investment cost increases. This is reflected in the curve for the total cost, which is nearly constant for cross sections larger than 100 mm^2. This indicates that for a constant load the total cost of all cross sections in this range will be fairly equal. This characteristic is often used when selecting cables for a system where the future load demand is uncertain. As the load might become larger than expected it is often reasonable to choose one of the larger cross sections in the range, as the cost of losses will be kept lower than if a smaller cross-section were selected.

Chapter 10

Economic sensitivity analysis

As discovered in chapter 9 it is obvious that investing in a BESS is far too expensive for the area in question. The distance to the external grid being only a few kilometers, constructing a new cable connection will be relatively cheap. To generalize the economic assessment a sensitivity analysis has been conducted, having especially a focus on the length of the weak supply connection. By doing this the study can be relevant for cottage areas that are even more rural than the one analyzed in this project. Additionally the future prices of battery storage systems will be accounted for, and an analysis will be done on how the expected price reduction will influence the results.

10.1 Variation of line length

Here the length of line section 6 of fig. A.1 will be increased incrementally in order to observe if a BESS may be more economically viable when the area of supply is located more remotely. The investment cost of the BESS will keep constant regardless of where it is located, while increasing length will increase the investment cost of the cables. Simulations are conducted in PowerFactory in the same way as was done in chapter 7 to obtain the maximum power losses for each step, but the results will not be shown here. These results have then been inserted into the economic analysis model, and the total present value of future costs is calculated the same way as was done in chapter 9.

The load situation will mimic the critical load scenario, as described in section 7.2. Alternative 1 causes the supply to be critically loaded, and is as such not an alternative. It will therefore not be included in the sensitivity analysis. Alternative 3 will also be disregarded in the sensitivity analysis as it does not make geographically much sense, meaning that alternatives 2 and 4 remains. Figure 10.1 presents the results of the line length variation, which shows that the battery becomes the most beneficial alternative when the line length exceeds approximately 37 kilometer.

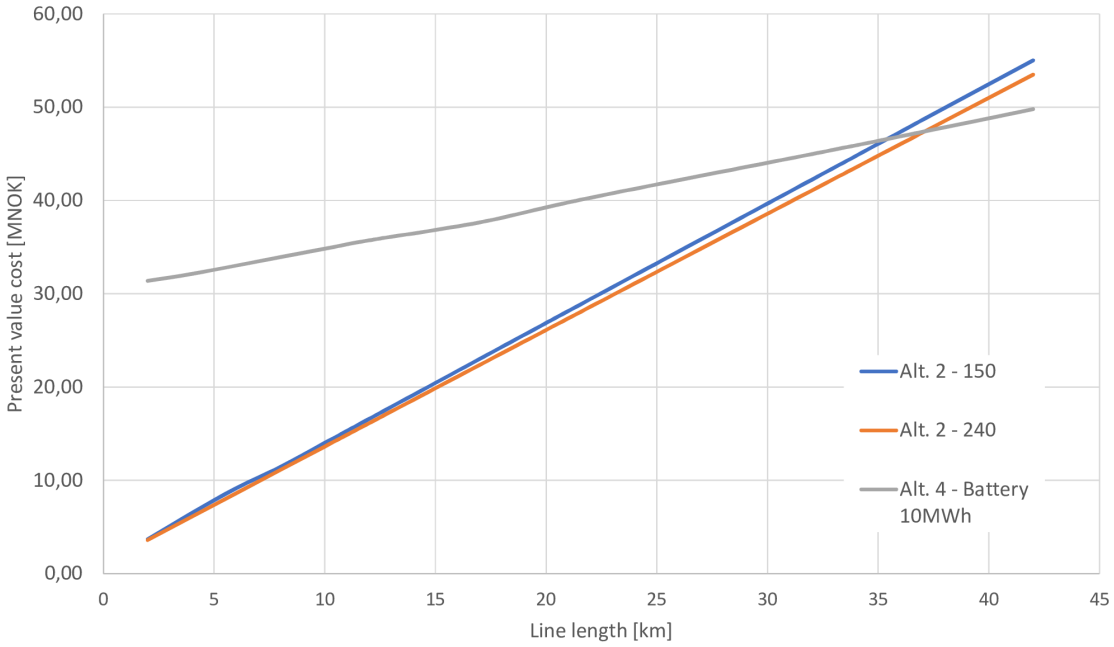

Figure 10.1: Present value of future costs with increasing length of grid connection.

The results show that the present value costs of all three alternatives increase linearly with respect to the line length. For alternative 2 the investment cost of the cable is given as a cost per kilometer, which as a result increases proportionally to the length. The investment cost of the BESS does not change, since no change is done to the battery parameters. The cost increase of alternative 4 is therefore solely due to the increased cost of losses. According to eq. (3.1) the power loss increases due to increased resistance in the line. As the load is kept constant the power loss increases linearly as a function of the line length, which causes also the cost of losses in eq. (3.3) to increase linearly. This applies to both variations of alternative 2 as well. Since both loss and investment cost increases for this alternative, however, the total cost increases faster than for alternative 4. Thus the BESS becomes economically viable compared to replacing the cable at approximately 37 km, which is a relatively long distance for a 22 kV distribution grid to cover. There are, however, examples of lines even longer than this in Norway, indicating that it is not an entirely unreasonable scenario [36].

During the simulation of this scenario, a large voltage drop in section 6 causes problems in the grid when the line becomes very long. The lowest voltage recorded is 0.73 p.u. which is an unacceptable value. Voltage drop in % is given by eq. (10.1) [51].

$$\Delta v = \frac{P}{V^2}\left(R + X \cdot tan\phi\right) \cdot 0.1 \tag{10.1}$$

From the formula it can be seen that reducing the power flow in the line will reduce the voltage drop as well. Therefore, an increase of battery discharge power will reduce the voltage drop in the line, and could as such be a solution to the voltage problem. This would, however, increase the investment cost further. Another possible way of improving the voltage is to operate the battery with voltage support in mind, which can be done through both active and reactive power. As the focus in this project has been on the peak shaving operation of the battery, the battery control system is operating to reduce the maximum power in the supply lines.

Therefore, the possibility of controlling the battery for voltage support operation has not been further investigated. Another possibility that not has been investigated, is tap changing of the transformers in order to increase the voltage. According to eq. (10.1) this could help to decrease the voltage drop. As such solutions not have been investigated, it is difficult to conclude that the battery is a viable option for the DSO for lengths above 37 km. What can be said, however, is that the battery also for this scenario is able to provide peak shaving such that the supply connection is not critically loaded.

10.2 Future battery pricing

As mentioned in section 8.3.2 the lithium-ion price is projected to continue its reduction the next ten years, according to [47] down to 70 $/KWh in 2030 from today's 209 $/kWh. In this chapter the future price of a battery energy storage system will be projected and inserted into the economic analysis model. Then the relevant alternatives will be compared as a function of the line length, in the same way as was done in the previous section.

The mentioned estimate for the year 2030 of 70 $/kWh includes the lithium-ion battery rack, but as discussed in section 8.3 the total enterprise cost contain much more than just the batteries. As a general principle, larger demand for a product causes a larger scale of production, which in turn may result in lower costs. Therefore, as the price of lithium-ion batteries decreases, the demand will increase for battery energy storage systems. As a result, the manufacturers of such systems has to increase their productions, which should decrease the costs of system components such as BMS, balance of system and suitable inverters. Thus, the cost for a BESS will obviously be driven down by reduction of the battery price, but its cost will also reduce due to other parts of the system becoming cheaper. In order to estimate the total BESS cost for an eight-hour system in the year 2030, the 70 $/kWh price point is therefore used in addition to a decrease of 30% for the remaining cost elements. [45, 52]

Using these assumptions, the future cost of a BESS is estimated on the basis of the costs given in table 8.4 and fig. 8.4. The resulting eight-hour discharge system cost is shown in fig. 10.2, which estimates a cost of 155 $/kWh. The main cost reduction obviously is due to the drastically cheaper lithium-ion batteries. For the 2018 estimation the battery rack cost accounts for 63% of the total system cost, while it for the 2030 estimation account for just 45% of the total system cost.

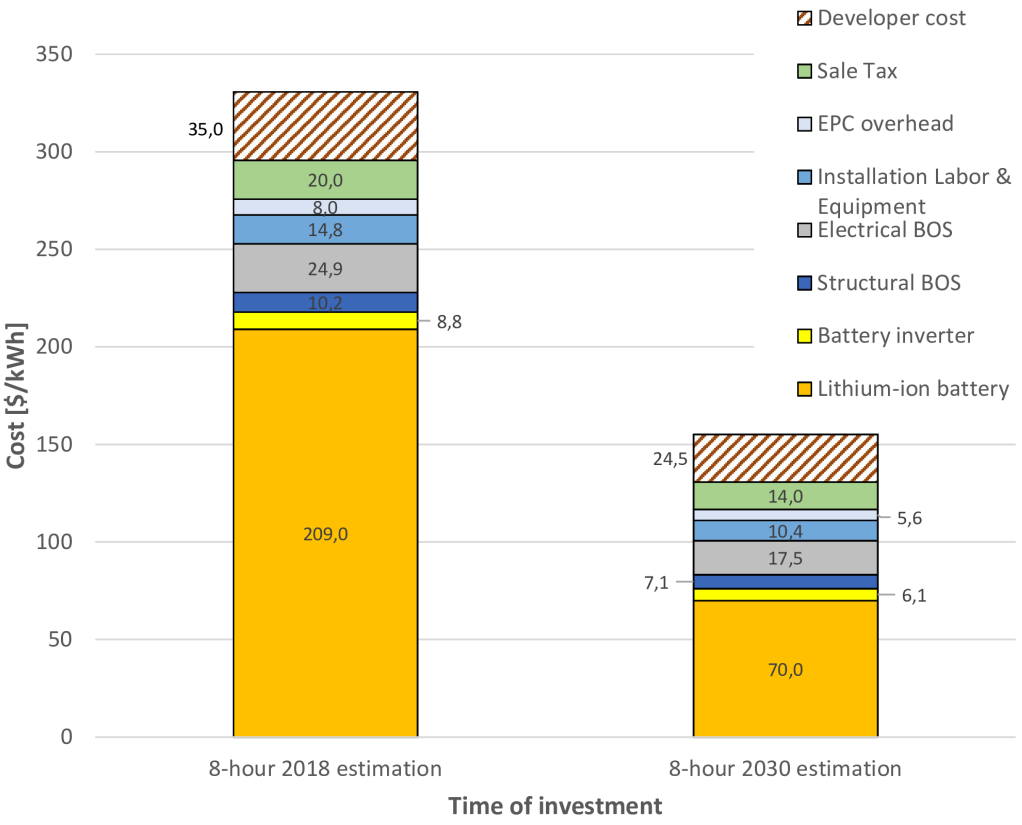

Figure 10.2: Investment cost for eight-hour BESS for 2018 and 2030.

Using the 155 $/kWh cost estimate in the sensitivity analysis model for reviewing the line length, generated the results shown in fig. 10.3. The cost of constructing the cable connections are assumed to be the same as earlier, as such mature technologies typically do not experience large cost reductions. It is observed that even with the cost reduction, the BESS alternative still is way too expensive for the analyzed grid area which has a total line connection length of 2 kilometers. At this length the present value for the analysis period is approximately 16 MNOK, which is over four times the cost of replacing the cable connection. The necessary line length for the battery to be beneficial has, however, decreased considerably compared to what was found in section 10.1. Due to the decreased investment cost of BESS the alternatives now meet each other at about 17 km. This still seem like a fairly long 22 kV connection, but may not be unrealistic in special cases. The present value at this point is approximately 22 MNOK for all alternatives, but the cost of the cable connection does increase more rapidly than the BESS alternative. This is because only the cost of losses is increasing for alternative 4, making it more and more beneficial compared to alternative 2.

Similarly to in section 10.1 the PowerFactory simulations causes worry regarding the voltage in the system at 17 km line length, which is 0.86 p.u. at the worst location. This has not been investigated further due to the limitations of this project, but possibly could have been solved by implementing voltage support in the battery control or by tap changing of the transformers.

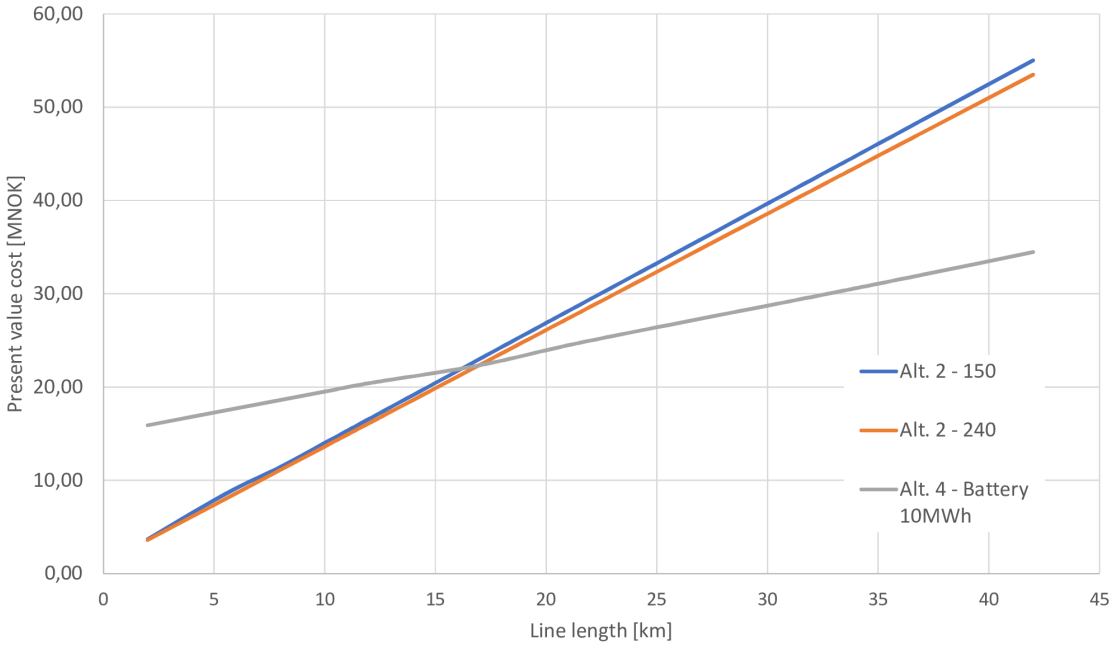

Figure 10.3: Present value of future costs with increasing length of grid connection and estimated 2030 cost of BESS.

Chapter 11

Energy storage in a broader perspective

This chapter will serve as a discussion of the findings in this report on a high level of abstraction, in order to widen one's perspective. Additionally, a discussion on the suitability of battery energy storage systems for the intended application is presented and compared to the applications where energy storage is used today.

11.1 Consequences of the model simplifications

During the work conducted in this project, battery energy storage has shown promising abilities to provide peak shaving in order to avoid overloading of weak supply grid components. There has, however, been observed other problems that the battery was unable to fix. For example in the case where a very long supply line was inserted, the battery was unable to keep the voltage at the required level. Simulations done with a reinforced cable of the same length showed that this reinforcement alternative was clearly better suited to uphold a reasonable voltage than the battery. In the case of this project, however, the intended battery application is peak shaving, and as a result the control algorithm for the battery is developed with this in mind. For a real system a much more clever energy and battery management system will control the battery behaviour, and will therefore be able to provide service for several applications at the same time such as e.g. peak shaving and voltage support. Therefore, problems observed in the simulation model, such as the low voltage, might not be an issue in a real life system.

The battery control algorithm that is utilized in this project include several simplifications that would not be present in real-world applications. The simulation model assumes fixed thresholds for charge and discharge, as presented in section 6.3, which cannot change during the simulation period. By having stringent thresholds like this, changes in demand magnitude and time variations would cause a suboptimal operation of the battery. It could, as a result, cause a situation where the battery is not providing peak shaving at all. In a real life system such fixed thresholds would not be present. In that case AI automation could e.g. conduct trend line learning, use historical demand data and utilize weather forecast to project the consumption profile for the upcoming period, and by doing this finding the optimal charge/discharge timing, magnitude and peak shaving dispatch [29]. This way the optimal operation of the BESS will be ensured, making it able to contribute to the daily operation of the grid when it is necessary.

Through the economic analysis of chapter 9 and the sensitivity analysis in chapter 10, it was discovered that both present and future prices of battery energy storage systems indicate that such a system is not economically feasible for the specific area that has been analyzed. The relatively short cable length that has to be reinforced causes this alternative to be fairly cheap,

while the prolonged high demand period of over eight hours requires a very large energy capacity of the battery. As a result, the BESS proves to be a very expensive investment, which is only beneficial compared to the cable reinforcement in cases where the necessary cable construction length is very long. The main reason for the exorbitant investment cost for the BESS is that the necessary discharge time is over eight hours, due to the consumption characteristic of the cottage user group. The load profile has, however, been manually estimated due to the lack of consumption data on the LV/MV transformer level. Therefore, this profile might estimate an unreasonably long high demand period, or an unreasonably short high demand period. If the period that needs peak shaving is shorter than the estimate, the BESS solution will be cheaper and thus more beneficial than what is presented in this study. If the necessary peak shaving period is longer, however, the battery system will be even more expensive and thus become less beneficial than presented in this thesis.

11.2 Global status of battery energy storage

When investigating the global status of energy storage it is evident that the majority of projects are designed for short duration applications, i.e. less than 4 hours discharge. Presently applications that improve the grid's ability to deal with momentary and short duration fluctuations are the most economically attractive, e.g. frequency regulation, spinning reserves and demand charge mitigation. Although the project economics are improving every year as costs are decreasing, even these short duration projects are dependent on subsidies or other incentives in many cases. Additionally, solar photovoltaics plus storage systems have proved to be economically attractive for commercial usage in some cases, while it generally seems unrealistic for residential and utility-scale applications. The unique position of short-duration battery projects, especially for frequency regulation, is illustrated by fig. 11.1. This figure show the intended application for utility-scale battery storage of the US in 2016, where 88% of the power and energy capacity was intended for frequency regulation. These market characteristics indicate that battery energy storage for long-duration energy management not at the present point in time is economically viable globally. As such the market trend correlate with the findings that has been observed in this project. [52, 53]

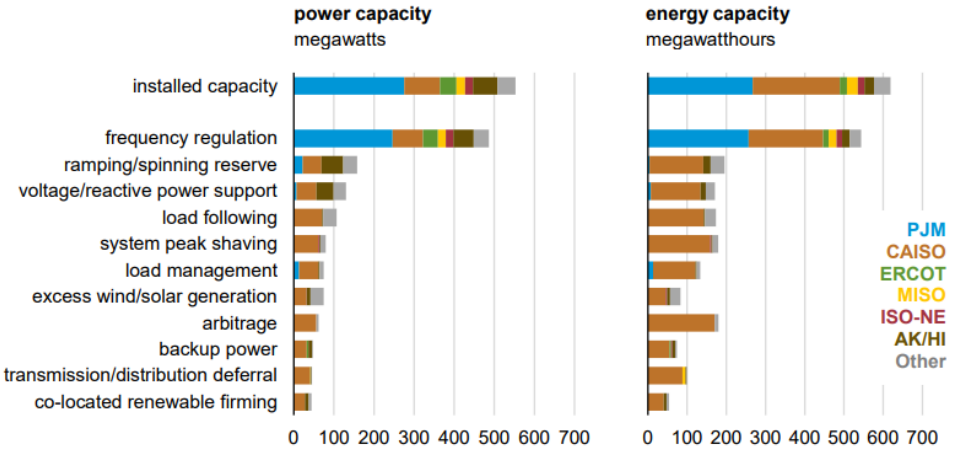

Figure 11.1: Applications for installed utility-scale battery storage in the U.S. [53].

In addition to the cost reduction of battery storage systems, there are measures that can be taken in order to increase the economic viability of an energy storage system. An important measure to increase the economic efficiency could be to aggregate several applications into one BESS, which enables the possibility of having more than one revenue stream. By efficiently applying multiple services, this permits the owner to gain income by always providing the service that is necessary. This concept can be referred to as "stacking services" and different applications can have preferable or undesirable synergies with each other. Figure 11.2 gives an indication of how well relevant applications generally fit together. Transmission and distribution upgrade deferral is given to have excellent synergies with electric energy time shift, electric supply capacity and voltage support. These applications often will result in the same operation pattern for the battery, and thus all could contribute together to improve the energy storage system economics. By taking the economic benefit of one or more of these applications into account during the analysis of the BESS in this project, increased revenue streams could have improved the viability of the alternative. As the DSO operates as a natural monopoly in Norway, however, they are not allowed to participate in other activities than operating the grid [54]. As a result, the DSO is not allowed to participate in sale of electricity through energy time shifting. [45, 55, 52]

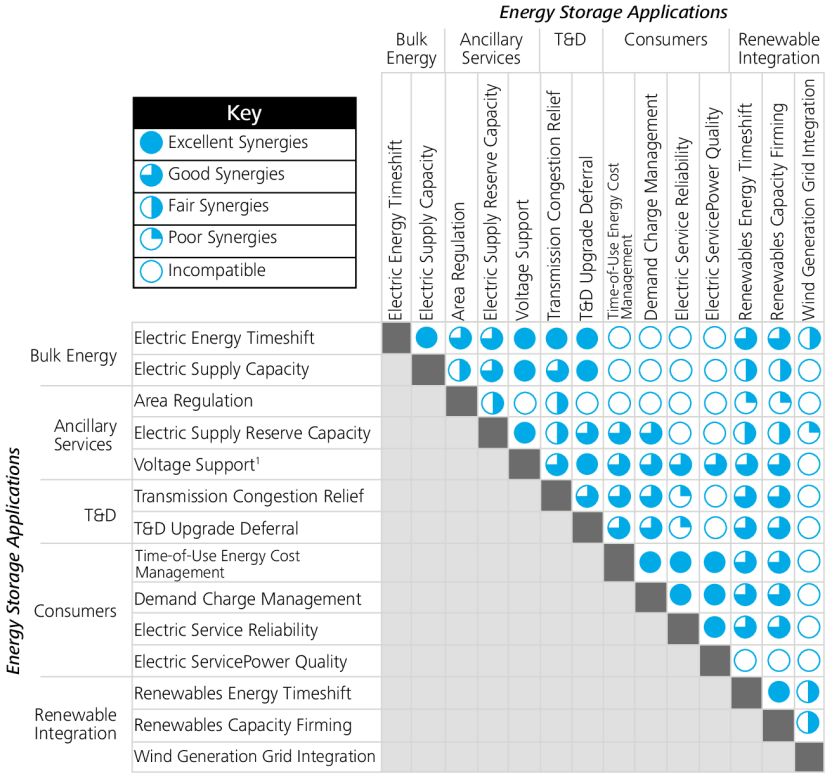

Figure 11.2: Application synergies for energy storage [55].

As was discovered in section 8.3.1 the global market for turnkey stationary battery energy storage systems is dominated by lithium-ion solutions, as there are few manufacturers providing such systems with other battery technologies. Figure 11.3a show the global share of power capacity for available electro-chemical energy storage technologies, which indicates that lithium-ion batteries represent 59% of the installed capacity. This corroborates the fact that

much of the focus on stationary energy storage is directed towards lithium-ion batteries, driven by the market development of electric vehicles which presently is a considerably larger market than stationary applications. By inspecting fig. 11.3b, showing the suitability of energy storage technologies for some grid service applications, in context of the globally deployed share of technologies, some interesting observations can be found. The lithium-ion technologies are shown to be excellently suited for frequency response and frequency containment reserve, while its suitability for load leveling is rated as medium. As a large share of the installed storage plants utilize the lithium-ion technology, and this is commercially the easiest available alternative, it is to be expected that most of the operators utilize their storage for frequency-related applications. This is precisely what is illustrated by fig. 11.1, as a large majority of the capacity is utilized for frequency regulation. If technologies such as vanadium redox flow batteries (VRFB) become more readily available in the market, one might see a rapid growth of storage facilities intended for energy management applications such as long duration peak shaving or load leveling. This technology is by fig. 11.3b stated as excellently suitable for load leveling, meaning that such applications could be much more viable than while utilizing lithium-ion batteries. A cost decline of VRFB through increased scale of manufacturing and by increasing the energy density, in addition to manufacturers providing turnkey units, could greatly increase the interest and demand for this technology in the global market. Thus costs for such systems would decrease accordingly. In that case battery energy storage systems with VRFB could make long duration applications a viable option, and thus enable grid investment deferral for systems such as the one analyzed in this project. [52]

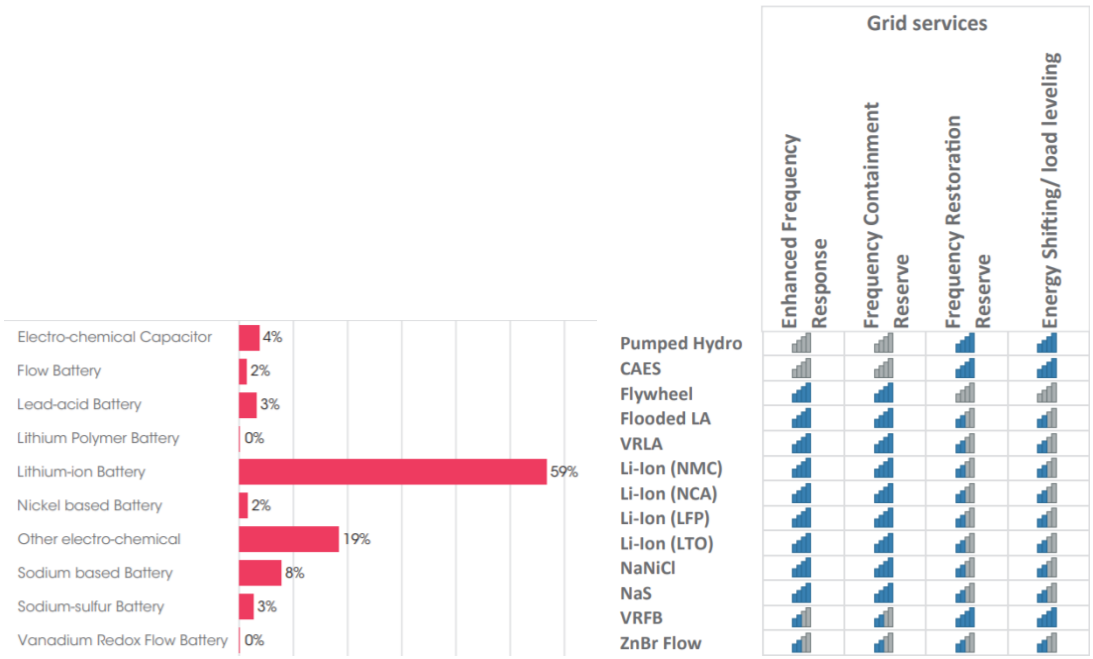

(a) Share of global energy storage power capacity by technology (2017). Cropped from [56].

(b) Suitability of energy storage technologies for different grid service applications [56].

Figure 11.3: Suitability and share of deployment for different energy storage technologies.

An opportunity to increase the economic viability for peak shaving application in cottage areas such as the one analyzed in this project, could be to utilize the principle of so-called

virtual aggregated power plants. This is a power plant that can aggregate the capacity of energy storage facilities located in different places, and operate it as one unit to provide a range of services through the use of AI, blockchain and predictive analysis [57]. If run by an independent market competitor the DSO could buy e.g. peak shaving services from the operator. As the electric vehicle penetration in Norway is rapidly increasing, more and more potential distributed energy storage facilities are appearing. In 2018 31% of all new cars sold in Norway was fully electric, and during the three first months of 2019 the share was 48% [58]. Still, only 7% of the total fleet of cars in the country are fully electric, but one would expect this to increase as old cars are being replaced with new EVs [59]. Energy capacities of up to 100 kWh are not uncommon for the most high-end models, indicating that there could be a large potential for utilizing the battery capacity of EVs to aggregate a virtual storage plant. This seems like a good fit for a cottage area such as the one analyzed since the load demand is highly dependent on users being present. While the user is present also the EV would be present, meaning that it could serve as an energy storage unit by connecting to the grid as a virtual storage facility. This way the virtual storage plant could be able to provide peak shaving to the DSO when the load situation is at the most critical, without the need for large capital investment in a BESS.

Chapter 12

Conclusion

In this project, the viability of using battery energy storage in a rural cottage area, instead of doing traditional grid upgrades, has been investigated. A given 22 kV distribution grid has been analyzed, where the supply to the cottage area is regarded as weak. Therefore, a battery energy storage system is modeled for the peak shaving application, and its technical and economic performance is compared to the performance of traditional grid upgrades.

By performing simulations in the developed power system model, it is clear that the peak shaving capability of a suitably dimensioned battery storage system is able to mitigate overloading of supply lines. Two different load scenarios have been analyzed. The first deals with a situation where the existing bottleneck is loaded at a maximum of 54%, while it has a maximum critical loading of 97% during the second load scenario. For the first scenario it is found that a 1 MW/9.5 MWh battery reduces the line loading to 41%. By doing this, however, the battery has caused the unfortunate effect of increasing the total losses in the system. Traditional grid reinforcement, by replacing the supply connection with a new cable, proved to be a much more reasonable alternative for this load scenario. Depending on the cable-cross section the maximum loading was decreased to 19% or 28%, while system loss was dramatically reduced compared both to the existing grid and the battery alternative. For the second load scenario keeping the existing grid unchanged is not an option, as the supply then becomes critically loaded. A 1.2 MW/10 MWh battery is found to be able to restrict the loading at a maximum of 80% during the entire high demand period, while also system losses are reduced compared to the initial state. Nevertheless, also for this load scenario traditional reinforcement seems like a more reasonable alternative, as the two modeled alternatives for replacing the supply connection resulted in maximum loading of 36% and 46%. At the same time losses are reduced with over 65% and 55% compared to the alternative where the battery was installed.

An economic analysis model was used to investigate the economic performance of the relevant alternatives. The model considered operation and maintenance cost, investment cost and the cost of losses, and utilized these to find the discounted cost of each solution alternative for the 30 year analysis period. It was found that a battery energy storage system is not an economically viable alternative for the given power system, as the present value of all future costs was considerably higher than the cheapest alternative for both load scenarios. In the first load scenario the battery was found to be over 29 times more expensive than doing nothing to the grid, while it was more than eight times more expensive than cable replacement in the second load scenario. The unfavourable economics of the battery is a result of several factors. The very long discharge duration caused by the consumption profile lead to 10 MWh energy capacity being necessary, which causes a huge investment cost given the present installation cost of 331 \$/kWh. Additionally, the cable replacement length is only 2 km, which has shown to be a much less expensive alternative. In a sensitivity analysis, it is found that the battery alternative with the present cost of installation is economically efficient if a 37 km cable has to be replaced. When projecting a future BESS installation cost of 155 \$/kWh, installing a battery becomes economically desirable when the cable length exceeds 17 km.

Chapter 13

Further work

This master's thesis project includes some simplifications, assumptions and limitations that can be looked into and further investigated. Some proposals for further work are therefore listed below.

- By monitoring the consumption in a MV/LV transformer in a cottage area, accurate load profiles for the user group may be obtained. Then the necessary discharge pattern might be established on the basis of better quality data, which may show a different load demand characteristic than what is estimated in this project.
- The possibility of using EVs as distributed energy storage could be investigated. This may include surveying the share of customers having EVs, and simulating different load scenarios while varying the amount of EVs present.
- Possible stacking services that are desirable in a cottage area may be investigated, modeled and simulated.
- Investigate the impact an energy storage system have on outages and its ability to reduce CENS.

Chapter 14

References

[1] Hanne Sæle, Maren Istad, and Synne Garnås. *The benefit of batteries in a flexible distribution grid. Results from the FlexNett project*. Tech. rep. SINTEF Energy Research AS, 2018.

[2] Vebjørn Hjelle. *Distributed Energy Storage as an Alternative to Grid Reinforcement*. Specialization project report. NTNU, 2018.

[3] DIgSILENT. *PowerFactory Applications*. Exported from https://digsilent.de on 2019/05/29. 2017. URL: https://www.digsilent.de/en/powerfactory.html.

[4] Karin Modig. *Powel og Validér når en ny milepæl i sitt samarbeid med leveranse av sentralsystemet*. Exported from https://valider.no on 2018/12/18. 2017. URL: https://www.valider.no/nyheter8.html.

[5] Hans Ørjasæter. COO Stryn Energi AS, Private communication. October 2018.

[6] Stig Julius Haugen et al. *Veileder for kraftsystemutredninger*. Tech. rep. Exported from https://publikasjoner.nve.no on 2019/06/02. Norges vassdrags- og energidirektorat, 2007.

[7] SINTEF Energi AS. *Planleggingsbok for kraftnett. Mål og rammebetingelser ved teknisk/økonomisk planlegging av kraftnett.* Exported from https://ren.no/planbok on 2019/03/15. SINTEF Energi AS, 2010.

[8] SINTEF Energi AS. *Planleggingsbok for kraftnett: Tapskostnader*. Exported from https://ren.no/planbok on 2019/04/17. SINTEF Energi AS, 2014.

[9] Eivind Solvang. "Nåverdier og kostnadselementer (investeringer, tap og avbudd)". Lecture notes from ELK-11: Cost-benefit analysis in distribution network planning, Unpublished. 2018.

[10] Trond Jensen, Ingrid Magnussen, and Stig Haugen. *Samfunnsøkonomisk analyse av energiprosjekter: Håndbok*. Exported from https://publikasjoner.nve.no on 2019/04/10. NVE, 2003. URL: http://publikasjoner.nve.no/haandbok/2003/haandbok2003_01.pdf.

[11] SINTEF Energi AS. *Planleggingsbok for kraftnett: Avbruddskostnader*. Exported from https://ren.no/planbok on 2019/03/28. SINTEF Energi AS, 2016.

[12] CEER. *Guidelines of Good Practice on Estimation of Costs due to Electricity Interruptions and Voltage Disturbances*. Exported from https://ceer.eu on 2019/04/10. CEER, 2010. URL: https://www.ceer.eu/documents/104400/3729293/C10-EQS-41-03_GGP+interuptions+and+voltage_7-Dec-2010.pdf/7dec3d52-934c-e1ea-e14b-6dfe066eec3e?version=1.0.

[13] NVE. *Referanserenten*. Exported from https://nve.no on 2019/04/08. 2019. URL: https://www.nve.no/reguleringsmyndigheten-for-energi-rme-marked-og-monopol/okonomisk-regulering-av-nettselskap/reguleringsmodellen/referanserenten/.

[14] SINTEF Energi AS. *Planleggingsbok for kraftnett: Grunnleggende økonomisk teori*. Exported from https://ren.no/planbok on 2019/03/28. SINTEF Energi AS, 2010.

[15] Investopedia. *Discounting*. Exported from https://investopedia.com on 2019/04/18. 2018. URL: https://www.investopedia.com/terms/d/discounting.asp.

[16] Investopedia. *Economic Life*. Exported from https://investopedia.com on 2019/04/18. 2018. URL: https://www.investopedia.com/terms/e/economic-life.asp.

[17] Investopedia. *Absolute Physical Life*. Exported from https://investopedia.com on 2019/04/18. 2018. URL: https://www.investopedia.com/terms/a/absolute_physical_life.asp.

[18] Hans Ørjasæter. COO Stryn Energi AS, Private communication. May 2019.

[19] Shuo Pang et al. "Battery state-of-charge estimation". In: *Proceedings of the 2001 American Control Conference. (Cat. No.01CH37148)*. Vol. 2. 2001, 1644–1649 vol.2.

[20] Gilbert M Masters. *Renewable and efficient electric power systems*. John Wiley & Sons, 2004.

[21] Christian Julien et al. *Lithium batteries*. Springer, 2016.

[22] N. Watrin, B. Blunier, and A. Miraoui. "Review of adaptive systems for lithium batteries State-of-Charge and State-of-Health estimation". In: *2012 IEEE Transportation Electrification Conference and Expo (ITEC)*. 2012, pp. 1–6.

[23] T. Guena and P. Leblanc. "How Depth of Discharge Affects the Cycle Life of Lithium-Metal-Polymer Batteries". In: *INTELEC 06 - Twenty-Eighth International Telecommunications Energy Conference*. 2006, pp. 1–8.

[24] HRESYS. "Smart Energy Solutions for a Cleaner World - Lithium Ion Battery Products". Company and product presentation, Unpublished.

[25] A. Zurfi and J. Zhang. "An electrical model for energy efficiency evaluation of NiMH batteries". In: *2017 IEEE 30th Canadian Conference on Electrical and Computer Engineering (CCECE)*. 2017, pp. 1–6.

[26] SINTEF Energi AS. *Planleggingsbok for kraftnett: Tekniske data*. Exported from https:// ren.no/planbok on 2019/04/28. SINTEF Energi AS, 2010.

[27] J Machowski, JW Bialek, and JR Bumby. *Power system dynamics: Stability and Control*. 2008.

[28] *DIgSILENT PowerFactory version 2018 User Manual*. Online Edition. DIgSILENT GmbH. Gomaringen, Germany, 2017.

[29] Micheal Austin. Vice president BYD US Operations, Private communication. 2019.

[30] PBES. *PBES CanPower: Low Emission Power Plant for Isolated Communities*. Exported from https://pbes.com on 2019/05/30. URL: https://www.pbes.com/wp-content/uploads/2019/05/CanPower-Low-Emission-Solution.pdf.

[31] Trond Leiv Toftevaag. Docent, Department of Electric Power Engineering NTNU, Private communication. May 2019.

[32] SINTEF Energi AS. *Planleggingsbok for kraftnett: Kostnadskatalog distribusjonsnett*. Exported from https://ren.no/planbok on 2019/04/28. SINTEF Energi AS, 2016.

[33] Hans Ørjasæter. COO Stryn Energi AS, Private communication. March 2019.

[34] SINTEF Energi AS. *Planleggingsbok for kraftnett: Brukstid for tap*. Exported from https:// ren.no/planbok on 2019/05/02. SINTEF Energi AS, 2014.

[35] Nicolai Feilberg. Private communication. March 2019.

[36] Kjell Sand. Vice Dean for Innovation, Faculty of Information Technology and Electrical Engineering (IE) at NTNU. Private communication. 2019.

[37] Paul Robson and Davide Bonomi. "Growing The Battery Storage Market 2018 - Exploring Four Key issues". In: *Energy Storage World Forum* (2018). Exported from https://energystorageforum.com on 2018/11/20. URL: https://energystorageforum.com/files/ESWF_Whitepaper_-_Growing_the_battery_storage_market.pdf.

[38] LG chem. *Product info: Battery Container-Long Duration*. Exported from https://lgesspartner.com on 2019/02/18. 2015. URL: https://www.lgesspartner.com/front/normal/en/product/productInfo.dev.

[39] BYD. *UTILITY ESS SOLUTION*. Exported from https://BYD.com on 2019/02/18. 2018. URL: https://en.byd.com/energy/utility-ess/.

[40] SAFT. *Intensium® Max, the megawatt energy storage system*. Exported from https://saftbatteries.com on 2019/02/18. URL: https://www.saftbatteries.com/products-solutions/products/intensium-max-megawatt-energy-storage-system.

[41] NAOKI Sonoda et al. "Development of Containerized Energy Storage System with Lithium-ion batteries". In: *Mitsubishi Heavy Industries Technical Review* 50.3 (2013). Exported from https://mhi.co.jp on 2019/02/18. URL: http://www.mhi.co.jp/technology/review/pdf/e503/e503036.pdf.

[42] PBES. *Containerized Energy Storage*. Exported from https://pbes.com on 2019/02/18. URL: https://www.pbes.com/containerized-ess/.

[43] Autarsys. *Autarsys Large ESS*. Exported from https://autarsys.com on 2019/02/18. URL: https://www.autarsys.com/products/product/large-ess/.

[44] HRESYS. *BC-OPzV-C Series Battery*. Exported from https://hresys.com on 2019/02/18. URL: http://www.hresys.com/yinginfo.php?id=308.

[45] Jimmy Zhang. Zhejiang Hengrui Technology Co Ltd, Private communication. 2019.

[46] Nils Johan Sylte. District manager Møre Trafo AS, Private communication. 2019.

[47] Bloomberg NEF. *New Energy Outlook 2018*. Exported from https://bnef.com on 2019/05/22. 2018. URL: https://about.bnef.com/new-energy-outlook/#toc-download.

[48] Ran Fu, Timothy Remo, and Robert Margolis. *2018 U.S. Utility-Scale Photovoltaics-Plus-Energy Storage System Costs Benchmark*. Tech. rep. Exported from https://nrel.gov/publications on 2019/05/22. Golden, CO: National Renewable Energy Laboratory, 2018. URL: https://www.nrel.gov/docs/fy19osti/71714.pdf.

[49] "IEEE Guide for the Characterization and Evaluation of Lithium-Based Batteries in Stationary Applications". In: *IEEE Std 1679.1-2017* (2018), pp. 1–47.

[50] Eivind Solvang. "Optimal cross section". Lecture notes from ELK-11: Cost-benefit analysis in distribution network planning. 2018.

[51] Eivind Solvang. "Optimal cross section (2)". Lecture notes from ELK-11: Cost-benefit analysis in distribution network planning. 2018.

[52] Lazard. *Lazard's Levelized Cost of Storage Analysis - version 4.0*. Exported from https://lazard.com on 2019/05/27. 2018. URL: https://www.lazard.com/perspective/levelized-cost-of-energy-and-levelized-cost-of-storage-2018/.

[53] U.S. Energy Information Administration. *U.S. Battery Storage Market Trends*. Exported from https://eia.gov on 2018/12/05. 2018. URL: https://www.eia.gov/analysis/studies/electricity/batterystorage/pdf/battery_storage.pdf.

[54] The Norwegian Water Resources and Energy Directorate. *Selskapsmessig og funksjonelt skille*. Exported from https://www.nve.no on 2019/05/30. 2018. URL: www.nve.no/reguleringsmyndigheten-for-energi-rme-marked-og-monopol/sluttbrukermarkedet/selskapsmessig-og-funksjonelt-skille/.

[55] Tomas Diaz de la Rubia et al. *Energy storage: Tracking the technologies that will transform the power sector*. Tech. rep. Exported from https://deloitte.com on 2019/05/29. Deloitte, 2016. URL: https://www2.deloitte.com/content/dam/Deloitte/no/Documents/energy-resources/energy-storage-tracking-technologies-transform-power-sector.pdf.

[56] IRENA. *Electricity Storage and Renewables: Costs and Markets to 2030*. Tech. rep. Exported from https://irena.org/publications on 2019/05/31. Abu Dhabi: International Renewable Energy Agency, 2017. URL: https://www.irena.org/publications/2017/Oct/Electricity-storage-and-renewables-costs-and-markets.

[57] Deloitte. *Supercharged: Challenges and opportunities in global battery storage markets*. Tech. rep. Exported from https://deloitte.com on 2019/05/31. Deloitte, 2018. URL: https://www2.deloitte.com/us/en/pages/energy-and-resources/articles/global-energy-storage-renewable-energy-storage.html.

[58] Norsk elbilforening. *Statistikk elbil*. Visited 2019/05/31. 2019. URL: https://elbil.no/elbilstatistikk/.

[59] Norsk elbilforening. *Elbilbestand*. Visited 2019/05/31. 2019. URL: https://elbil.no/elbilstatistikk/elbilbestand/.

Appendices

Appendix A

Modeling data

A.1 Grid modeling data

Table A.1: Cable parameters [26].

Cable	Resistance [Ω/km]	Reactance [Ω/km]	Resulting cap. [µF/km]	Rated current [A]	SC current (1s) [kA]
TXSE 3x1x50	0.641	0.140	0.160	185	4.5
TSLF 3x1x95	0.320	0.120	0.200	275	8.6
TXSE 3x1x150	0.206	0.120	0.230	355	13.5
TXSE 3x1x240	0.125	0.110	0.280	455	21.6

Table A.2: Overhead line parameters [26].

Line	Resistance [Ω/km]	Reactance [Ω/km]	Resulting capacitance [nF/km]	Rated current [A]
FeAl 1x16	1.126	0.409	8.89	171
FeAl 1x25	0.723	0.380	9.576	266

Table A.3: Line section component type and length, related to section numbers in fig. 2.2.

Line section	Type	Length [km]
1	TXSE 3x1x50	0.485
2	FeAl 1x16	0.448
3	FeAl 1x25	0.077
4	FeAl 1x25	0.831
5	TXSE 3x1x50	0.147
6	TXSE 3x1x50	0.342
7	TXSE 3x1x50	0.700
8	TSLF 3x1x95	1.010
9	TXSE 3x1x50	0.562
10	TXSE 3x1x50	0.432
11	TXSE 3x1x50	0.578
12	TXSE 3x1x50	0.753
13	TXSE 3x1x50	0.445
14	TXSE 3x1x50	0.553

Table A.4: Prerequisites for I_{th} of the overhead lines [26].

Parameter	Value
Vind speed across line	v = 1 m/s
Solar irradiance	$S_i = 900W/m^2$
Solar absorption coefficient	Y = 0.5
Emissivity compared to a black body	$K_e = 0.6$
Temperature of aluminium	$T_2 = 80°C$
Ambient temperature	$T_1 = 20°C$

Table A.5: Prerequisites for I_{th} of cables [26].

Parameter	Value
Maximum conductor temperature	90°C for PEX-insulated
Thermal resistivity in ground	1.0°C m/W
Temperature in ground	15°C
Cable depth in ground	0.7m above 1kV
Temperature in air	25°C

A.2 Load data

Table A.6: Calculation of average peak load from node "Hydla".

Measuring point	Peak 1h [kW]	Peak 10 min [kW]	Peak 1 min [kW]
6970631403764705	5.00	5.25	5.56
6970631403764859	7.50	7.875	8.34
6970631403765405	7.90	8.30	8.78
6970631403763210	5.00	5.25	5.56
6970631403763036	8.50	8.93	9.45
6970631403763036	10.20	10.71	11.34
6970631403766709	6.00	6.30	6.67
6970631407538272	8.00	8.40	8.89
6970631403763135	2.00	2.10	2.22
6970631403762640	7.30	7.67	8.12
6970631403766426	7.20	7.56	8.01
6970631403765924	5.20	5.46	5.78
6970631407538258	5.60	5.88	6.23
6970631401396557	7.15	7.51	7.95
6970631403765498	4.50	4.73	5.00
6970631407538234	8.30	8.72	9.23
Average	6.58	6.91	7.32

Table A.7: Peak load calculation for each node in the existing situation based on the average peak.

Node	Transformer type	Number of customers	Peak load (10 min) [kW]
Lida	Nat. ind	3	53
Stryn Skisenter 230	Møre Trafo OTW4650	3	18.6
Stryn Skisenter 415	Møre Trafo OTW51160	1	-
Kvia	Møre Trafo OTW3640	4	29
Hydla	Møre Trafo OTW51160	84	580
Hydla 2	NT EcoSmart	0	-
Bøanedsetra 1	Møre Trafo OTW51160	57	394
Bøanedsetra 2	Møre Trafo OTW51160	66	456
Bøanedsetra 3	Møre Trafo OTW51160	31	214
Tonningsetra	Møre Trafo OTW3640	22	152
Fossen	ABB	9	62
Skansen	Møre Trafo OTW4640	14	97
TOTAL			2056

A.3 Reactive load data

Table A.8: Calculation of average reactive load from node "Hydla".

Measuring point	P [kW]	Q [KVAr]	$cos\phi$
6970631400964191	0.769	0.184	0.972
	1.203	0.25	0.979
	0.515	0.157	0.957
6970631401263156	1.79.1	0.835	0.906
	1.673	0.784	0.906
6970631401120640	0.671	0.198	0.959
6970631404105811	8.755	0.395	0.999
6970631404105811	6.766	0.72	0.994
	2.894	1.024	0.943
	2.104	1.097	0.887
6970631403763036	6.927	0.44	0.998
	2.221	0.024	0.999
6970631401396557	2.501	0.565	0.975
	1.614	0.346	0.977
6970631407538234	1.912	0.314	0.987
	6.723	0.157	0.999
6970631403765955	11.778	0.311	0.999
	6.249	1.2	0.982
6970631403765498	1.553	0.195	0.992
	4.435	0.212	0.998
6970631403763210	1.24	0.206	0.986
	1.65	0.836	0.892
6970631403764705	4.283	1.026	0.972
	2.523	0.327	0.992
6970631403766709	2.745	0.286	0.994
	0.354	0.134	0.935
Average			0.969

A.4 PowerFactory single-line diagram

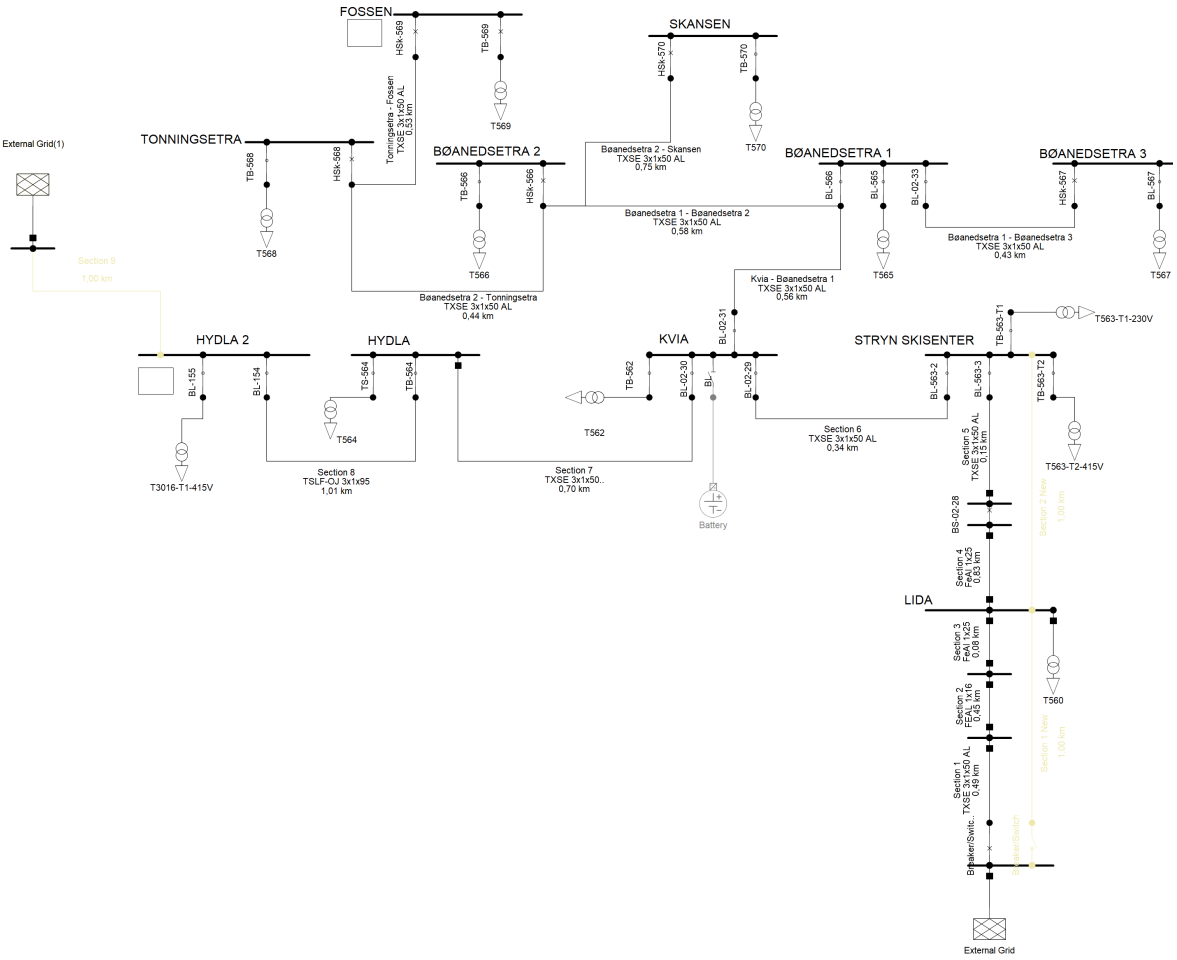

Figure A.1: PowerFactory model of cottage area.

Appendix B

Economic data

B.1 Construction costs

B.1.1 Cost of cables

Table B.1: Costs (in NOK/km) for 24 KV cables [32].

Type	Material	Labor	Machines	Equipment	Planning	Total
TSLE/TSLF 3x1x50 Al	143 091	17 381	5 156	6 385	7 025	179 038
TSLE/TSLF3x1x95 Al	173 279	17 381	5 156	8 006	7 025	210 847
TSLE/TSLF3x1x150 Al	225 689	22 277	5 156	8 006	7 918	269 046
TSLE/TSLF3x1x240 Al	270 012	22 277	5 156	11 244	7 918	316 607
TSLE/TSLF3x1x400 Al	333 173	23 297	5 156	13 457	7 918	383 001
TSLE/TSLF3x1x630 Al	658 025	23 297	5 156	18 321	7 918	712 716

Table B.2: Cost elements included in 50 and 240 mm^2 cables [32].

Cost element	Cost 50mm^2 [NOK]	Cost 240mm^2[NOK]	Amount	Unit
24 kV cable	131 618	248 745	1,05	km
Cable marking, protection and plate	12 861	12 861	1	km
Cable stretching	2 958	6 661	1	km
Engineering	8 507	8 507	1.5	
Joint PEX 3x1x240	-	8 819	1	pcs
Registration in NIS	558	558	1,5	pcs
Startup and decommisioning	22 537	22 537	1	pcs

B.1.2 Cost of trenches

Table B.3: Trench digging cost in NOK/km [32].

Type	Material	Labor	Machines	Equipment	Planning	Other	Total
City area			109 797	349 374	17 168	223 250	699 589
Suburb			87 316	157 708	17 168	171 058	433 249
Countryside			111 126	121 296	17 168	59 108	308 697

Table B.4: Cost element of one km trench in countryside [32].

Cost element	Cost [NOK]	Amount	Unit
Trench: Depth 0.6 m, width 0.5-0.7 m	89 541	0.7	km
Trench: Depth 1.2 m, width 0.4-0.9 m	107 690	0.3	km
Compacting	5 255	120	m^2
Sanding	27 950	1	km
Exchange of material	5 773	36	m^2
Drilling and blasting	11 260	20	m
Remove old and lay new asphalt	39 366	0.1	km
Securing trench	3 059	1	km
Documentation and measuring	4 464	1	km
Intersecting obstacles in ground	1 634	1	pcs
Engineering	12 704	1	km

B.2 Cost of losses

B.2.1 Annual specific cost of losses

Table B.5: Equivalent annual cost of energy losses and cost of maximum power losses for the analysis period [8].

Year	k_{weq} [NOK/kWh]	k_p [kr/kW year]
2019	0.259	584
2020	0.261	592
2021	0.266	599
2022	0.262	607
2023	0.265	616
2024	0.265	624
2025	0.265	633
2026	0.265	643
2027	0.265	652
2028	0.265	663
2029	0.265	673
2030	0.265	684
2031	0.265	695
2032	0.265	707
2033	0.265	719
2034	0.265	731
2035	0.265	745
2036	0.265	745
2037	0,265	745
2038	0.265	745
2039	0.265	745
2040	0.265	745
2041	0.265	745
2042	0.265	745
2043	0.265	745
2044	0.265	745
2045	0.265	745
2046	0.265	745
2047	0.265	745
2048	0.265	745

Appendix C

Load scenario data

C.1 Load scenario 1

Table C.1: Load scenario 1: Peak load calculation for each node based on average peak.

Node	Transformer type	Number of customers	Peak load (10 min) [kW]
Lida	Nat. ind	3	53
Stryn Skisenter 230	Møre Trafo OTW4650	3	18.6
Stryn Skisenter 415	Møre Trafo OTW51160	1	-
Kvia	Møre Trafo OTW3640	4	29
Hydla	Møre Trafo OTW51160	84	580
Hydla 2	NT EcoSmart	200	1304
Bøanedsetra 1	Møre Trafo OTW51160	57	394
Bøanedsetra 2	Møre Trafo OTW51160	66	456
Bøanedsetra 3	Møre Trafo OTW51160	31	214
Tonningsetra	Møre Trafo OTW3640	22	152
Fossen	ABB	9	62
Skansen	Møre Trafo OTW4640	14	97
TOTAL			3360

C.2 Load scenario 2

Table C.2: Load scenario 2: Peak load calculation for each node based on average peak.

Node	Transformer type	Number of customers	Peak load (10 min) [kW]
Lida	Nat. ind	3	53
Stryn Skisenter 230	Møre Trafo OTW4650	3	18.6
Stryn Skisenter 415	Møre Trafo OTW51160	1	-
Kvia	Møre Trafo OTW3640	4	29
Hydla	Møre Trafo OTW51160	84	580
Hydla 2	NT EcoSmart	600	4000
Bøanedsetra 1	Møre Trafo OTW51160	57	394
Bøanedsetra 2	Møre Trafo OTW51160	66	456
Bøanedsetra 3	Møre Trafo OTW51160	31	214
Tonningsetra	Møre Trafo OTW3640	22	152
Fossen	ABB	9	62
Skansen	Møre Trafo OTW4640	14	97
TOTAL			6002.6

Appendix D

Battery control

NOTE: The Latex code environment (listings) does not support the DIgSILENT programming language (DPL). Therefore, not all functions and keywords are highlighted correctly in the code blocks that are following[1].

The battery control algorithm presented in this appendix is based on [28] and [2], and is updated to fit the desired functionality.

D.1 Parameters of control system

Table D.1: State variables and parameters of control system [28].

Parameter	Unit	Description
SOC	%	State of charge
Eini	MWh	Storage energy size
SOCini	%	Initial state of charge
SOCmin	%	Minimum state of charge
SOCmax	%	Maximum state of charge
Pstore	MW	Rated charging power
PStartStore	MW	Pmeas where charging starts
PFullStore	MW	Pmeas where maximum charging is reached
Pfeed	MW	Rated discharging power
PStartFeed	MW	Pmeas where discharging starts
PFullFeed	MW	Pmeas where maximum discharging is reached
orientation	-	1=terminal j is closest to storage, otherwise -1

D.2 Initialisation

```
double pmeas;

SOC = SOCini;
pmeas = 0.;

! measured power operation area
chargeP = 0.;
if ({PFullStore >= PStartStore}.or.{PStartFeed >= PFullFeed}) {
  chargeP = 0;  ! Error
  Warn('PFullStore must be < than PStartStore and PFullFeed > than PStartFeed');
}
else if (pmeas > PStartFeed) {
```

[1]For reference, the Fortran style is used.

```
  chargeP = 3;
}
else if (pmeas <  PStartStore) {
  chargeP = 1;
}
else {
  chargeP = 2;
}

! energy operation area
iniSOCoob = 0; ! Inside bounds
if (SOCmin >= SOCmax) {
  chargeE = 0;  ! Error
  Warn('SOCmin must be < than SOCmax.');
}
else if (SOC > SOCmax) {
  chargeE = 3;
  iniSOCoob = 1;
}
else if (SOC = SOCmax) {
  chargeE = 3;
}
else if (SOC = SOCmin) {
  chargeE = 1;
}
else if (SOC < SOCmin) {
  chargeE = 1;
  iniSOCoob = 1;
}
else {
  chargeE = 2;
}
```

Listing D.1: Initialisation

D.3 Load flow equations

```
double Pgen,
       Qgen,
       redFac;

Pmeas = Pline*orientation + Pset; ! negative=load

redFac = 1.0;
if ({chargeP = 3}.and.{chargeE >= 2}.and.{chargeE > 0}) {
  if (Pmeas < PFullFeed) {
    redFac = 1 - ((PFullFeed - Pmeas)/(PFullFeed - PStartFeed));
  }
  Pgen = Pfeed * redFac;  ! discharge = GEN, feeding
  Qgen = Qfeed * redFac;  ! discharge = GEN, feeding
}
else if ({chargeP = 1}.and.{chargeE <= 2}.and.{chargeE > 0}) {
  if (Pmeas > PFullStore) {
    redFac = 1 - ((PFullStore - Pmeas)/(PFullStore - PStartStore));
  }
  Pgen = -Pstore * redFac;  ! charge = LOAD, storing
  Qgen = -Qstore * redFac;  ! charge = LOAD, storing
}
else {
  Pgen = 0.;
  Qgen = 0.;
}

SetEquation(0, Pset - Pgen);
SetEquation(1, Qset - Qgen);
```

Listing D.2: Load flow equations

D.4 Load flow control

```
Pmeas = Pline*orientation + Pset; ! negative=load

! measured power operation area
if (chargeP > 0) {  ! Not initial error
  if (Pmeas > PStartFeed) {
    chargeP = 3;
  }
  else if (Pmeas < PStartStore) {
    chargeP = 1;
  }
  else {
    chargeP = 2;
  }
}

! energy operation area
if (chargeE > 0) {  ! Not initial error
  if (SOC >= SOCmax) {
    chargeE = 3;
    if ({iniSOCoob = 0}.and.{SOC > SOCmax}) {
      SOC = SOCmax;
    }
```

```
  }
  else if (SOC <= SOCmin) {
    chargeE = 1;
    if ({iniSOCoob = 0}.and.{SOC < SOCmin}) {
      SOC = SOCmin;
    }
  }
  else {
    chargeE = 2;
    iniSOCoob = 0; ! Inside limits now
  }
}
```

Listing D.3: Load flow control

D.5 Quasi-dynamic simulation equations

```
SOC. = -Pset * 100. / (Eini * 3600.);  ! slope of charge/discharge in %
```

Listing D.4: Quasi dynamic equations

D.6 Quasi-dynamic simulation control

```
! energy operation area
if (chargeE > 0) {  ! Not initial error
  if (SOC >= SOCmax) {
    chargeE = 3;
    if ({iniSOCoob = 0}.and.{SOC > SOCmax}) {
      SOC = SOCmax;
    }
  }
  else if (SOC <= SOCmin) {
    chargeE = 1;
    if ({iniSOCoob = 0}.and.{SOC < SOCmin}) {
      SOC = SOCmin;
    }
  }
  else {
    chargeE = 2;
    iniSOCoob = 0; ! Inside limits now
  }
}
```

Listing D.5: Quasi dynamic control

Appendix E

BESS cost component regression

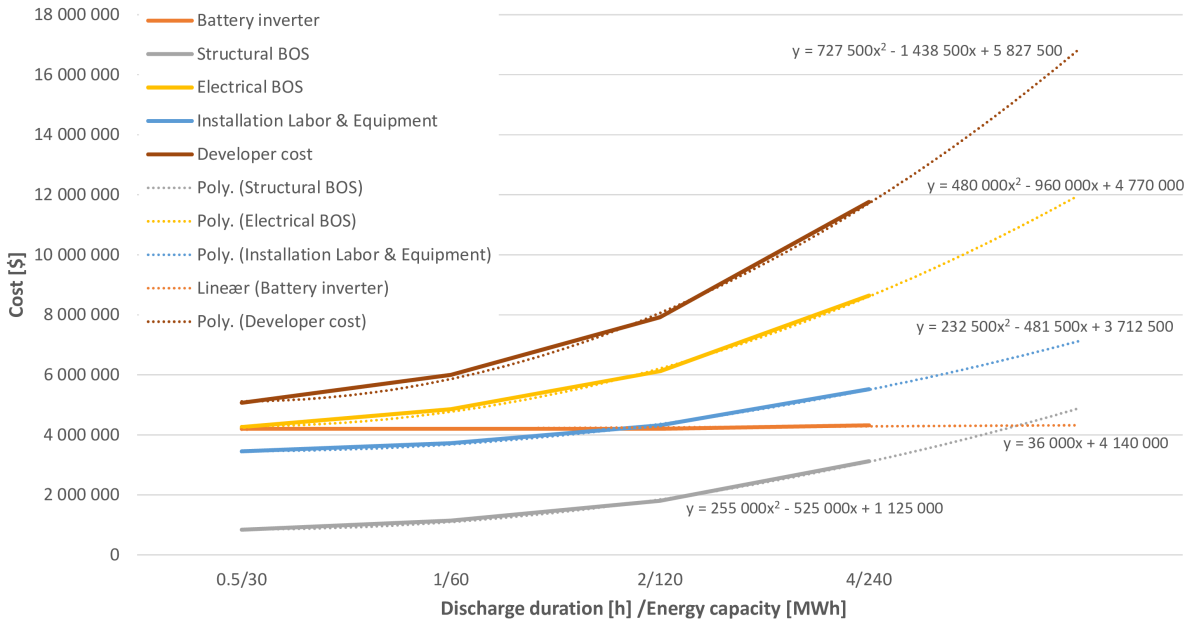

Figure E.1: BESS component cost regression. Based on values from [48].

Vebjørn Hjelle

Energy Storage for Reinforcement of a High Voltage Distribution Grid

NTNU
Norwegian University of
Science and Technology